

Analysis of E3 ligases and identification of ubiquitination sites regulating turnover of the plant immune signaling kinase BIK1

By

Lauren E. Grubb

A thesis submitted to the Department of Biology
in conformity with the requirements for the
Degree of Master of Science

Queen's University
Kingston, Ontario, Canada
(September 2018)
Copyright © Lauren E. Grubb, 2018

ABSTRACT

Plants possess sophisticated mechanisms for responding to the threat of pathogens. Microbial patterns such as bacterial flagellin are perceived by receptor complexes located at the plant plasma membrane. This perception initiates a signaling cascade which culminates in a robust immune response including an influx of Ca^{2+} into the cytosol, an apoplastic burst of reactive oxygen species, and up-regulation of defence genes. The receptor-like cytoplasmic kinase BIK1 is activated by many different receptor complexes and is a key component of the immune system. Although necessary for survival, the plant immune response must be tightly regulated to avoid fitness costs and maintain normal growth and development. As an important component in several immune responses, BIK1 must be maintained at optimal levels; however, the mechanism for this is poorly understood. Previous work identified the calcium-dependent protein kinase CPK28 to be a negative regulator of immunity and of BIK1 accumulation. It also provided evidence for proteasome-mediated turnover. Our collaborators identified the plant U-box proteins PUB25 and PUB26 as E3 ligases responsible for destabilization of BIK1 through polyubiquitination. The major objectives of my thesis were to determine which residues on BIK1 were polyubiquitinated, and to determine how CPK28, PUB25 and PUB26 regulate BIK1 turnover. I found that PUB25 and PUB26 associate with CPK28 and used epistasis analysis to place CPK28 upstream of PUB25 and PUB26 in this immune signaling pathway. This thesis also presents work toward determining CPK28- and PUB25- or PUB26-mediated BIK1 ubiquitination sites, as well as providing a dataset of ubiquitinated plasma membrane proteins through generation of a ubiquitome. Overall, the work presented in this thesis provides insight into the regulation of BIK1 turnover and contributes to our understanding of plant immune homeostasis.

CO-AUTHORSHIP

All data presented in this thesis was generated by me, however I was fortunate to benefit from the following collaborations:

Danielle Ciren (Queen's University)

- Performed site-directed mutagenesis (Appendix Table S3)
- Expressed and purified BIK1 single mutants in *E. coli*

Heather Galley (St. Lawrence College and Queen's University)

- Performed LR Reactions (Appendix Table S2)
- Performed floral dips

Mansuba Rana (Queen's University)

- Helped with generation of the quintuple *pub22 pub23 pub24 pub25 pub26*
- Performed some floral dips

Jacqueline Monaghan (Queen's University)

- Helped with genetic crosses (Appendix Table S1)
- Performed some qPCR
- Provided seed lines (Appendix Table S1)

Jinlong Wang and Jian-Min Zhou (Chinese Academy of Sciences, Beijing, China)

- Provided seed lines (Appendix Table S1)
- Provided clones for split-luciferase assays and ubiquitination assays (Appendix Table S6-S8)
- Provided unique knowledge and tools to allow for project design prior to the work being published

Marco Trujillo (University of Freiburg, Germany)

- Provided *pub22 pub23 pub24* seeds

Jan Sklenar, Paul Derbyshire, Frank Menke (The Sainsbury Laboratory, Norwich, UK)

- Ran mass spectrometry reps, and helped with analyses

Work in Chapter 3.1-3.4 has been published as part of a larger study:

Wang *et al.*, (2018). A regulatory module controlling homeostasis of a plant immune kinase. *Molecular Cell*, 69(3), 493–504.

- I provided data presented in Figure 1D-E, Figure 4A-B, and Figure S1G, S1I, and S1J-L

ACKNOWLEDGEMENTS

I would firstly like to thank my supervisor, Dr. Jacqueline Monaghan, for her guidance throughout the course of my Master's thesis. Thanks to her, I have become a better scientist, and have learned many valuable skills. Next, I would like to thank my committee members, Dr. Wayne Snedden and Dr. Virginia Walker for providing advice throughout my thesis, and for their encouragement to pursue research prior to my graduate degree. Next, I would like to thank Dr. Frank Menke and Dr. Cyril Zipfel at The Sainsbury Lab (TSL) in Norwich, UK for hosting me during my NSERC-MSFSS, as well as Dr. Jan Sklenar, Dr. Paul Derbyshire and Ana Lopez-Vazquez of the TSL Proteomics support team for providing such a welcoming environment. I am grateful to our collaborators, Dr. Jian-Min Zhou and Dr. Jinlong Wang for providing seeds, and clones for many of my experiments (Appendix Table S1, Appendix Table S6-S8), as well as for providing us with unique knowledge and tools prior to publication, allowing us to form the basis of the first part of my thesis project. Thank you also to Danielle Ciren, Heather Galley and Suba Rana for their assistance throughout my project. I would also like to thank Jeffrey Rowbottom, Dale Kristensen and Olivia Siemons for plant care. Of course, I am also grateful for my fellow Monaghan Lab members, namely Dr. Melissa Bredow, Kristen Siegel, Irina Sementchoukova, Danalyn Holmes, Ruxandra Bogdan, Alex Johnson-Dingee, Sydney Pascetta, Alysha Thomson, Kathy Sihavong, Lindsey Marck, Andrew Ji, Cailun Tanney, and Jennifer Wesley for making our lab such a fun, enriching environment. In addition, thanks to all members of the Plaxton, Snedden and Regan Labs for continuous assistance and fun throughout my Master's degree. Finally, I would like to thank my friends and family for their encouragement and continued support. My research has been generously supported by an NSERC CGS-M, NSERC MSFSS, and OGS, as well as by NSERC Discovery and CFI grants awarded to Dr. Jacqueline Monaghan.

TABLE OF CONTENTS

ABSTRACT	ii
CO-AUTHORSHIP.....	iii
ACKNOWLEDGEMENTS.....	iv
TABLE OF CONTENTS.....	v
LIST OF TABLES	viii
LIST OF FIGURES	ix
LIST OF ABBREVIATIONS.....	x
1. INTRODUCTION.....	1
1.1- Introduction to plant immune signaling	1
1.2- Immune signaling at the plasma membrane	2
1.3- Immune homeostasis and regulation of BIK1	5
1.3.1- BIK1 activity is negatively regulated by a protein phosphatase	8
1.3.2- BIK1 levels are positively regulated by heterotrimeric G proteins	8
1.3.3- BIK1 is negatively regulated by a calcium-dependent protein kinase	9
1.4- E3 ligases and ubiquitination.....	10
1.5- Research objectives.....	14
2. MATERIALS AND METHODS	16
2.1- Plant growth conditions.....	16
2.2- Generation of plant materials	17
2.2.1- Genetic crosses.....	17
2.2.2- <i>Agrobacterium</i>-mediated transformation by floral dip.....	17
2.2.3- Allele-specific genotyping	18
2.3- Molecular cloning.....	19
2.3.1- Gateway cloning	19
2.3.2- Site-directed mutagenesis	20
2.3.3- Gibson assembly	21
2.4- RNA extraction, reverse transcription and qPCR.....	21
2.5- Immune-induced oxidative burst assays.....	22
2.6- Transient protein expression in <i>N. benthamiana</i>	22
2.7- Split-luciferase complementation assays.....	23

2.8- Co-immunoprecipitation assays	23
2.9- Identification of ubiquitination sites on plasma-membrane proteins using liquid chromatography followed by tandem mass spectrometry (LC-MS/MS).....	25
2.9.1- Preparation of microsomal fractions and trypsin digests.....	25
2.9.2- Column desalting.....	26
2.9.3- Immunoprecipitation using α -K- ϵ -GG	26
2.9.4- Sample purification with C18 Micro-spin columns	27
2.9.5- MAPK activation assays	27
2.9.6- LC-MS/MS determination of BIK1 ubiquitination sites	28
2.10- Expression and protein purification from <i>E. coli</i>	28
2.11- Cell-free degradation assays	30
2.12- <i>In vitro</i> ubiquitination assays	30
2.13- SDS-PAGE and immunoblotting.....	31
3A. REGULATION OF BIK1 TURNOVER BY THE CALCIUM-DEPENDENT PROTEIN KINASE CPK28 AND E3 UBIQUITIN LIGASES PUB25 AND PUB26	33
3.1- PUB25 and PUB26 associate with CPK28	33
3.2- PUB25 and PUB26 negatively regulate plant immunity	34
3.3- Epistasis analysis to determine genetic interaction between PUB25/26, CPK28 and BIK1 in PAMP-induced ROS burst	36
3.4- PUB22, PUB23 and PUB24 may also contribute to BIK1 turnover	38
3B. IDENTIFICATION OF BIK1 UBIQUITINATION SITES.....	47
3B.1- Generation of a plasma membrane ubiquitome	47
3B.2- Analysis of ubiquitinated proteins	48
3B.3- Determination of ubiquitinated residues on BIK1	50
3B.4- Site-directed mutagenesis and generation of <i>in planta</i> BIK1 mutants	51
3B.5- Development of ubiquitination assays to test which BIK1 lysines are subject to regulation by the CPK28-PUB25/26 regulatory module	53
3B.5.1- <i>In vitro</i> ubiquitination assays.....	53
3B.5.2- Cell-free degradation assays	54
3B.5.3- <i>In vivo</i> transient ubiquitination assays in <i>N. benthamiana</i>	55
4. DISCUSSION	62
4.1- CPK28, PUB25 and PUB26 contribute to BIK1 turnover	63
4.2- Analysis of PUB22, PUB23 and PUB24 as other factors in BIK1 turnover	65

4.3- Identifying BIK1 ubiquitination sites	68
4.4- Troubleshooting ideas for ubiquitination assays	70
4.5- Identification of ubiquitinated proteins upon elf18 treatment	72
4.6- Future directions	74
4.7- Concluding remarks	75
SUMMARY	77
LITERATURE CITED	79
APPENDIX	90

LIST OF TABLES

Table 3B.1. BIK1 peptides identified by mass spectrometry	57
Table S1. Germplasm used in this thesis	90
Table S2. BIK1 ^{mut} constructs used for <i>Agrobacterium tumefaciens</i> -mediated transformation and expression and purification of recombinant protein from <i>E. coli</i>	91
Table S3. Primers used in this thesis for site-directed mutagenesis and Gibson assembly ..	93
Table S4. Primers used in this thesis for colony PCR and sequencing	95
Table S5. Primers used in this thesis for genotyping and qPCR.....	96
Table S6. Constructs used for split-luciferase complementation assays.....	97
Table S7. Constructs used for co-immunoprecipitation assays	98
Table S8. Constructs for <i>in vitro</i> ubiquitination assays.....	99
Table S9. Antibodies and titres used in this thesis.....	100
Table S10. Plasma membrane ubiquitinated proteins as identified by di-Gly enrichment and LC-MS/MS.....	103
Table S11. GO term enrichment for mock treated di-Gly microsomal fractions.....	119
Table S12. GO term enrichment for elf18 treated di-Gly microsomal fractions	137

LIST OF FIGURES

Figure 2.1. General workflow for determination of BIK1 ubiquitination sites by mass spectrometry	32
Figure 3A.1. PUB25 and PUB26 associate with CPK28 via split-luciferase assays	41
Figure 3A.2. PUB25 and PUB26 associate with CPK28 via co-IP assay	42
Figure 3A.3. Genetic analysis of <i>pub25 pub26</i> double knockout mutants and PUB25-OE and PUB26-OE overexpression lines.....	43
Figure 3A.4. Characterization of <i>pub25-1 pub26-1</i> mutants and PUB25-OE and PUB26-OE lines.....	44
Figure 3A.5. Epistasis analysis places CPK28 upstream of PUB25 or PUB26	45
Figure 3A.6. Generation of <i>pub22 pub23 pub24//35S:BIK1-HA</i> lines.....	46
Figure 3B.1. MPK3, MPK4/11 and MPK6 are activated upon elf18 treatment	56
Figure 3B.2. Validation of BIK1 ubiquitination at residues K31, K41, K61, K358, K366, K369, K370, K374 and K388.....	58
Figure 3B.3. Ubiquitinated lysine residues on BIK1	59
Figure 3B.4. Optimization of <i>in vitro</i> ubiquitination assays for determination of BIK1 lysines responsible for its CPK28-, PUB25- and PUB26-mediated degradation	60
Figure 3B.5. Optimization of <i>in vivo</i> ubiquitination assays in <i>N. benthamiana</i>	61
Figure S1. Analysis of flg22-induced ROS burst on <i>pub25 pub26</i> knockout mutants and PUB25-OE and PUB26-OE overexpression lines.....	101
Figure S2. Epistatic analysis of flg22 ROS burst	102

LIST OF ABBREVIATIONS

ABA	Abscisic acid
ABC	Ammonium bicarbonate
ABI	ABA INSENSITIVE
ACN	Acetonitrile
ACRE	Avr9/Cf-9 RAPIDLY ELICITED
AGB1	ARABIDOPSIS G-PROTEIN BETA SUBUNIT1
AGG1/2	ARABIDOPSIS G-PROTEIN GAMMA SUBUNIT1/2
ANOVA	Analysis of variance
AP2C1	ARABIDOPSIS PP2C-TYPE PHOSPHATASE1
APC	ANAPHASE PROMOTING COMPLEX
ARC1	ARMADILLO REPEAT CONTAINING1
ARM	Armadillo repeat
BAK1	BRASSINOSTEROID INSENSITIVE 1-ASSOCIATED RECEPTOR KINASE1
BIK1	BOTRYTIS INDUCED KINASE1
BKI1	BRI1 KINASE INHIBITOR1
BR	Brassinosteroid
BRI1	BRASSINOSTEROID INSENSITIVE1
BSA	Bovine serum albumin
BTB	BRIC-A-BRAC, TRAMTRACK, AND BROAD COMPLEX
CAMV	Cauliflower mosaic virus
CBB	Coomassie Brilliant Blue
CDG1	CONSTITUTIVE DIFFERENTIAL GROWTH1

CDPK	Calcium-dependent protein kinase
CERK1	CHITIN ELICITOR RECEPTOR KINASE1
Cluc	C-terminal luciferase
co-IP	Co-immunoprecipitation
Col-0	Columbia ecotype
CPK28	CALCIUM-DEPENDENT PROTEIN KINASE28
CPR5	CONSTITUTIVE EXPRESSION OF PATHOGENESIS RELATED GENES5
CRL	CULLIN Ring Ligase
CV	Column volume
DAMP	Damage associated molecular pattern
DDB	Damaged DNA binding
DMP	Dimethyl pimelimidate
dpi	Days post infiltration
DTT	Dithiothreitol
DUB	Deubiquitinating enzyme
DWF4	DWARF4
ECL	Enhanced chemiluminescent
EDTA	Ethylenediaminetetraacetic acid
EFR	ELONGATION FACTOR TU RECEPTOR
EIL1	ETHYLENE INSENSITIVE3-LIKE1
EIN3	ETHYLENE INSENSITIVE3
ET	Ethylene
ETI	Effector-triggered immunity

elf18	18 amino acid peptide from Elongation factor-Tu
FER	FERONIA
flg22	22 amino acid conserved sequence from bacterial flagellin
FLS2	FLAGELLIN SENSING2
GFP	Green fluorescent protein
GO	Gene ontology
GST	Glutathione S-transferase
HA	Hemagglutinin
HECT	HOMOLOGOUS TO THE E6-AP CARBOXYL TERMINUS
His	Histidine
HPLC	High performance liquid chromatography
HR	Hypersensitive response
HRP	Horseradish peroxidase
IAM	Iodoacetamide
IAP	Immuno-affinity purification
IP	Immunoprecipitation
IPTG	Isopropyl β -D-1-thiogalactopyranoside
JA	Jasmonic acid
kDa	Kilodaltons
LB	Luria Broth
LC-	Lipid chromatography- tandem mass spectrometry
MS/MS	
LB	Luria broth

LIP1/2	LOST IN POLLEN TUBE GUIDANCE1/2
LRR	Leucine-rich repeat
LYK5	LYSIN MOTIF RECEPTOR KINASE5
MAPK	Mitogen activated protein kinase
MES	2-(N-morpholino)ethanesulfonic acid
MHC	Major histocompatibility complex
MS	Murashige and Skoog
NB	Nucleotide binding
NEB	New England Biolabs
Nluc	N-terminal luciferase
OD	Optical density
OE	Overexpression
PAD4	PHYTOALEXIN DEFICIENT4
PAMP	Pattern associated molecular pattern
PBL	PBS1-LIKE
PBS	Phosphate buffered saline
PBS1	AvrPphB SUSCEPTIBLE PROTEIN1
PCR	Polymerase chain reaction
Pep	Plant elicitor peptide
PEPR1/2	PLANT ELICITOR PEPTIDE RECEPTOR1/2
PMSF	Phenylmethylsulfonyl fluoride
PP2C	Protein phosphatase2C
PRM	Parallel reaction monitoring

PRR	Pattern recognition receptor
PTI	PAMP-triggered immunity
PTM	Post-translational modification
PUB	Plant U-box
PVDF	Polyvinylidene fluoride
RBOHD	RESPIRATORY BURST OXIDASE HOMOLOGUE D
RGS1	REGULATOR OF G-PROTEIN SIGNALING1
RING	REALLY INTERESTING NEW GENE
RIPK	RPM1-INDUCED PROTEIN KINASE
RLCK	Receptor-like cytoplasmic kinase
RLK	Receptor-like kinase
RLP	Receptor-like protein
ROS	Reactive oxygen species
RT-qPCR	Reverse transcription, quantitative polymerase chain reaction
SA	Salicylic acid
SCF	SFP, Cullin, F-box containing complex
SDS-	Sodium dodecyl sulfate-polyacrylamide gel electrophoresis
PAGE	
SGI	Seedling growth inhibition
STRING	Search tool for the retrieval of interacting genes/proteins
TBS	Tris buffered saline
TCAG	The Centre for Applied Genomics
TCEP	Tris(2-carboxyethyl)phosphine

TE	Tris-EDTA
TFA	Trifluoroacetic acid
TPK1b	TOMATO PROTEIN KINASE1b
TPR	Tetratricopeptide repeat
Tris	Tris(hydroxymethyl)aminomethane
TSL	The Sainsbury Laboratory
XLG2	EXTRA LARGE G PROTEIN2
YFP	Yellow fluorescent protein

1. INTRODUCTION

1.1- Introduction to plant immune signaling

Plant diseases are responsible for the loss of at least 10% of annual global food production, which has devastating impacts on food security (Strange & Scott, 2005). The world population is rising dramatically, and births in developing countries account for approximately 95% of these individuals (Christou & Twyman, 2018). Many farmers in these developing countries have reduced access to pesticides and herbicides, leaving their crops vulnerable to drastic yield losses due to pathogens. Crop plants have been bred for desirable traits such as flavour profiles rather than for traits conferring strong disease resistance, contributing to instances of severe crop loss due to disease. Co-evolution between plants and their pathogens has resulted in adaptive mechanisms of pathogenesis and virulence, as well as defence mechanisms in the targeted plants. Thus, studying plant immune signaling is an important, ever-evolving field of study.

Although they evolved independently, animal and plant immune systems are quite similar; however, there are also some major differences. There are two forms of immunity in animals, innate and adaptive, whereas plant immune systems are limited to innate immunity (Ausubel, 2005; Nürnberger *et al.*, 2004). Adaptive immunity is an antigen-specific immune response, that results in generation of immune cells that are specific for that antigen (Boehm & Swann, 2014). This is a slower response but generates of a sort of memory for more efficient responses upon subsequent pathogen exposure. Innate immunity is the activation of non-specific defence mechanisms that are the first line of defence including a defined set of receptors that recognize microbe-associated molecules.

1.2- Immune signaling at the plasma membrane

The first layer of plant innate immune signaling is pattern-triggered immunity (PTI), which consists of receptors located at the plant plasma membrane, called pattern recognition receptors (PRRs) that perceive conserved pathogen-associated molecular patterns (PAMPs) (Boller & Felix, 2009; Couto & Zipfel, 2016; Li *et al.*, 2016; Saijo *et al.*, 2018; Tang *et al.*, 2017). Well-studied *Arabidopsis* PRRs include FLAGELLIN SENSING2 (FLS2), which recognizes a 22 amino acid peptide of flagellin (flg22), and ELONGATION FACTOR-TU RECEPTOR (EFR), which recognizes an 18 amino acid epitope from bacterial EF-Tu (elf18) (Gómez-Gómez & Boller, 2000; Gómez-Gómez *et al.*, 1999; Kunze *et al.*, 2004; Zipfel *et al.*, 2006). Fungal chitin can also be perceived as an elicitor in *Arabidopsis* and is recognized by the PRRs CHITIN ELICITOR RECEPTOR KINASE1 (CERK1) and LysM-RK LYSINE MOTIF RECEPTOR KINASE5 (LYK5) (Cao *et al.*, 2014; Miya *et al.*, 2007). Aside from these PAMPs, there are plant PRRs that recognize endogenous “self” molecules indicative of cell damage, known as damage-associated molecular patterns (DAMPs), which can consist of molecules that are passively released upon cell damage, or of peptides that are processed and/or secreted upon infection to contribute to immune responses (called phytochemicals) (Gust *et al.*, 2017). The second category includes plant elicitor peptides (Peps), a family of 7 small proteins derived from larger PROPEP precursors, which are recognized by PEP1 RECEPTOR1 and PEP1 RECEPTOR2 (PEPR1 and PEPR2) (Huffaker & Ryan, 2007; Yamaguchi, *et al.*, 2010; Yamaguchi *et al.*, 2006).

The second layer of plant innate immune defences is that of effector-triggered immunity (ETI). Pathogens have evolved mechanisms of injecting effector proteins directly into the cell as a way of by-passing PTI machinery (Rafiqi *et al.*, 2009). Many effectors target important

components of PTI (Macho & Zipfel, 2015; Zhang *et al.*, 2010). In turn, plants have evolved intracellular receptors that recognize either the effector or changes in target proteins induced by the effector (Rafiqi *et al.*, 2009). Most of these receptors consist of a leucine-rich repeat (LRR) domain and a nucleotide binding (NB) domain termed NB-LRRs. In order to quell the infection, ETI often results in localized cell death at the pathogen infection sites, known as the hypersensitive response (HR) (Dangl *et al.*, 1996).

Components of PRR complexes involved in PTI consist of receptor-like kinases (RLKs), receptor-like cytoplasmic kinases (RLCKs) or receptor-like proteins (RLPs). The *Arabidopsis* genome encodes greater than 600 total RLKs and RLCKs predicted to function in plant responses to microbial infection, hormones, and endogenous and environmental cues (Shiu & Bleecker, 2001, 2003). Many well-studied RLKs at the plasma membrane consist of an extracellular series of leucine-rich repeats (LRRs), a transmembrane domain and an intracellular kinase domain (Rao *et al.*, 2018; Wu & Zhou, 2013). Upon elicitor perception, it is common for there to be formation of a receptor complex that relays the signal for the plant to respond to the pathogen threat. For example, upon perception of flg22, FLS2 associates with another LRR-RLK BRASSINOSTEROID INSENSITIVE1-ASSOCIATED RECEPTOR KINASE1 (BAK1) (Lu *et al.*, 2010; Zhang *et al.*, 2010). BAK1 and other related proteins are known to associate with several different PRRs upon recognition of PAMPs, and this association results in a phosphorylation cascade activating downstream components of immune signaling pathways (Couto & Zipfel, 2016).

Several RLCKs, which lack an extracellular domain, have been found to be important for downstream signaling from RLKs. They are thought to mediate signal transduction from the RLKs at the membrane upon their ligand perception, or to function as intracellular receptors of

effectors (Zhang *et al.*, 2010). The 45-member RLCK subfamily VII consists of numerous candidates that serve roles in various important signaling pathways. For instance, CONSTITUTIVE DIFFERENTIAL GROWTH1 (CDG1) associates with BRASSINOSTEROID INSENSITIVE1 (BRI1) to regulate plant growth and brassinosteroid (BR) signaling, and the closely related LOST IN POLLEN TUBE GUIDANCE1 (LIP1) and LIP2 are involved in LURE1-induced pollen tube guidance (Kim *et al.*, 2011; Liu *et al.*, 2013). Another member of this subfamily is RPM1-INDUCED PROTEIN KINASE (RIPK), which functions downstream of FERONIA (FER) to regulate root growth (Du *et al.*, 2016). The RLCK VII members BOTRYTIS INDUCED KINASE1 (BIK1) and closely related PBS1-LIKE kinases, regulate PTI by directly associating with and phosphorylating FLS2, EFR, CERK1 and PEPR1 (Liu *et al.*, 2013; Lu *et al.*, 2010; Zhang *et al.*, 2010). BIK1 and PBLs contribute to defence against bacterial and fungal pathogens as well as aphid herbivory (Lei *et al.*, 2014; Lu *et al.*, 2010; Veronese *et al.*, 2006; Zhang *et al.*, 2010). To emphasize the importance of BIK1 and PBLs in PTI signaling, a number of pathogen effector proteins have been found to target them including the *Pseudomonas syringae* effector AvrPphB, *Xanthomonas campestris* effector AvrAC, and *Xanthomonas oryzae pv oryzae* effector XopR which modify these kinases to inhibit their function in immunity (Feng *et al.*, 2012; Guy *et al.*, 2013; Wang *et al.*, 2016; Zhang *et al.*, 2010).

Upon PAMP perception, a cascade of responses mediated by RLCKs occur that culminate in the plant immune response and resistance to the invading pathogen stressor. Early responses include an influx of calcium (Ca²⁺), a burst of apoplastic reactive oxygen species (ROS), activation of mitogen-activated protein kinases (MAPKs) and calcium-dependent protein kinases (CDPKs), activation of defence-related genes, callose deposition and stomatal closure to halt the invading pathogen (Blume *et al.*, 2000; Couto & Zipfel, 2016; Nühse *et al.*, 2000, 2007).

Importantly, BIK1 is directly involved in the production of ROS via its phosphorylation of the NADPH oxidase RBOHD which generates apoplastic ROS (Kadota *et al.*, 2014).

Phosphorylation of RBOHD by another RLCK VII subfamily member PBL13 inhibits its ROS production (Lin, *et al.*, 2015). Thus, regulation of BIK1 and other immune-related PBLs can provide important insights into the regulation of plant immune signaling.

1.3- Immune homeostasis and regulation of BIK1

BIK1 was first identified through increased transcript induction upon infection with the necrotrophic pathogen *Botrytis cinerea* (Veronese *et al.*, 2006). Lack of *BIK1* can leave the plant highly susceptible to necrotrophic pathogens such as *Botrytis cinerea* and *Alternaria brassicicola*, through increased accumulation of salicylic acid (SA) and attenuated jasmonic acid (JA)- and ethylene (ET)-regulated defence responses (Veronese *et al.*, 2006). *bik1* mutant plants show more root hair growth, possess a lodging phenotype with crinkled leaf margins, and flower earlier with fewer and shorter siliques, indicating that BIK1 is also essential for normal growth and development (Veronese *et al.*, 2006).

BIK1 is a dual-specificity kinase, reported to phosphorylate serines, threonines as well as tyrosines (Lin *et al.*, 2014; Xu *et al.*, 2013). BIK1 is an RD-kinase, meaning that phosphorylation of the activation loop is often required for its activation (Nolen *et al.*, 2004). BIK1 and related PBLs are plasma-membrane localized due to an N-terminal N-myristoylation motif, and are convergent substrates of several PRRs including FLS2, EFR, PEPR1, CERK1 and BAK1 (Veronese *et al.*, 2006; Zhang *et al.*, 2010). BIK1 is phosphorylated at Thr²³⁷ in an FLS2 and BAK1-dependent manner within a minute of PAMP perception (Lu *et al.*, 2010; Zhang *et al.*, 2010). Upon perception BIK1 phosphorylates FLS2 and its co-receptor BAK1 (Lin *et al.*, 2014; Liu *et al.*, 2013; Lu *et al.*, 2010; Zhang *et al.*, 2010). Following activation of its kinase activity

by hyperphosphorylation, BIK1 dissociates from the receptor complex, where it may go on to interact with downstream targets to potentiate immune signaling (Benschop *et al.*, 2007; Liu *et al.*, 2013; Lu *et al.*, 2010; Zhang *et al.*, 2010). One of these BIK1 substrates is the NADPH oxidase RBOHD, which associates with both BIK1 and FLS2 as well as EFR, and upon phosphorylation by BIK1 on Ser³⁹ and Ser³⁴³ in response to flg22, EF-Tu, chitin and the DAMP Pep1, dissociates from FLS2 or EFR and generates ROS, promotes stomatal closure, and is involved in the increase in cytosolic Ca²⁺ (Kadota *et al.*, 2014; Li *et al.*, 2014). In addition, both BIK1 and PBL1 are required for PAMP-induced Ca²⁺ elevation (Li *et al.*, 2014; Monaghan, *et al.*, 2015; Ranf *et al.*, 2014).

Interestingly, BIK1 is also required for seedling growth responses to ET and glucose, acting through ET signaling (Laluk *et al.*, 2011). ET signaling has increasingly been shown to be involved in PTI responses. For example, FLS2 transcription is positively regulated by ETHYLENE INSENSITIVE3 (EIN3) and ETHYLENE INSENSITIVE3-LIKE1 (EIL1), two closely-related transcription factors involved in the ET-signaling pathway (Boutrot *et al.*, 2010; Mersmann *et al.*, 2010). It has been determined that Pep peptides, PEPRs and BIK1 can act in the ET signaling pathway to mediate plant immune signaling through BIK1 interaction and phosphorylation by PEPR1 (Liu *et al.*, 2013). In addition to its role in microbial immune signaling, the tomato homolog of BIK1, TOMATO PROTEIN KINASE1b (TPK1b) plays an important role in plant resistance to insect herbivory (Abuqamar *et al.*, 2008). BIK1 was found to act as a negative regulator of plant defence response against aphids, possibly through increased ROS and cell death in the *bik1* mutant leaves that had been gnawed by aphids, and although the mutant also shows increased ET and SA accumulation, aphid defence responses have shown to be independent of these factors (Lei *et al.*, 2014). The resistance of the *bik1* mutant was

determined to be through the relief of repression on the lipase-like protein PHYTOALEXIN DEFICIENT4 (PAD4) (Lei *et al.*, 2014). BIK1 also has been shown to be required for signaling to the actin cytoskeleton to increase actin filament abundance during immune responses (Henty-Ridilla *et al.*, 2013). In contrast to its positive regulation of PTI and ethylene signaling, BIK1 negatively regulates BR signaling through association with BRI1, through which it is phosphorylated for BR signal transduction (Lin *et al.*, 2013).

Although imperative for plant defence against pathogen stressors, heightened immune responses can have extensive fitness costs for the plant. A major indicator of the growth-defence trade-off is the 80% reduction in plant growth seen in plants grown continually in the presence of PAMPs (Gómez-Gómez *et al.*, 1999; Zipfel *et al.*, 2006). Growth suppression is also often seen in plants with genetically elevated immune signaling, where mutants show a dwarf phenotype (Clarke *et al.*, 2000; Huot *et al.*, 2014; Zhang *et al.*, 2003). As BIK1 functions at an early step downstream of several PRRs, plays a role in both immunity and development, and is involved in the generation of ROS through RBOHD (Kadota *et al.*, 2014; Li *et al.*, 2014), it is an important candidate for regulating the strength of the plant immune response. There are several modes through which protein accumulation can be regulated. Many plasma membrane-associated proteins undergo clathrin-mediated endocytosis to target them to the vacuole for degradation, can be subject to bulk degradation for nutrient remobilization via selective autophagy, or are ubiquitinated and recycled by the 26S proteasome (Liu *et al.*, 2018). Indeed, BIK1 kinase activity is regulated by phosphorylation/dephosphorylation, and the protein is maintained at optimal levels via ubiquitin-mediated proteasomal degradation.

1.3.1- BIK1 activity is negatively regulated by a protein phosphatase

Proteins can be activated or inhibited through either phosphorylation by a protein kinase, or dephosphorylation by a protein phosphatase (Macho & Zipfel, 2014). Protein kinases and protein phosphatases have been implicated in several immune responses. The protein phosphatase ARABIDOPSIS PP2C-TYPE PHOSPHATASE1 (AP2C1) has been found to negatively regulate basal responses to *Pseudomonas syringae* by deactivating MAPKs, and PROTEIN PHOSPHATASE 2C (PP2C)26 and PP2C62 have been implicated in both photosynthesis and suppression of the plant immune system (Akimoto-Tomiya *et al.*, 2018; Shubchynskyy *et al.*, 2017). The protein phosphatase PP2C38 negatively regulates BIK1 activity and immunity conferred by BIK1 through association with BIK1 as well as the PRRs FLS2 and EFR, but not their co-receptor BAK1 (Couto *et al.*, 2016). PP2C38 dephosphorylates BIK1 in absence of pathogen to prevent its activation. This negative regulation is relieved upon PAMP activation, where PP2C38 is phosphorylated on S77, leading to its release from the PRR complex. It is presumed that BIK1 hyperphosphorylation upon PAMP treatment is responsible for the phosphorylation and release of PP2C38, relieving its repression such that it can activate downstream signaling (Couto *et al.*, 2016). In this way, BIK1 is kept at a lower activity level in absence of pathogen threat, and its repression is relieved upon PAMP treatment to allow the plant to mount sufficient defence responses to quell the invading pathogen threat.

1.3.2- BIK1 levels are positively regulated by heterotrimeric G proteins

Heterotrimeric G proteins are important in animal signaling pathways. They also have many regulatory and stress response roles in plants including in cell division (Bommert *et al.*, 2013; Chen *et al.*, 2003, 2006; Ding *et al.*, 2007; Ma *et al.*, 2015; Pandey *et al.*, 2006; Sun *et al.*, 2014; Ullah *et al.*, 2001, 2003; Wang *et al.*, 2001; Warpeha *et al.*, 2006). Many studies have also

indicated a role for heterotrimeric G proteins in plant immunity (Cheng *et al.*, 2015; Escudero *et al.*, 2017; Ishikawa, 2009; Llorente *et al.*, 2005; Trusov *et al.*, 2006; Zhu *et al.*, 2009). In *Arabidopsis*, the heterotrimeric G proteins EXTRA-LARGE GUANINE NUCLEOTIDE-BINDING PROTEIN2 (XLG2), ARABIDOPSIS G-PROTEIN BETA SUBUNIT1 (AGB1) and ARABIDOPSIS G-PROTEIN GAMMA SUBUNIT1 and 2 (AGG1/2) have been shown to regulate immune signaling pathways downstream of PRRs (Ishikawa, 2009; Liu *et al.*, 2013; Lorek *et al.*, 2013; Maruta *et al.*, 2015; Torres *et al.*, 2013; Zhu *et al.*, 2009). The heterotrimeric G protein triplet composed of the non-canonical G α protein XLG2, the G β protein AGB1 and the G γ proteins AGG1 and AGG2 have been shown to act in flg22-triggered immunity by interacting with the FLS2-BIK1 immune signaling complex (Liang *et al.*, 2016). In absence of PAMP, these G proteins act to stabilize BIK1 levels, blocking it from proteasome-mediated degradation to prime the plant cell for optimum immune induction. Interestingly, perception of flg22 triggers BIK1/PBL-mediated phosphorylation on REGULATOR OF G-PROTEIN SIGNALING (RGS1), promoting its dissociation from XLG2 and FLS2 for FLS2-mediated immune signaling, indicating the importance of phosphorylation and feedback loops for de-repression of G proteins and activation of immune responses (Liang *et al.*, 2018).

1.3.3- BIK1 is negatively regulated by a calcium-dependent protein kinase

Calcium-dependent protein kinases are activated in response to PAMP perception by PRRs at the plasma membrane (Couto & Zipfel, 2016; Macho & Zipfel, 2014; Saijo *et al.*, 2018). Monaghan and colleagues (2014) discovered a role for the calcium-dependent protein kinase (CPK) CPK28 in negatively regulating PAMP-triggered immune responses in *Arabidopsis*. A member of the CDPK subgroup IV, CPK28 was previously known for its role in the vegetative stage transition (Boudsocq & Sheen, 2013; Hamel *et al.*, 2014; Matschi *et al.*, 2013). CPK28 was also found to

interact with and phosphorylate BIK1 (Monaghan *et al.*, 2014). Mutant *cpk28-1* lines display higher ROS burst in response to flg22, elf18, AtPep1 and chitin, as well as enhanced sensitivity to elf18 and AtPep1 in seedling growth inhibition assays, whereas CPK28 overexpression lines display severely reduced ROS burst higher bacterial growth and impaired flg22-induced stomatal closure (Monaghan *et al.*, 2014). CPK28 contributes to BIK1 turnover via the 26S proteasome following polyubiquitination, revealing a regulatory mechanism to ensure optimal levels of immune signaling (Monaghan *et al.*, 2014). CPK28 also contributes to the PAMP-induced Ca²⁺ burst, supporting its role as a negative regulator of BIK1 (Monaghan *et al.*, 2015). Proteasome-mediated turnover of BIK1 indicated the action of an E3 ligase to polyubiquitinate BIK1 targeting it for degradation by the 26S proteasome (Monaghan *et al.*, 2014; Liang *et al.*, 2016).

1.4- E3 ligases and ubiquitination

In response to various environmental stressors and developmental cues, plants employ mechanisms that involve protein post-translational modifications (PTMs) to modulate and transduce signals for induction of appropriate responses. These PTMs, including protein acetylation, methylation, phosphorylation and ubiquitination all play important roles in various plant developmental stages and interactions with their environment, and there is often sophisticated crosstalk between them (Friso & van Wijk, 2015; Hashiguchi & Komatsu, 2016; Withers & Dong, 2017).

The ubiquitin-proteasome system is an important process that functions in ubiquitination and degradation of a target protein and may be employed to degrade a protein when its function is no longer required, or to maintain optimal levels (Adams & Spoel, 2018). The ubiquitination process begins with a ubiquitin-activating enzyme (E1), which activates the ubiquitin moiety in an ATP-dependent manner through a thioester bond between the C-terminus of ubiquitin and a

cysteine residue of E1. The thioester-linked ubiquitin is then transferred onto a cysteine residue of the ubiquitin-conjugating enzyme (E2) (Haas *et al.*, 1982). Next the ubiquitin is transferred from the E2 to a lysine residue on the target protein via a ubiquitin ligase (E3). This transfer may be direct as in the case of HOMOLOGOUS TO THE E6AP CARBOXYL TERMINUS (HECT)-type E3s, or indirect as is the case for REALLY INTERESTING NEW GENE (RING), U-box and CULLIN-based E3s (Shu & Yang, 2017). Although ubiquitination typically occurs on lysine residues, cysteine, serine, threonine and N-terminal methionines may also be modified by ubiquitin (Chen *et al.*, 2016; Ishikura *et al.*, 2010; Shimizu *et al.*, 2010). With lysine residues, ubiquitination forms a covalent isopeptide bond, while Ser/Thr, Cys or N-terminal Met ubiquitination forms oxyester or thioester linkages, respectively (Chen *et al.*, 2016). While mono-ubiquitination can regulate DNA repair, histone function, gene expression and receptor endocytosis, a polyubiquitin chain of four or more is targeted for degradation by the 26S proteasome, a large complex composed of a 20S proteolytic core with 2 cap-like 19S regulatory flanking particles (Callis, 2014; Vierstra, 2009). After the 19S regulatory particle recognizes the polyubiquitination, the protein is guided into the central core where it is unfolded and subjected to protease activity to be degraded into small peptides and ubiquitin moieties, which are recycled for future use (Kurepa & Smalle, 2008; Smalle & Vierstra, 2004).

Ubiquitin is a highly conserved protein consisting of 76 amino acids, and has been dubbed a ‘ubiquitous polypeptide’ as it exists in most organisms including animals, plants, bacteria and yeast (Schlesinger, 1975). Ubiquitins contain 7 lysine residues at positions 6, 11, 27, 29, 33, 48, and 63, as well as an N-terminal methionine, through which they can attach to each other to form polyubiquitin chains for degradation (Sadowski *et al.*, 2012; Trujillo, 2018). Each of these distinct individual ubiquitin linkage types have been identified in plants, with the

exception of Met1 and Lys27 (Maor *et al.*, 2007). RING E3 ligases can autoubiquitinate on Lys 6, 27 and 48 (Sadowski *et al.*, 2012). Typically Lys48-linked polyubiquitin chains target proteins for proteasomal degradation while Lys63-linked polyubiquitin chains on protein that are endocytosed targets the substrate for transport to the vacuole via endosomal sorting complexes (Isono *et al.*, 2010; Vierstra, 2009). Importantly, ubiquitin homeostasis can be tightly regulated by de-ubiquitinating enzymes (DUBs) (Kimura & Tanaka, 2010).

The greatest specificity in the ubiquitin-proteasome pathway exists in the range of E3 ligases. While *Arabidopsis* possesses only two E1s and 37 E2s, there are over 1400 predicted E3 ligases encoded in its genome (Hatfield *et al.*, 1997; Vierstra, 2012; Vierstra, 2009). E3 ubiquitin ligases can be grouped based on whether they are single- or multi-subunit. The single-subunit group includes subfamilies based on mechanisms of action and domain presence. This includes HECT, RING and U-box type E3s. The multi-subunit group, also known as Cullin-RING box1-Ligases (CRLs) consists of four subfamilies: S phase kinase-associated protein 1-Cullin 1-F-box(SCF), Bric-a-brac-Tramtrack-Broadcomplex (BTB), DNA Damage-Binding domain-containing (DDB) and anaphase-promoting complex (APC) (Vierstra, 2009).

Plant U-box (PUB) proteins possess a conserved U-box motif of approximately 70 amino acids that is a modified RING-finger domain that lacks the scaffold and zinc-chelating cysteine and histidine residues of the typical RING domain (Shu & Yang, 2017). There are 64 predicted PUBs in *Arabidopsis*, 77 in rice, and 125 reported in soybean, while the human genome encodes only 8 U-box E3s (Azevedo *et al.*, 2001; Wang *et al.*, 2016; Wiborg *et al.*, 2008; Zeng *et al.*, 2008). PUBs can have a variety of additional domains including armadillo (ARM) repeats, a Ser/Thr protein kinase domain, WD40 repeats, a tetratricopeptide (TPR) domain, or peptidyl-prolyl isomerase domain (Azevedo *et al.*, 2001; Trujillo, 2018; Yee & Goring, 2009). The largest

class of PUBs in *Arabidopsis* is the ARM domain-containing PUB proteins, which contain tandem ARM motif repeats located in the C-terminus (Mudgil *et al.*, 2004; Samuel *et al.*, 2006).

PUBs are involved in many plant responses to environment and stressors, including cell proliferation during development, adaptation to drought, and immune responses during pathogen infection (Trujillo, 2018). The first PUB protein studied was the *Brassica napus* Arm Repeat-Containing 1 (ARC1), a member of the PUB-ARM family, which was determined to be a positive regulator of *Brassica* self-incompatibility (Stone *et al.*, 1999; Stone *et al.*, 2003). ARC1 is proposed to impede self-pollination by regulating degradation of an exocyst component Exo70A1, which mediates early tethering of vesicles during exocytosis resulting in down-regulation of the secretory pathway and delivery of required pollen germination factors (Indriolo *et al.*, 2014; Safavian *et al.*, 2015; Samuel *et al.*, 2009). PUBs have also been implicated in various abiotic stress responses. Ubiquitination and proteolytic systems are involved in abscisic acid (ABA) signaling, responsible for plant responses to drought and osmotic stress, with PUB12 and PUB13 acting as E3 ligases in the degradation of ABA INSENSITIVE1 (ABI1) in response to ABA (Kong *et al.*, 2015; Yu *et al.*, 2016).

Many PUBs have been implicated in plant responses to biotic stress. *Nicotiana tabacum* PUB genes, Avr9/Cf-9 RAPIDLY ELICITED74 and 276 (*NtACRE74* and *NtACRE276*) were two PUB genes found to be upregulated in response to treatment with the fungal pathogen *Clostridium fulvum* Avr9 peptide (Durrant *et al.*, 2000). Parsley *PcCMPG1* (so named after its first 4 amino acids, Cys, Met, Pro, Gly), and the *Arabidopsis* ortholog *AtCMPG1/AtPUB20* were also shown to be up-regulated in early defence responses against pathogen elicitors (Heise *et al.*, 2002; Kirsch *et al.*, 2001). *Arabidopsis AtPUB20, AtPUB21, AtPUB17, AtPUB12* and *AtPUB5* were identified as upregulated genes upon flagellin elicitor treatment (Navarro *et al.*, 2004).

Subsequently, both PcCMPG1 and NtACRE276/AtPUB17 were confirmed as E3 ligases responsible for positive regulation of HR in defence against pathogen stress, where *pub17* mutants showed decreased resistance to the *Pseudomonas Pto* gene (Gonzalez-Lamothe *et al.*, 2006; Yang *et al.*, 2006). In addition, PUBs have also been implicated in suppressing signaling from plasma membrane localized receptors (Trujillo, 2018). In *Arabidopsis*, PUB12 and PUB13 have been shown to contribute to FLS2 ubiquitination and turnover dependent on the presence of the FLS2 co-receptor BAK1 (Lu *et al.*, 2011; Zhou *et al.*, 2015). Activated FLS2 is internalized and transported to the vacuole for its degradation via the endocytic pathway (Beck *et al.*, 2012; Mbengue *et al.*, 2016; Spallek *et al.*, 2013). PUB13 has also has been shown to interact with and contribute to ubiquitination of the chitin receptor LYK5 *in vitro* (Liao *et al.*, 2017). While PUB-ARM E3 ligases AtPUB22 and AtPUB23 were initially identified as negative regulators of drought tolerance (Cho *et al.*, 2008), Trujillo *et al.* (2008) later identified the same genes as negative regulators of plant defence responses, with *pub22 pub23 pub24* knockouts showing additive effects in the generation of the oxidative ROS burst as well as resistance to bacterial and oomycete pathogens. PUB22 has also been shown as a mediator of the degradation of the exocyst subunit Exo70B2 upon FLS2 activation (Stegmann *et al.*, 2012). These examples implicate PUBs as key negative regulators of immune responses, maintaining an optimal balance in the plant between defence responses and growth/development.

1.5- Research objectives

Since BIK1 is a key regulator downstream of multiple PRRs, and plays additional roles in ethylene and BR signaling, it appears to be an important point for regulating plant immune homeostasis. Proteasome-mediated turnover of BIK1 was shown by Monaghan *et al.* (2014), implicating the involvement of an E3 ligase in its ubiquitination and turnover. Our collaborators

from the Zhou lab in Beijing performed an *in vivo* pull-down assay with PBL1, a closely related homolog of BIK1, to identify interacting partners in *Arabidopsis*. This screen uncovered PUB25 and PUB26 as PUB-ARM U-box E3 ligases putatively associating with PBL1. Because PBL1 and BIK1 are functionally redundant (Zhang *et al.*, 2010), they also tested whether PUB25 and PUB26 could associate with BIK1. Key findings from these experiments include: (1) PUB25 and PUB26 interact with and promote degradation of non-phosphorylated BIK1, and (2) PUB25 and PUB26 negatively regulate plant immunity by controlling BIK1 levels (Wang *et al.*, 2018). As CPK28 associates with BIK1 and its over-expression leads to lower BIK1 accumulation (Monaghan *et al.*, 2014), it would be interesting to determine the mechanism of PUB25, PUB26 and CPK28-mediated turnover of BIK1. Thus, the main goals of my thesis have been to (1) determine which residues on BIK1 are ubiquitinated by PUB25 and PUB26 *in vivo*, and (2) determine how CPK28 contributes to this regulation. These goals have been addressed using three objectives: (1) determine if PUB25 and PUB26 associate with CPK28, (2) assess the biological function of PUB25 and PUB26 and their genetic interactions with CPK28, and (3) identify and functionally analyze ubiquitination sites on BIK1 and determine which of these sites are regulated by PUB25 and PUB26. Knowledge gained from this research will add to the understanding of plant immune signaling and homeostasis and could lead to the engineering of crops that are more tolerant of pathogen stress.

2. MATERIALS AND METHODS

2.1- Plant growth conditions

Unless otherwise described, *Arabidopsis thaliana* seeds to be used for soil assays were stratified in 0.1% agar at 4°C for 48-72 h prior to sowing in 10 cm round pots. Seedlings were grown under climate-controlled short-day conditions (22 °C with 10 h light period, 30% humidity and 150 $\mu\text{E m}^2\text{s}^{-1}$) for approximately 7 d, followed by individual transplantation to either 10 cm square pots or 72-well flats, depending on the assay. Growth was continued under short-day conditions for 4-5 weeks.

For plants grown in sterile conditions, seeds were first rinsed with 70% ethanol for 30 s, incubated in 40% bleach for 17 min with gentle shaking, and then rinsed 5 times with sterile water. In between each incubation or wash, seeds were briefly vortexed and centrifuged at 5,000 x g for 1 min. The seeds were resuspended in a final volume of sterile water or 0.1% agar and plated on MS agar plates (0.5X Murashige and Skoog Media + vitamins, 0.8% agar) containing the appropriate antibiotic selection (Appendix Table S1). The seeds were stratified at 4 °C for 48-72 h, and then germinated under 12 h photoperiod for 7-14 d prior to transplanting to 6-well liquid MS plates or to soil. For seed collection, plants were moved to a long-day growth chamber (16 h light period) after 35 d to enhance the transition to vegetative stage. The plants were fertilized with 1.5 g/L 20:20:20 N:P:K bi-weekly, and grown in the Queen's University Phytotron facility maintained by Jeffrey Rowbottom and Dale Kristensen.

Nicotiana benthamiana seeds were similarly stratified and grown in 15 cm pots under long-day conditions prior to use at 4-6 weeks of age. Plants were fertilized as above but supplemented with 0.3 g/L iron. Plants were grown on a shelf in the Monaghan Lab under

ambient temperature (22-28°C), with light levels of approximately 140 $\mu\text{E m}^2\text{s}^{-1}$, and were maintained by Danalyn Holmes, Jennifer Wesley, Olivia Siemons, and Jeffrey Rowbottom.

2.2- Generation of plant materials

Experiments performed in *Arabidopsis thaliana* were done using the Columbia ecotype (Col-0, wild-type). Genotypes used in this thesis are listed in Appendix Table S1. Lines that we generated were made either by crossing, or by *Agrobacterium tumefaciens*-mediated transformation by floral dip (Clough & Bent, 1998).

2.2.1- Genetic crosses

Crosses were performed by emasculating the flowers of one genotype at a stage where there are 5-6 inflorescences, to expose the style, followed by hand-pollination with the other genotype. To generate the *cpk28-1/35S:PUB25-OE* and *cpk28-1/PUB26-OE* lines, we crossed a homozygous *cpk28-1* plant with either a homozygous Col-0/35S:PUB25-FLAG or Col-0/35S:PUB26-FLAG transgenic line. The *pub25-1 pub26-1/CPK28-OE1* line was generated by crossing a homozygous *pub25-1 pub26-1* plant with a homozygous C-terminal yellow-fluorescent protein (YFP)-tagged Col-0/35S:CPK28-YFP transgenic line. Finally, to generate the quintuple *pub22 pub23 pub24 pub25 pub26* plant, we crossed a homozygous *pub22 pub23 pub24* plant with a homozygous *pub25-1 pub26-1* plant. Higher-order mutants were genotyped in the F2 and/or F3 generation using a combination of antibiotic selection and polymerase chain reaction (PCR)-based genotyping.

2.2.2- *Agrobacterium*-mediated transformation by floral dip

C-terminal hemmagglutinin (HA)-tagged pGWB14-cBIK1^{mut}-HA constructs (Appendix Table S2) for use in *Agrobacterium*-mediated transformation by floral dip were transformed into *Agrobacterium tumefaciens* GV3101 by electroporation, and single transfected colonies were

confirmed by colony PCR using primers outlined in Appendix Table S4. Starter 5 mL cultures were grown in Luria Broth (LB; BioShop) overnight with 200 rpm shaking at 28 °C with appropriate antibiotics (with 50 µM/mL kanamycin). This was used to inoculate a larger 200 mL LB culture containing appropriate antibiotics, which was grown to mid-log phase. This larger culture was centrifuged at 2,831 x g for 20 min using a JA-10 rotor (Beckman Coulter), in an Avanti® J-E centrifuge prior to pellet resuspension in 50 mL of 5% sucrose. Cultures were then diluted to an optical density (OD)₆₀₀ of approximately 0.8 for dips. *Arabidopsis* plants were grown in long-day conditions for 4-6 weeks until flowering, at which point bolts were clipped to encourage secondary inflorescence growth (Bent, 2006). Prior to floral inoculation, Silgard Xiameter OFX-8803 was added to a final concentration of 0.05%. Plants were inverted, and flowers were submerged into the *Agrobacterium* suspension and agitated for 10-20 s. Plants were placed on their side on top of paper towel in a covered tray overnight in the dark. After 12-24 h, the plants were returned upright and grown for another 3-4 weeks prior to seed harvesting.

Selection of T1s was done by sterilizing and selecting the seeds on 0.5X MS plates with appropriate antibiotics (as indicated in Appendix Table S1) for 10-14 d prior to transplantation to soil for recovery. Transgenic lines were confirmed using a combination of allele-specific PCR genotyping and western blots.

2.2.3- Allele-specific genotyping

Leaf material was pressed into a Whatman FTA card (GE Healthcare) for 2-5 s and left to sit for at least 1 h prior to use. A 1.20 mm biopsy punch (Harris UniCore) was used to excise FTA card punches, which were then incubated in 50 µL 1X FTA (10 mM Tris-HCl, pH 8.0, 2 mM EDTA, pH 8.0, 0.1% Tween-20) for 5 min at room temperature in a skirted 96-well plate (Diamed). The 1X FTA was removed and replaced with 200 µL TE-1 (10 mM Tris-HCl, pH 8.0, 2 mM EDTA,

pH 8.0) for 2 washes, incubated for 5 min each. The final wash of TE-1 was removed and replaced with a PCR MasterMix. PCR amplification was done using 0.2 μ L GeneDirex Taq polymerase (FroggaBio), 10 mM dNTPs, 2.5 μ L PCR Buffer (1 M KCl, 1 M MgCl₂, 1 M Tris-HCl pH 8.0), and 0.5 μ L of each primer. 20 μ L of PCR product was run on a 1% agarose gel to visualize amplicons. Typical thermal cycling parameters were: 94°C initial denaturation for 5 min, followed by 35 cycles of 94°C denaturation for 30 s, 53°C annealing for 45 s, 72°C extension for 2 min, with a final 72°C for 10 min. All primers used for PCR genotyping are listed (Appendix Table S5). For T-DNA alleles obtained from stock centres, plants were genotyped by confirming presence or absence of an amplicon for gene-specific and T-DNA insertion reactions for each individual plant.

2.3- Molecular cloning

2.3.1- Gateway cloning

Gateway technology (Invitrogen) was used to create both the cauliflower mosaic virus (CaMV) 35S promoter-driven and C-terminally tagged with 3x hemagglutinin (HA) 35S:BIK1^{mut}-HA constructs in the pGWB14 vector (Karimi *et al.*, 2002). The pENTR-cBIK1 wild-type entry clone, containing only the open reading frame but no stop codon, was previously described (Liu *et al.*, 2013) and was used for site-directed mutagenesis (section 2.3.2) to create the BIK1 lysine to arginine (K→R) point mutations (BIK1^{mut}). The pENTR-PUB25 and pENTR-PUB26 constructs, containing only open-reading frames and no stop codons, were made using Gibson assembly (Gibson *et al.*, 2009) (section 2.3.3). An LR reaction was performed to shuttle the cBIK1^{mut} inserts into the destination vector pGWB14. The LR reactions were performed using a quarter of the recommended reaction volume with 75 ng of entry vector and 75 ng of destination vector in Tris-EDTA (TE) buffer (pH 8.0) up to 4 μ L total, and 1 μ L Gateway LR clonase II

Enzyme Mix (Invitrogen) incubated at 25°C overnight. The clonase was then deactivated by addition of 0.5 µL Proteinase K (2 µg/µL) at 37°C for 10 min. The entire reaction was then used to transform Top10 *Escherichia coli* cells using the heat-shock method. Colonies were confirmed using colony PCR and Sanger sequencing (TCAG, Toronto, Canada). All primers are listed in Appendix Table S4.

2.3.2- Site-directed mutagenesis

Overlapping, reverse-complemented primers were designed for site-directed mutagenesis of a lysine residue (AAA, AAG) to an arginine (AGA, AGG) using primers described in Appendix Table S3. PCR was performed with Phusion Taq (Invitrogen) as per manufacturer's instructions, with the pENTR-cBIK1 vector as template. Successful amplification was confirmed on a 1% agarose gel prior to carrying forward with column purification using a GenepHlow™ Gel/PCR Kit (GeneAid), following manufacturer's instructions. The remaining *E. coli*-replicated template was digested away with *DpnI* restriction enzyme (New England Biolabs: NEB) for 3 h at 37°C, followed by 20 min inactivation at 65°C. The entire product was then transformed into Top10 *E. coli* cells via heat-shock and plated on LB agar plates supplemented with kanamycin (50 µg/mL). Constructs that proved difficult to create in this way (pENTR-cBIK1^{K41R} and pENTR-cBIK1^{K358R}) were subjected to mutagenesis with the NEB site-directed mutagenesis kit using manufacturer's instructions, using non-overlapping primers generated from the NEB database, outlined in Appendix Table S3. In all cases, single colonies were grown in 5 mL overnight cultures, plasmids were purified with Presto™ Mini Plasmid Kit (GeneAid), and mutagenesis was confirmed by Sanger Sequencing (TCAG) using primers outlined in Appendix Table S4. Site-directed mutant constructs were constructed as a joint effort between myself, Danielle Ciren and Heather Galley (Appendix Table S2).

2.3.3- Gibson assembly

Gibson assembly from Gibson *et al.*, (2009) was used for cloning of all constructs into the Gateway-compatible pENTR entry vector or the *E. coli* expression vectors pGEX6p.1 (GE Healthcare) and pET44a(+) (Novagen). Desired backbone and insert fragments were amplified by PCR with Phusion Taq (Invitrogen) using compatible primers as outlined in Appendix Table S3. Any *E. coli*-derived template was digested away by incubation with *DpnI* restriction enzyme (NEB) for 3 h at 37°C followed by column purification with a GenopHlow™ Gel/PCR Kit (GeneAid), and DNA was quantified using a NanoDrop One™ spectrophotometer (Thermo Scientific). The reaction was set up using 0.02 pmol backbone DNA and 0.06 pmol insert DNA and 1X Gibson Assembly Master Mix (NEB) in 10 µL total volume and incubated at 50°C for 30 min, followed by addition of 5 µL of pure water. Top10 *E. coli* cells were then used for transformation by heat shock. Correct assembly was confirmed using colony PCR and purified plasmids were confirmed by Sanger sequencing (TCAG) using primers outlined in Appendix Table S4.

2.4- RNA extraction, reverse transcription and qPCR

Approximately 6 leaves per genotype were ground in liquid nitrogen, followed by RNA extraction using the Aurum™ Total RNA Minikit (BioRad) according the manufacturer's instructions. The extracted RNA was run on a freshly-prepared 1% agarose gel for quality control, and concentration was determined by NanoDrop One™ Spectrophotometer (Thermo Scientific). Reverse transcription was performed using 2 µg total RNA, 50 µM oligo(dT)20, 500 µM dNTPs, 1 x First-Strand™ Buffer (Invitrogen), 40 U RNaseOUT™ Recombinant RNase Inhibitor (Invitrogen), and 200 U SuperScript™ III Reverse Transcriptase (Invitrogen). This was

incubated at 50°C for 1 h, followed by 70°C inactivation for 15 min, and dilution with 100 µL sterile pure water.

Quantitative PCR (qPCR) was carried out using Sso Advanced™ Universal SYBR® Green Super (BioRad) in a skirted 96-well plate (BioRad). All reactions were performed in triplicate, and gene expression was analyzed using a BioRad CFX96 Touch™ Real-time PCR Detection System to measure fluorescence. Melt curves were tested for each primer to ensure only one amplicon, and values were normalized to the housekeeping gene UBOX. Primers used are listed in Appendix Table S5.

2.5- Immune-induced oxidative burst assays

Between 6-12 leaf discs were taken for each genotype using a 4 mm biopsy punch (Miltex) from 4-5-week-old *Arabidopsis* plants, added to 100 µL water in an opaque white 96-well plate (Evergreen Scientific), and incubated in the dark at room temperature overnight for recovery. On the day of the assay, the water was removed with a multi-channel pipette and replaced with a solution of 100 µM luminol (Sigma-Aldrich), 10 µg/mL horseradish peroxidase (HRP; Sigma-Aldrich), and 100 nM PAMP (flg22, and elf18, and 500 nM AtPep1; EZ Biolabs). PAMP-induced production of reactive oxygen species (ROS) was immediately measured as relative light units using the LUM module on a Spectramax spectrophotometer (Paradigm) over 40 min, with measurements every 2 min, with an integration time of 1 s.

2.6- Transient protein expression in *N. benthamiana*

A. tumefaciens strains containing plant expression vectors (Appendix Table S2) were freshly streaked from cryogenic stocks on LB agar plates containing appropriate antibiotics 2-3 d prior to infiltration. As all constructs were driven by CaMV 35S, *A. tumefaciens* containing the viral suppressor P19 (Lakatos *et al.*, 2004) was co-infiltrated to reduce anti-viral silencing in *N.*

benthamiana. The day before infiltration, overnight LB cultures containing appropriate antibiotics were made and incubated at 28°C with 200 rpm shaking. On the day of infiltration, 4-5 week old *N. benthamiana* plants were watered to improve efficiency of stomatal infiltration, and bacterial cultures were centrifuged at 1,592 x g for 15 min. The pellet was resuspended in induction buffer (10 mM MgCl₂, 10 mM MES, pH 6.3), and allowed to rock at room temperature for 2-3 h. Each culture was diluted to OD₆₀₀ of 0.2 and mixed according to the experiment to be performed. Leaves were infiltrated using a needleless syringe and tissue was collected 3 d post-infiltration (dpi).

2.7- Split-luciferase complementation assays

Split-luciferase complementation assays were done as previously described (Liang *et al.*, 2016). Leaf discs were obtained 3 dpi from *N. benthamiana*, transiently expressing protein from N-Luc and C-Luc tagged vectors kindly provided by Jian-Min Zhou (Liang *et al.*, 2016) (Appendix Table S6) with a 4 mm biopsy punch. All constructs, including controls, were infiltrated on the same leaf for direct comparison. For each reaction and control, 3-6 leaf discs were collected into individual wells of an opaque white 96-well plate containing 100 µL of water. Luciferin (Gold Biotech) was added to the wells for a final concentration of 1 mM. The 96-well plate was left in dark for 10-15 min, followed by measurements of all wavelengths of light by the LUM module in the spectrophotometer for an integration time of 1 s.

2.8- Co-immunoprecipitation assays

Entire *N. benthamiana* leaves were infiltrated with *A. tumefaciens* containing desired constructs as outlined in Appendix Table S7 3 d after infiltration, whole leaves were treated with water or 100 nM flg22 using vacuum infiltration, incubated for 10 min, and then flash frozen in liquid nitrogen. Proteins were extracted in buffer containing 5 mM dithiothreitol (DTT), 1% (v/v)

protease inhibitor P9599 (Sigma Aldrich), 1% (v/v) Igepal, 2 mM Na₂MoO₄, 2.5 mM NaF, 1.5 mM activated sodium orthovanadate (Na₃VO₄), 50 mM Tris-HCl pH 7.5, 150 mM NaCl, 1 mM phenylmethylsulfonyl fluoride (PMSF) for 1 h at 4°C. Samples were then centrifuged at 15,800 x g for 30 min at 4°C, and filtered through Miracloth to clarify the extracts. Coomassie Protein Assay Kit (ThermoFisher Scientific) was used for protein sample quantification and normalization using bovine serum albumin (BSA) as protein standards. An input fraction was reserved for each sample, and the remaining protein extract was incubated with either μMacs α-green fluorescent protein (GFP) microbeads (Miltenyi Biotec) or GFP-Trap agarose beads (ChromoTek) as described below.

For immunoprecipitation (IP) assays using μMacs magnetic beads, protein extracts were incubated with 30 μL of beads for 2 h at 4°C with rocking. Columns were equilibrated with wash buffer (20 mM Tris-HCl pH 7.5, 150 mM NaCl, 1% (v/v) P9599 (Sigma-Aldrich), 1 mM DTT, 1% (v/v) Igepal), followed by application of protein samples. After flow-through, the columns were washed three times with wash buffer, followed by elution of bound protein with 30 μL of μMacs supplied elution buffer preheated to 80°C. Eluted proteins were separated by sodium dodecyl sulfate, polyacrylamide gel electrophoresis (SDS-PAGE) and analyzed by immunoblot.

For IPs using ChromoTek GFP-Trap beads, protein extracts were incubated with 20 μL slurry following washing of beads with wash buffer as described above for μMacs IPs. The incubation lasted 2 h at 4°C with rocking, followed by centrifugation at 100 x g for 30 s to collect beads. Beads were washed 3 times with the same wash buffer as above, with centrifugation and vacuum-assisted aspiration between each wash. For elution, 50 μL of 5X SDS Loading buffer was added to each sample, followed by denaturation at 80°C for 5 min. Samples

were then centrifuged at 15,871 x g for 30 s, proteins separated by SDS-PAGE, and immunoblotted.

2.9- Identification of ubiquitination sites on plasma-membrane proteins using liquid chromatography followed by tandem mass spectrometry (LC-MS/MS)

2.9.1- Preparation of microsomal fractions and trypsin digests

For each genotype, 20 mg of seeds were sterilized and stratified at 4°C for 48 h, and then added to flasks containing 50 mL 0.5X MS media with 0.05% sucrose. Seedlings were shaken at 100 rpm for 8 d, followed by treatment with 50 µM MG-132 for 1 h, and then vacuum infiltrated with water (mock) or 1 µM elf18, followed by shaking for 10 min. Samples were flash frozen and ground to a coarse powder in liquid nitrogen, then homogenized in urea lysis buffer (8 M urea, 50 mM Tris-HCl pH 8.0, 150 mM NaCl, 1 mM EDTA, 1 mM P9599 protease inhibitor (Sigma), 1 mM PMSF, 50 µM PR-619) using equal volume to tissue in a Potter tube for 10 min at 1,000 rpm. 1 mL was removed, centrifuged at 15,000 x g, and supernatant kept for analysis of MAPK activation as described in section 2.9.5. The remaining homogenate was transferred to Sorvall tubes, centrifuged in a Sorvall SS34 rotor at 5,856 x g for 1 h at 4°C. The supernatant was transferred to a polycarbonate tube, diluted to the top in lysis buffer, and centrifuged in a ThermoFisher Ultracentrifuge at 110,000 x g for 1 h at 4°C. The pellet was resuspended in 2 mL of lysis buffer with PMSF, and protein concentration was determined by Bradford Assay (BioRad) according to manufacturer's instructions. Samples with 3 mg protein in 2 mL lysis buffer, had tris(2carboxyethyl)phosphine (TCEP) added to a final concentration of 5 mM with rocking at room temperature for 45 min. 10 mM iodoacetamide (IAM) was then added and incubated 30 min at room temperature in the dark. Samples were diluted to 5 mL with 50 mM

Tris-HCl pH 8.0 and 30 μ g of trypsin (diluted in 50 mM ammonium bicarbonate (ABC) buffer, pH 9.0) was added, with incubation at 37°C overnight. General workflow is shown in Figure 2.1.

2.9.2- Column desalting

Following trypsin digestion, samples were acidified with 50% trifluoroacetic acid (TFA) to pH 3.0 and diluted to 10 mL in Tris-HCl pH 8.0. Centrifugation at 1,600 x g was done to remove precipitate, and supernatant was used for C18 Peptide Clean-up with 2.5 mL C18 silica Reversed-Phase Chromatography columns Sep-Pak (Waters). Columns were equilibrated with 1 column volume (CV) of MeOH, then 1 CV of Activation Buffer (80% acetonitrile (ACN), 0.1% TFA), then 5 CV of Wash Buffer (2% ACN, 0.1% TFA). Sample was added to the column and allowed to drip by gravity flow, collected and put through the column a second time. Columns were then washed with 5 CV Wash Buffer. Trypsin-digested peptides were eluted in 2 CV Elution Buffer (40% ACN, 0.1% TFA), and then placed in a freeze drier for 48 h.

2.9.3- Immunoprecipitation using α -K- ϵ -GG

The PTMScan® Ubiquitin Remnant Motif K- ϵ -GG antibody (Cell Signaling) was first crosslinked to the beads by washing each tube 3 times with 1 mL of 100 mM sodium borate pH 9.0, with centrifugation at 2,000 x g between each wash. The beads were then resuspended in fresh 20 mM dimethyl pimelimidate (DMP) in 100 mM sodium borate, with incubation for 1 h at room temperature with end-over-end rotation. Washing was done 2 times with 1 mL of 200 mM ethanolamine pH 8.0, and then beads were resuspended in 200 mM ethanolamine and incubated overnight at 4°C with end-over-end rotation prior to IP.

For the immunoaffinity purification (IP), crosslinked beads were first washed 3 times with 1.5 mL IAP buffer (50 mM MOPS pH 7.2, 10 mM sodium phosphate, 50 mM NaCl), with centrifugation at 2,000 x g for 1 min between each wash. Freeze-dried peptide samples were

resuspended in 1.5 mL IAP buffer, sonicated for 10 min, and centrifuged at 16,000 x g for 5 min. 1300 μ L of peptide sample was added to 300 μ L K- ϵ -GG beads in IAP buffer, saving the remaining 200 μ L as crude sample for liquid chromatography tandem mass spectrometry (LC-MS/MS). Samples were incubated with the beads for 2 h at 4°C with end-over-end rotation, followed by centrifugation for 1 min at 2,000 x g, with supernatant kept as unbound sample for LC-MS/MS as control for efficiency of di-Gly enrichment. Beads were washed 2 times with 1.5 mL IAP buffer, then 3 times with high performance liquid chromatography (HPLC) grade water prior to elution with 100 μ L of 0.15% TFA, centrifugation 1 min at 2,000 x g, saving supernatant as elution sample for LC-MS/MS.

2.9.4- Sample purification with C18 Micro-spin columns

Crude, unbound and elution samples were partially purified using C18 Micro-Spin Stagetips columns (The Nest Group Inc.). 50% TFA was added to bring pH to 3.0, and columns were placed in 2 mL microcentrifuge tubes and equilibrated by washing 3 times with 200 μ L MeOH and centrifuged at 135 x g for 30 s between each wash. Equilibration continued with 3 washes of 200 μ L Equilibration Buffer (80% ACN, 0.1% TFA) and centrifugation for 2 min at 185 x g, followed by 6 times with Wash Buffer (2% ACN, 0.1% TFA) with centrifugation for 2 min at 185 x g. Peptide solutions were loaded twice into the columns and centrifuged 4 min at 240 x g. Columns were then washed 6 times with Wash Buffer, centrifuged at 240 x g for 2 min, followed by elution twice with 150 μ L elution buffer each (40% ACN, 0.1% TFA) by centrifuging 3 min at 240 x g.

2.9.5- MAPK activation assays

To ensure efficiency of elf18 treatment, total protein lysate samples were subjected to a MAPK activation assay prior to mass spectrometry analysis. 20 μ g protein was loaded and separated by

SDS-PAGE, followed by immunoblotting with phosphor-p44/42 MAPK (Erk1/2) (Cell Signaling) antibody, which binds phosphorylated MPK3, MPK4/11, and MPK6 (Rubinfeld & Seger, 2005) .

2.9.6- LC-MS/MS determination of BIK1 ubiquitination sites

Following dehydration using vacuum centrifugation (SpeedVac), crude, unbound and elution samples were resuspended in 2% ACN and 0.1% TFA for submission to the mass spectrometer. They were vortexed, sonicated for 10 min, then centrifuged at 13,000 rpm for 10 min. 40 μ L supernatant was loaded into a 96-well plate for analysis on an Orbitrap Fusion Mass Spectrometer (ThermoFisher). Mascot program was used to extract mass spectrometer scores and transferred to Scaffold 4 for further analysis.

2.10- Expression and protein purification from *E. coli*

For use in *in vitro* assays to study ubiquitination of BIK1, we used N-terminally 6x Histidine-tagged wheat E1 (His-WE1), His-AtUBC8 and His-PUB25 and His-PUB26 in the vector pET28a received from the lab of Jian-Min Zhou, as well as N-terminally tagged glutathione S-transferase (GST) tagged BIK1 mutant variants (GST-BIK1^{mut}) cloned as described in section 2.3.3. These vectors were transformed into *E. coli* (BL21-CondonPlus(DE3)-RIL cells (Novagen; maintained in the Monaghan Lab). Transformed cells from single colonies were grown in a 5 mL overnight culture prior to culturing at 37°C in 200 mL LB broth containing 50 μ g/mL kanamycin to an OD₆₀₀ of 0.6-0.8, which corresponds to mid-log phase. Protein expression was induced by the addition of 0.5 mM isopropyl β -D-1-thiogalactopyranoside (IPTG; BioShop) overnight with shaking at 30°C. Cells were harvested by centrifugation at 2,831 x g for 15 min, and pellets were flash-frozen in liquid nitrogen, and stored at -80°C until further use.

For GST-tagged proteins, the pellet was resuspended in 30 mL GST extraction buffer (1 mM DTT, 1 mM PMSF, 6 mM MgCl₂, 1:50 DNase I), and His-tagged proteins in Ni Binding buffer (50 mM Tris-HCl pH 7.5, 300 mM NaCl, 20 mM Imidazole). Resuspended samples were lysed by passage through a French Pressure cell at 20,000 psi. The lysate was clarified by centrifugation at 23,708 x g for 30 min at 4°C, and supernatant was used as soluble lysate for purification. For GST purification, glutathione agarose (Sigma-Aldrich) was used to prepare columns with a column volume (CV) of 500 µL and equilibrated with phosphate buffered saline (PBS). Soluble lysate was incubated with glutathione agarose resin for 1 h at 4°C and then put through the column. Columns were then washed with 10 CV PBS, and recombinant protein was then eluted with 5 CV GST elution buffer (50 mM Tris-HCl pH 8.0, 5 mM DTT, 10 mM reduced glutathione (Sigma-Aldrich)) collected in 500 µL fractions.

For His-tagged protein purification, the columns were prepared using 1 mL His60-Ni Superflow Resin (Takara) for a total column of 500 µL and equilibrated with 10 CV Ni Binding Buffer. 20 mM Imidazole was added to the protein sample, and it was passed over the column via gravity flow following batch purification at 4°C for 1 h. Columns were washed with 10 CV Ni Wash Buffer (50 mM Tris-HCl pH 7.5, 300 mM NaCl, 40 mM Imidazole), and then eluted with 5 CV of Ni Elution Buffer (50 mM Tris-HCl pH 7.5, 300 mM NaCl, 300 mM Imidazole) in individual fractions. Protein elution samples were quantified by separation in SDS-PAGE, stained with Coomassie Brilliant Blue (CBB) and the use of ImageJ or BioRad ImageLab software.

2.12 *In vivo* transient ubiquitination assays in *N. benthamiana*

N. benthamiana was infiltrated as described in section 2.6 with the pGWB14-BIK1^{mut}-HA constructs and tissue was collected after 3 dpi. Total protein was extracted using native protein

extraction buffer (50 mM Tris-MES pH 8.0, 0.5 M sucrose, 10 mM EDTA, 5 mM DTT, 1 mM MgCl₂). co-IPs were performed with μ Macs magnetic beads as described in section 2.8, however when incubating with the magnetic beads, 50 μ M MG-132 was added. Proteins were eluted in 50 μ L from the column and were resolved on a 10% SDS-PAGE gel after boiling samples at 80°C for 10 min followed by quick centrifugation. Immunoblotting was performed with α -ubiquitin P41 (Cell Signaling) at an antibody titre of 1:2500.

2.11- Cell-free degradation assays

Total protein was extracted from Col-0 or PUB25-OE tissue using a native protein extraction buffer (50 mM Tris-MES pH 8.0, 0.5 M sucrose, 10 mM EDTA, 5 mM DTT, 1 mM MgCl₂) (Wang *et al.*, 2018b) as previously described in section 2.8. 200 ng of purified GST- or His-BIK1 was incubated with 200 μ L total protein extracts (1 mg/mL) for the specified time at 28°C. Reactions were stopped by the addition of 5X 10 μ L SDS-PAGE loading buffer to the 20 μ L of sample and boiled at 80°C for 10 min. Samples were then centrifuged briefly, separated by SDS-PAGE, and subject to immunoblotting with an α -GST antibody at a titre of 1:5,000.

2.12- *In vitro* ubiquitination assays

In vitro ubiquitination assays were performed as previously described (Wang *et al.*, 2018). In short, 12.5 ng His-E1, 250 ng His-E2 (AtUBC8), 1 μ g His-PUB25 or His-PUB26, and 4 μ g HA-Ubiquitin (Boston Biochem, cat. no. U-110) were incubated in 30 μ L ubiquitination reaction buffer (50 mM Tris-HCl pH 7.4, 10 mM MgCl₂, 5 mM ATP, 2 mM DTT) for 2 h at 30°C in a thermomixer (Eppendorf). For GST-BIK1 polyubiquitination, 60 ng GST-BIK1 was added to the reaction. Termination of the reaction was done by adding 5X SDS Loading buffer and heating at 80°C for 10 min. Samples were quickly centrifuged, separated by SDS-PAGE, and detected by immunoblotting with α -His or α -GST antibodies (Appendix Table S9).

2.13- SDS-PAGE and immunoblotting

5X Laemmli SDS loading buffer (45% v/v glycerol, 1% SDS, 0.5 M Tris-HCl pH 6.8, 0.02% bromophenol blue, 50 mM DTT; BioShop) was added to each sample for 1X final concentration. The samples were then heat-denatured for 10 min at 80°C on a thermal block and quickly collected by centrifugation. 10-25 µL of each sample was then run through 5% polyacrylamide stacking gel for 25 min at 75 V, followed by 10% resolving gel for 1 h at 150 V using BioRad Mini-PROTEAN Tetra Cell Systems with 1X SDS Running Buffer (25 mM Tris-HCl pH 6.8, 190 mM glycine, 0.1% (w/v) SDS). Proteins were next transferred onto polyvinylidene fluoride (PVDF) membrane (BioRad) using a wet transfer for 1.5 h at 90 V at 4°C in 1X TG buffer (25 mM Tris-HCl pH 6.8, 190 mM glycine, 20% ethanol). Following transfer, the membrane was blocked in 5% skim milk in Tris-buffered saline (TBS) containing 0.1% Tween-20 (TBS-T) for 1 h, and then incubated with primary antibody overnight at 4°C in the 5% skim milk with rocking. Following incubation with primary antibody, the membranes were washed 3 times with TBS-T, followed by incubation with secondary antibody in 5% milk/TBS-T conjugated to HRP for 2 h at room temperature. Membranes were then washed twice with TBS-T, including a final wash in TBS prior to imaging with Clarity Western Enhanced Chemiluminescence (ECL) on a ChemiDoc™ Touch Imaging System (both BioRad). Antibodies and the titres used are listed in Appendix Table S9.

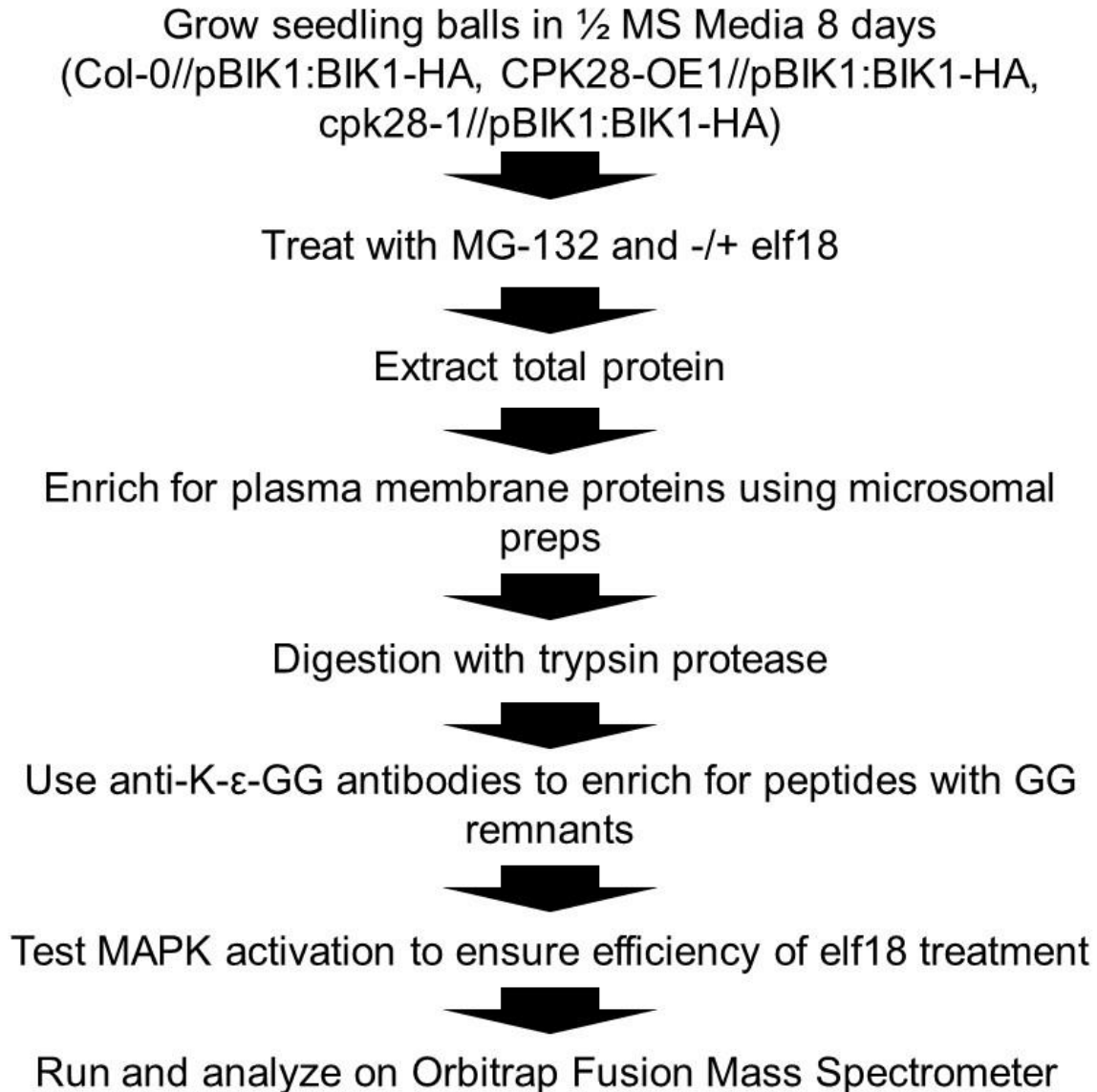


Figure 2.1. General workflow for determination of BIK1 ubiquitination sites by mass spectrometry. Seeds were shaken in flasks of 0.5X MS media for 8 days until they formed seedling balls, then treated with MG132 and +/- elf18. Total protein was extracted, and microsomal preps were performed the enrich for plasma membrane-associated proteins. Samples were then digested with trypsin and ubiquitinated peptides were enriched using α -K-ε-GG antibody. MAPK activation was analyzed prior to submission of samples for LC-MS/MS. These assays were performed at The Sainsbury Laboratory (Norwich, UK), and 3 repetitions were performed using this experimental workflow.

3A. REGULATION OF BIK1 TURNOVER BY THE CALCIUM-DEPENDENT PROTEIN KINASE CPK28 AND E3 UBIQUITIN LIGASES PUB25 AND PUB26

3.1- PUB25 and PUB26 associate with CPK28

Our collaborators from the lab of Jian-Min Zhou identified PUB25 and PUB26 as interacting partners of BIK1 and related PBLs via an *in vivo* mass spectrometry pull-down assay in *A. thaliana* (Wang *et al.*, 2018). Other key findings from previous experiments include: 1) PUB25 and PUB26 interact with and promote degradation of non-phosphorylated BIK1, and 2) PUB25 and PUB26 negatively regulate plant immunity by ubiquitinating BIK1 resulting in its degradation (Wang *et al.*, 2018). Previous published work implicated CPK28 as an important regulator in the turnover of BIK1, evidenced by its increased degradation in CPK28-OE lines, and stabilization in *cpk28* mutants (Monaghan *et al.*, 2014). Furthermore, CPK28 associates with and can phosphorylate BIK1 (Monaghan *et al.*, 2014). We thus sought to determine whether CPK28 also associates with PUB25 and PUB26, which may point to the existence of a multi-protein regulatory complex in controlling BIK1 accumulation. We found that PUB25 and PUB26 do indeed associate with CPK28 through a split-luciferase complementation assay evidenced by the reconstitution of N- and C-luciferase (Figure 3A.1). Association between CPK28 and BIK1 was used as a positive control, and CPK28 with the CONSTITUTIVE EXPRESSOR OF PR GENES5 (CPR5) as a negative control. CPR5 plays a role in programmed cell death immune responses associated with the hypersensitive response (HR) (Bowling *et al.*, 1997), and thus is not expected to associate with CPK28. Although the association between CPK28 and PUB25 or PUB26 was not as strong as that between the positive control CPK28 and BIK1, it was

significantly stronger than that of the negative control, suggesting that CPK28 associates with both PUB25 and PUB26 in this assay.

I next sought to confirm the interaction of PUB25 and PUB26 with CPK28 using another protein:protein interaction assay. For this we chose to perform co-immunoprecipitation (co-IP) of proteins transiently expressed in *N. benthamiana*. I found that CPK28 was able to associate with PUB25 (Figure 3A.2a), PUB26 (Figure 3A.2b), and the BIK1 positive control (Figure 3A.2c). Importantly, BIK1 was not pulled down in the beads control, which consisted of incubation of BIK1-HA with anti-GFP beads, indicating its specificity for its substrate. These were tested with and without flg22 elicitation, but no difference was observed, suggesting that these proteins may constitutively form a complex. We next tested whether all three proteins, CPK28, PUB25 or PUB26 and BIK,1 existed in a complex through a 3-way co-IP assay. CPK28 was found to pull down PUB25 or PUB26 and BIK1 together (Figure 3A.2d-e), suggesting the existence of a CPK28-BIK1-PUB25/PUB26 complex.

3.2- PUB25 and PUB26 negatively regulate plant immunity

The characterization of plant phenotypes associated with loss-of-function and overexpression lines can be used to determine more about the function of a protein. We obtained loss of function T-DNA mutants *pub25-1* (Salk_147032) and *pub26-1* (GABI_308D07) from Jian-Min Zhou, as well as segregating lines of the double mutant *pub25-1 pub26-1*, which I genotyped to homozygosity. *PUB25* (At3g19380) and *PUB26* (At1g49780) each consist of one exon, and the positioning of the T-DNA insertions is shown in Figure 3A.3a-b. T2 over-expression lines from Jian-Min Zhou were also screened to homozygosity using antibiotic selection; four *PUB25*-OE lines (OE1, OE6, OE9, OE27) and three *PUB26*-OE lines (OE1, OE6, OE27) were analyzed. RT-qPCR was used to confirm lines as loss-of-function (Figure 3A.3c-d) or over-expression

(Figure 3A.3e-f), with Col-0 showing significantly higher and lower *PUB25* and *PUB26* transcript level than the knockout and overexpression lines, respectively. Our collaborators observed that overexpression of *PUB25* and *PUB26* reduced BIK1 abundance, whereas the *pub25-1*, *pub26-1* and *pub25-1 pub26-1* accumulated BIK1 to greater levels than Col-0 (Wang *et al.*, 2018). This indicated *PUB25* and *PUB26* involvement in negatively regulating BIK1 overall protein abundance. To determine whether this regulation was at the transcript or protein level, I performed reverse transcription (RT)-qPCR to detect *BIK1* transcript levels in the *pub25-1 pub26-1* and *PUB25*-OE and *PUB26*-OE lines. As *BIK1* transcript levels were similar to Col-0 wild-type (Figure 3A.3g-h), enhanced BIK1 turnover in these lines was at the post-translational level, which is in agreement with *PUB25* and *PUB26* as the E3 ligases responsible for BIK1 turnover (Wang *et al.*, 2018).

While the loss-of-function single and double mutant lines grew similarly to wild-type on soil (Figure 3A.4a), all *PUB25*-OE and *PUB26*-OE lines showed altered phyllotaxy and curled leaves in comparison to wild-type (Figure 3A.4b). This type of altered rosette phenotype has been observed in plants with hypersensitive BR signaling, such as that seen in *Arabidopsis* over-expressing the BR receptor *BRI1* or the BR-biosynthetic enzyme *DWARF4* (*DWF4*) (Choe *et al.*, 2001; Wang *et al.*, 2018; Wang *et al.*, 2001). Antagonistic crosstalk exists between immune and BR pathways at the transcriptional level (Lozano-Durán & Zipfel, 2015). In addition, while *BIK1* positively regulates immune signaling, it has been shown to associate with *BRI1* and negatively regulate BR signaling (Lin *et al.*, 2013). As *PUB25*-OE and *PUB26*-OE lines accumulate low levels of *BIK1* (Wang *et al.*, 2018), these phenotypes are similar to those seen in *bik1* loss-of-function plants (Veronese, 2006).

Immune phenotypes were examined using measurement of ROS upon application of a peptide elicitor. As BIK1 is known to phosphorylate and activate the ROS-producing NADPH oxidase RBOHD (Kadota *et al.*, 2014b; Li *et al.*, 2014b), this assay served as an indirect indicator of BIK1 levels. As shown previously (Monaghan *et al.*, 2014), *cpk28-1* and BIK1-OE lines had significantly higher ROS burst than Col-0 (Figure 3A.4c). The *pub25-1 pub26-1* mutant displayed a higher elf18 ROS burst phenotype than Col-0 in (Wang *et al.*, 2018), consistent with lower levels of BIK1 accumulation observed in the *pub25-1 pub26-1* plants than in *cpk28-1*, however in our assays this was not consistently statistically significant (Figure 3A.4c). Similar results were seen with flg22 and AtPep1-induced ROS burst (Appendix Figure S1). In addition, as PUB25 and PUB26 are part of a gene family containing other PUBs known to negatively regulate immune signaling (Trujillo *et al.*, 2008), this could suggest the possibility of other E3 ligases involved in BIK1 turnover. While loss-of-function lines can sometimes be difficult to interpret due to genetic redundancy, the examination of over-expression lines can reveal gain-of-function phenotypes. Examination of the ROS burst phenotype for PUB25-OE and PUB26-OE lines showed a significantly lower elf18-elicited ROS burst compared to Col-0, as did control lines CPK28-OE and *bik1 pbl1* (Figure 3A.4d). The flg22 and AtPep1- induced ROS burst was similar (Appendix Figure S1). These results are in agreement with the lower accumulation of BIK1 in *bik1 pbl1*, CPK28-OE (Monaghan *et al.*, 2014), and PUB25-OE and PUB26-OE lines (Wang *et al.*, 2018).

3.3- Epistasis analysis to determine genetic interaction between PUB25/26, CPK28 and BIK1 in PAMP-induced ROS burst

Double mutant *A. thaliana* lines were generated by performing crosses to analyze genetic relationships between CPK28 and PUB25 or PUB26. As overexpression of CPK28 results in

lower BIK1 accumulation, it can genetically suppress the high ROS in BIK1-OE lines (Monaghan *et al.*, 2014). We used PAMP-induced ROS to analyze the genetic interactions of CPK28 with PUB25 or PUB26. We first analyzed the mutants *cpk28-1*/PUB25-OE and *cpk28-1*/PUB26-OE. The *cpk28-1* mutant has a high ROS burst, consistent with increased stability of BIK1 (Figure 3A.5a) (Monaghan *et al.*, 2014). As discussed in section 3.2, the PUB25-OE and PUB26-OE lines have a low ROS burst, consistent with increased turnover of BIK1 (Wang *et al.*, 2018; Figure 3A.5a). We found that overexpressing *PUB25* or *PUB26* suppressed the high elf18-induced ROS burst of *cpk28-1* mutants (Figure 3A.5a), suggesting that they act genetically downstream of CPK28. Similar results were seen with flg22 as an elicitor (Appendix Figure S2).

We next analyzed the *pub25-1 pub26-1*/CPK28-OE lines to further characterize the genetic interactions of CPK28 and PUB25 or PUB26. The *pub25-1 pub26-1* mutant had a comparable ROS burst to wild-type, and the CPK28-OE lines had low ROS burst, consistent with previous studies (Monaghan *et al.*, 2014; Wang *et al.*, 2018; Figure 3A.5b). We observed a partially complementation of the elf18-induced ROS burst with *pub25-1 pub26-1* in CPK28-OE background (Figure 3A.5b), suggesting that CPK28 acts genetically upstream of PUB25 and PUB26. Similar results were also observed with flg22-induced ROS burst (Appendix Figure S2).

The results from these epistasis analyses serve as a complement to biochemical approaches for determining the contribution and placement of a protein within a pathway. Using ROS generation as a proxy for BIK1 accumulation levels in these double mutants, we provided further support for the role of CPK28, PUB25 and PUB26 as negative regulators of BIK1 accumulation, as well as their involvement in the same immune signaling pathway. We were also able to further confirm that PUB25 and PUB26 are the E3 ligases involved in BIK1 ubiquitination and turnover, in agreement with other biochemical, genetic and proteomic

approaches discussed in Wang *et al.*, (2018). The results from our epistasis analysis indicate a place for CPK28 upstream of PUB25 and PUB26, which in turn are upstream of BIK1 to catalyze its turnover through polyubiquitination targeting it for degradation by the 26S proteasome. The *cpk28-1/PUB25-OE* and *cpk28-1/PUB26-OE* lines showed suppression of the high *cpk28-1* ROS burst (Monaghan *et al.*, 2014), consistent with the role of PUB25 and PUB26 involvement in BIK1 turnover. Interestingly, the ROS burst was not completely suppressed, which may indicate a requirement for CPK28 in activating PUB25 and PUB26 for optimal activity in turning over BIK1. Indeed, PUB25 and PUB26 were found to be phosphorylated by CPK28 on T94 and T95, respectively, enhancing their activity and promoting ubiquitination of BIK1 (Wang *et al.*, 2018). Interestingly, our *pub25-1 pub26-1/CPK28-OE* lines show partial complementation of the low ROS generation in CPK28-OE (Monaghan *et al.*, 2014; Wang *et al.*, 2018). With the over-expression of *CPK28*, we might normally expect more activation of PUB25/26. However, in this double mutant, these PUB25 and PUB26 are knocked out, so we did not expect there to be a difference in BIK1 accumulation. The observed decrease in ROS compared to Col-0 may suggest either direct regulation of BIK1 by CPK28, or the involvement of other E3 ligases in BIK1 turnover.

3.4- PUB22, PUB23 and PUB24 may also contribute to BIK1 turnover

As the *pub25-1 pub26-1* mutants did not present a consistent significantly higher ROS burst than wild-type (Figure 3A.4c), and based on the epistasis analysis discussed above, it may be possible that other players are involved in the turnover of BIK1. In addition, *cpk28-1* mutants display consistently much higher ROS burst than *pub25-1 pub26-1*, suggesting the possibility for multiple substrates. Previously, the closely related PUB22, PUB23 and PUB24 were found to negatively regulate immunity (Trujillo *et al.*, 2008), and are in the same sub-group of U-box E3

ligases as PUB25 and PUB26 (Azevedo *et al.* 2001). Indeed, overexpression of *PUB22* and *PUB23* resulted in decreased accumulation of BIK1 (Wang *et al.*, 2018), providing support for their role as additional regulators of BIK1 turnover. We sought to further investigate the role of PUB22, PUB23 and PUB24 in the turnover of BIK1. Dr. Jacqueline Monaghan had previously dipped *pub22 pub23 pub24* triple mutant plants with a 35S:BIK1-HA construct and had selected to the T2 generation. I selected these lines to homozygosity and analyzed their developmental phenotypes and BIK1 accumulation. Interestingly, the plants show stunted growth and development, with the first true leaves being photobleached, and having slower growth and development of the entire plant (Figure 3A.6a). The plants eventually recovered and set seed, and further work will be completed by a future student to document growth over time, as well as look further into hyperimmune phenotypes through analysis of ROS, seedling growth inhibition, upregulation of defence-related genes and levels of SA. These rosette phenotypes could be caused by an even higher accumulation of BIK1, which could be detrimental to plant development. We therefore sought to test the hypothesis that the *pub22 pub23 pub24/35S:BIK1-HA* lines showed higher BIK1 accumulation than wild-type overexpressing BIK1, which indeed they did (Figure 3A.6b). Based on the high levels of BIK1 in the pBIK1 line, more work is required to determine the mechanism through which the *pub22 pub23 pub24/35S:BIK1-HA* plants are developmentally affected. To investigate the contribution of PUB22, PUB23, PUB24, PUB25 and PUB26 to the turnover of BIK1, we sought to generate a quintuple mutant *pub22 pub23 pub24 pub25 pub26* by crossing a *pub22 pub23 pub24* plant with a *pub25-1 pub26-1* plant. As both the *pub22 pub23 pub24* and the *pub25-1 pub26-1* mutants both have higher ROS burst than WT (Trujillo *et al.*, 2008; Wang *et al.*, 2018), I hypothesize that the quintuple mutant may have an even higher ROS burst than the triple or double individually. Together with summer

student Mansuba Rana, we are close to having a quintuple mutant, however due to time constraints this was not completed before finishing my thesis. Overall, these first experiments suggest that PUB22, PUB23, PUB24, PUB25 and PUB26 all act in controlling BIK1 levels, and play a role in balancing optimal immune signaling with growth and development.

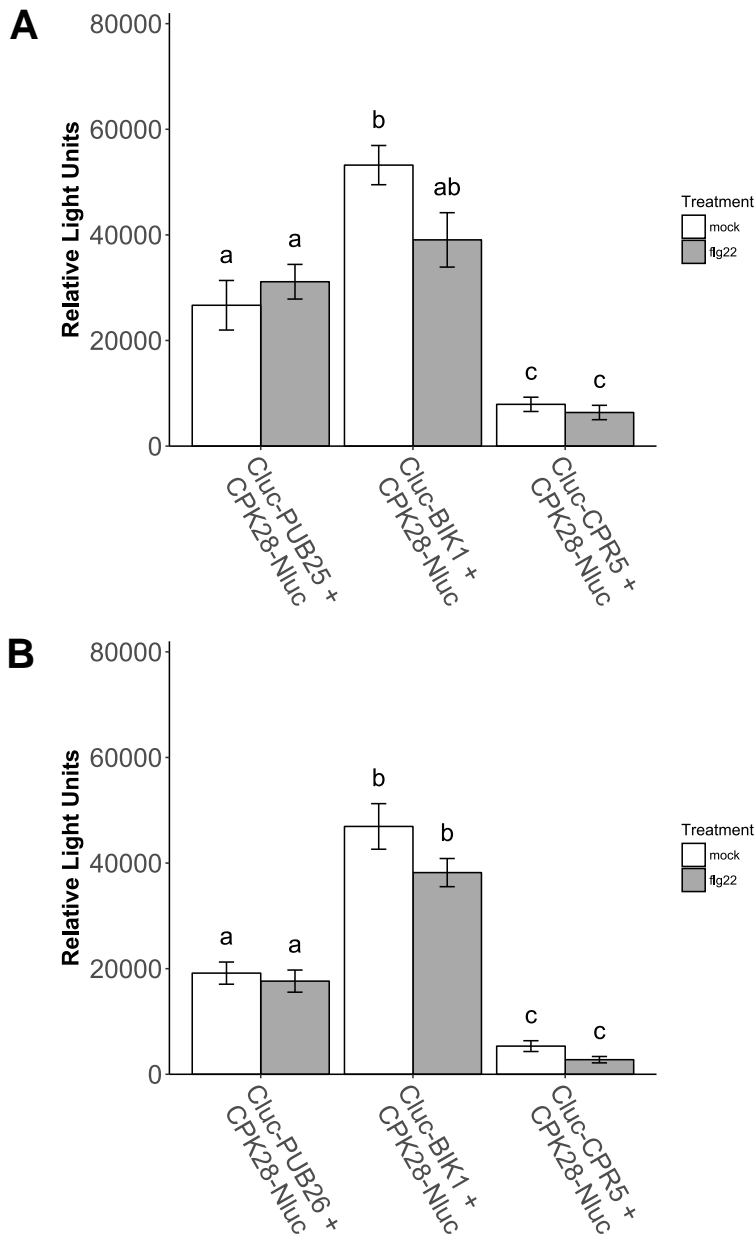


Figure 3A.1. PUB25 and PUB26 associate with CPK28 via split-luciferase assays. N-luciferase and C-luciferase constructs were expressed in 4-5 week old *N. benthamiana* plants through *Agrobacterium*-mediated transformation. Tissue was harvested at 3 dpi, treated with or without 200 nM flg22, and split-luciferase complementation was performed as described in section 2.7. Light signal (measured in relative light units) was observed with CPK28-NLuc + CLuc-PUB25 (A) and with CPK28-NLuc + CLuc-PUB26 (B). CPK28-NLuc + BIK1-CLuc was used as a positive control and CPK28-NLuc + CLuc-CPR5 as a negative control for both. Split-luciferase complementation assays were performed 3 times with similar results. Letters denote statistically significant groups ($p < 0.05$) based on a one-way ANOVA followed by Tukey HSD. No significant difference was observed with mock or flg22 treatment.

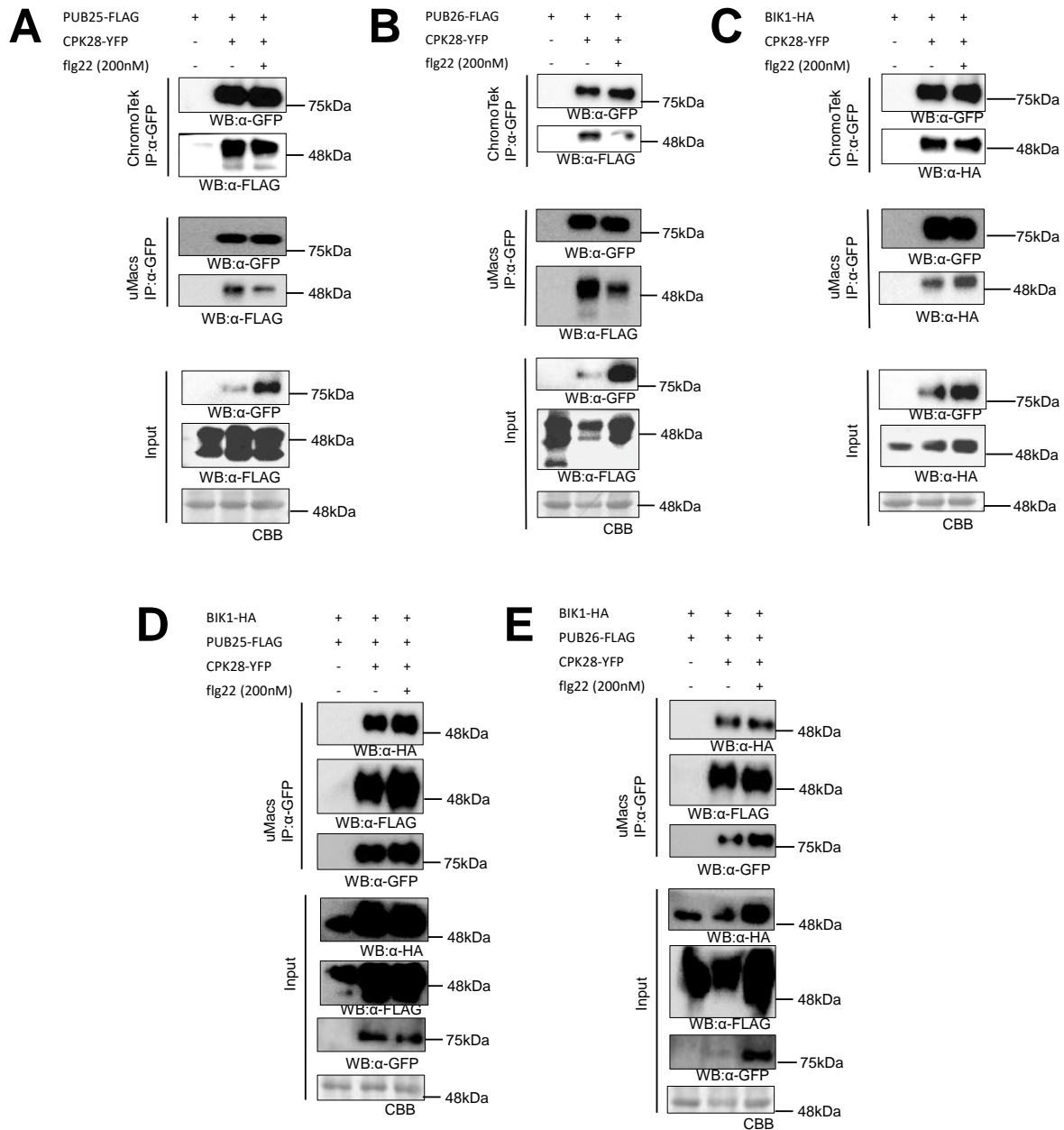


Figure 3A.2. PUB25 and PUB26 associate with CPK28 via co-IP assay. CPK28-YFP was expressed with PUB25-FLAG (A), PUB26-FLAG (B) or BIK1-HA (C) or with PUB25/26 and BIK1-HA (D-E) in 4-5 week old *N. benthamiana* plants alongside a negative control lacking CPK28-YFP. Tissue was harvested at 3 dpi, and tissues were vacuum infiltrated with water (mock) or 200 nM flg22. Total protein was extracted, and co-IP followed by immunoblotting was performed using anti-GFP microbeads. As PUB25/26-FLAG was present with CPK28-YFP on its own and in combination with BIK1-HA, it suggests that PUB25 and PUB26 may interact with CPK28 *in planta* and with CPK28, PUB25/26 and BIK1 all in complex. There was no difference in association with flg22 elicitor treatment. These assays were performed 3 times with similar results.

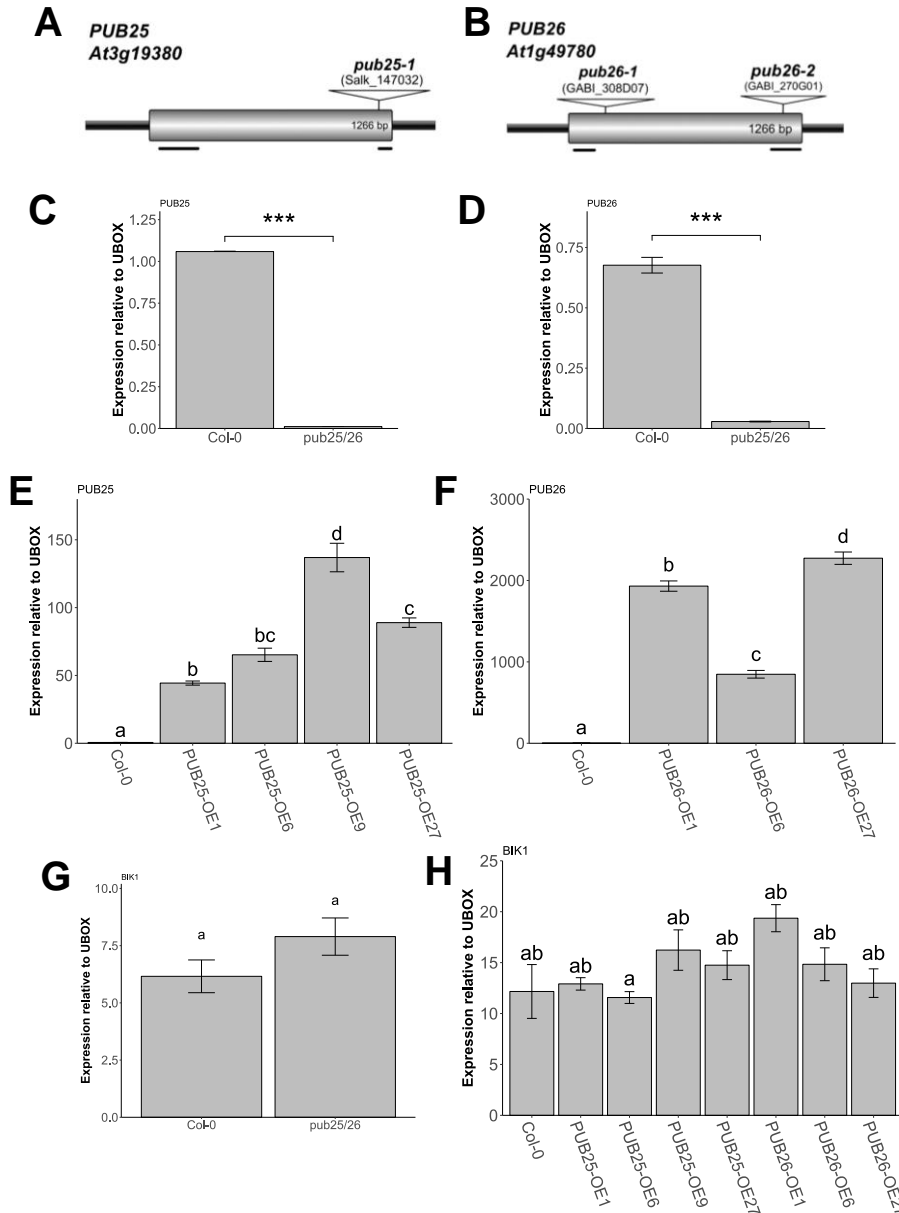


Figure 3A.3. Genetic analysis of *pub25 pub26* double knockout mutants and *PUB25-OE* and *PUB26-OE* overexpression lines. A-B) Gene schematic of *PUB25* (At3g19380) and *PUB26* (At4g49780) with T-DNA insertion allele indicated. C-D) qPCR analysis of gene expression relative to the housekeeping gene *UBOX* of *PUB25* and *PUB26* in *pub25-1 pub26-1* compared to Col-0. E-F) Gene expression determined by qPCR of *PUB25* and *PUB26* relative to *UBOX* in *PUB25-OE* and *PUB26-OE* lines compared to Col-0. G-H) Gene expression determined by qPCR relative of *BIK1* relative to *UBOX* in the indicated genotypes compared to Col-0. Asterisks indicate $p < 0.001$ based on a one-way ANOVA followed by a Tukey post-hoc test. Letters are based on ANOVA ($p < 0.05$) followed by Tukey HSD. All qPCR tests were performed 3 times with similar results.

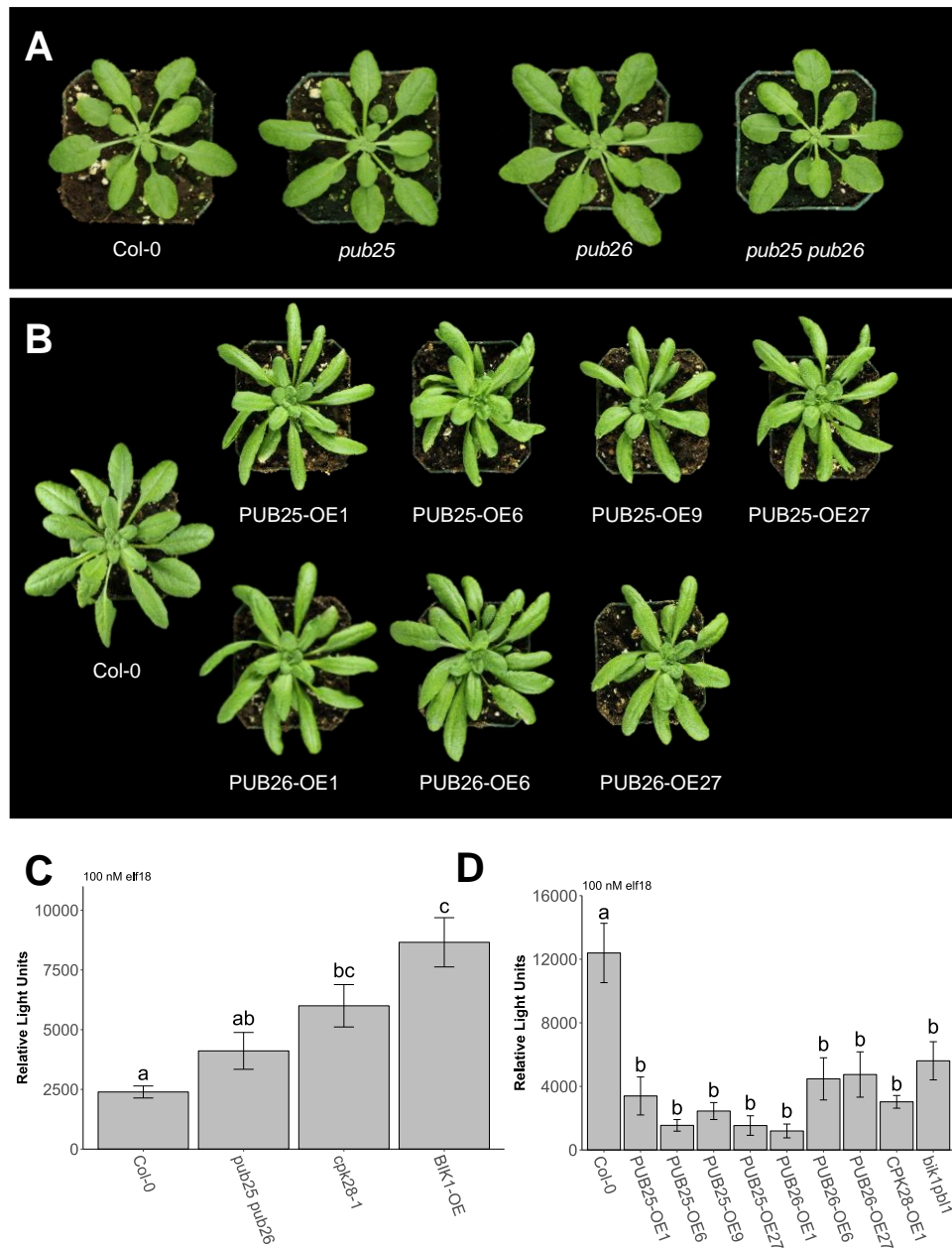


Figure 3A.4. Characterization of *pub25-1 pub26-1* mutants and PUB25-OE and PUB26-OE lines. A-B) Rosette phenotype of 5-week old *pub25-1 pub26-1* knockout and PUB25 and PUB26 overexpression lines, respectively.. C-D) Oxidative burst of 4-5 week old T3 homozygous *Arabidopsis* upon treatment with 100 nM elf18 of *pub25-1 pub26-1* and PUB25-OE and PUB26-OE lines in comparison to previously studied genotypes (Monaghan *et al.*, 2014; Veronese *et al.*, 2006; Zhang *et al.*, 2010). 6 leaf discs from different plants were tested per genotype. Letters indicate statistically significant groups ($p < 0.05$) based on a one-way ANOVA followed by Tukey post-hoc test. ROS burst assays were performed 3 times with similar results. ROS burst totals are indicative of area under the dynamic curve of ROS generation over a period of 40 min.

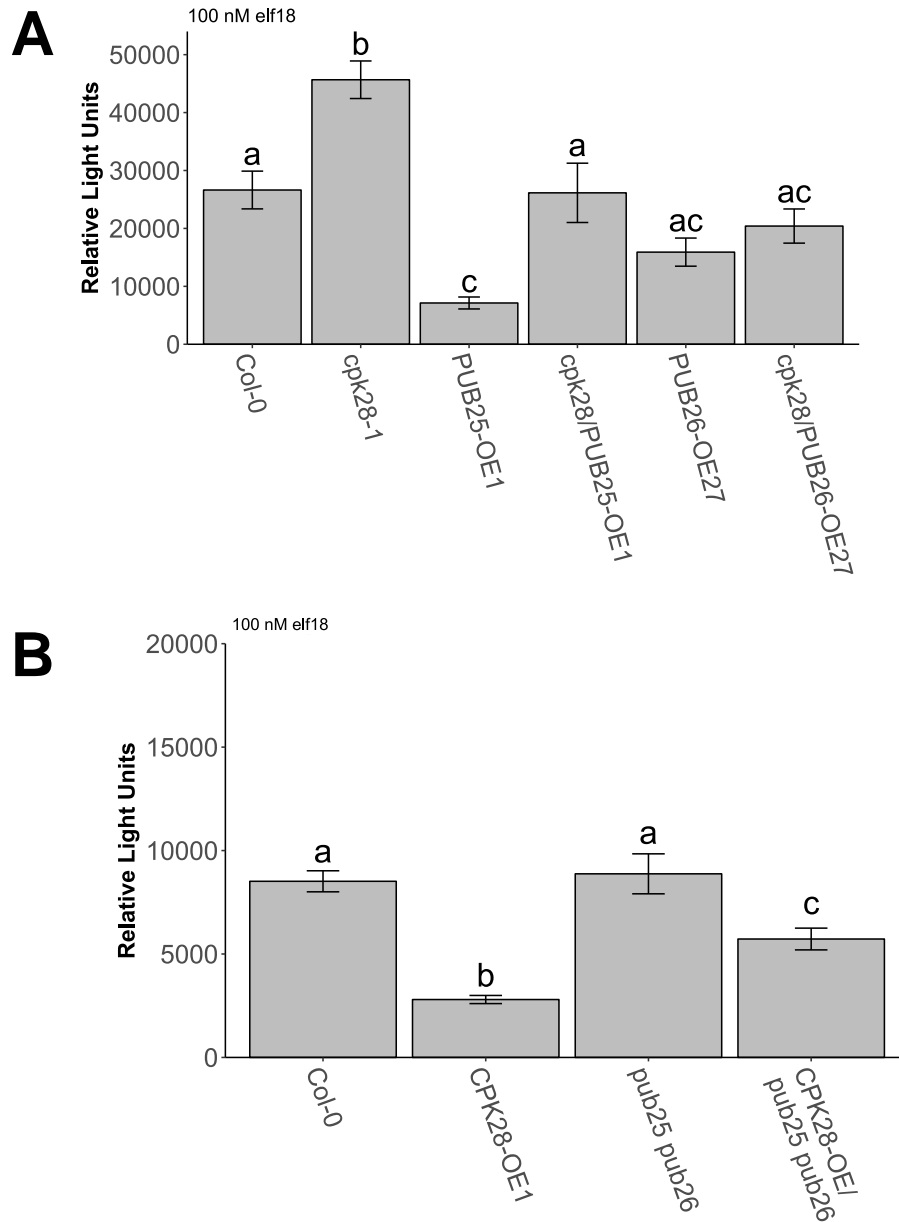


Figure 3A.5. Epistasis analysis places CPK28 upstream of PUB25 and PUB26. A) Oxidative burst assay of T2 generation of 4-5 week old *Arabidopsis* with treatment of 100 nM elf18 on *cpk28-1/PUB25-OE1* and *cpk28-1/PUB26-OE* for epistasis analysis to determine whether PUB25 or PUB26-OE could suppress the high ROS burst of *cpk28-1*. B) Epistasis analysis of oxidative burst of CPK28-OE/ *pub25-1 pub26-1* to determine whether *pub25-1 pub26-1* can restore the low ROS of CPK28-OE. Leaf discs were treated with 100 nM elf18. Three repetitions were performed with similar results, and 12 leaf discs were tested per genotype. Letters indicate groups which are statistically significant ($p < 0.05$) based on a one-way ANOVA with Tukey post-hoc test.

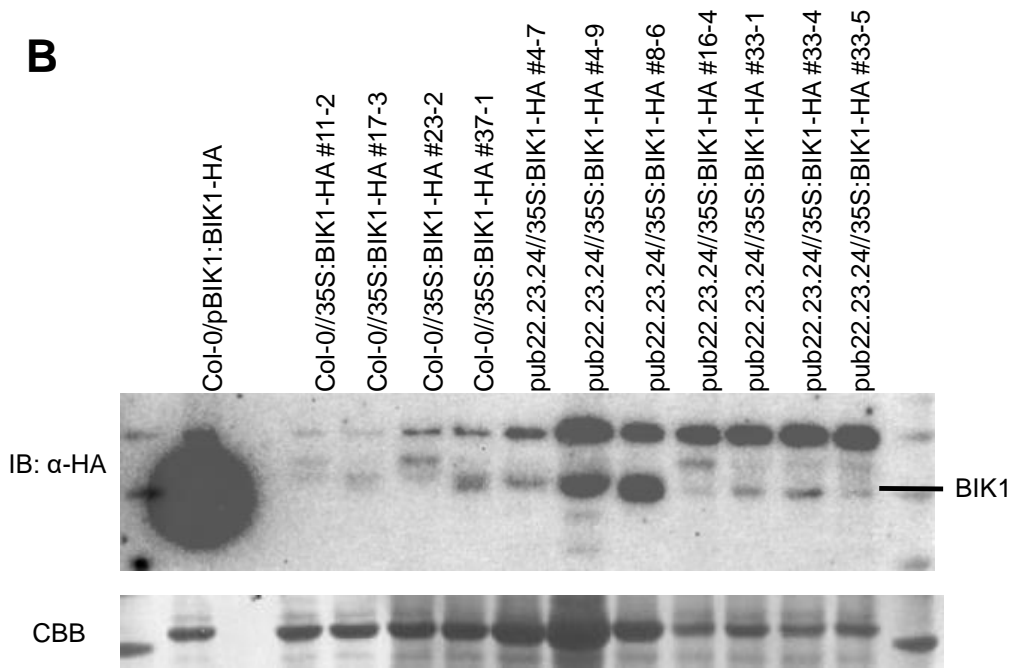
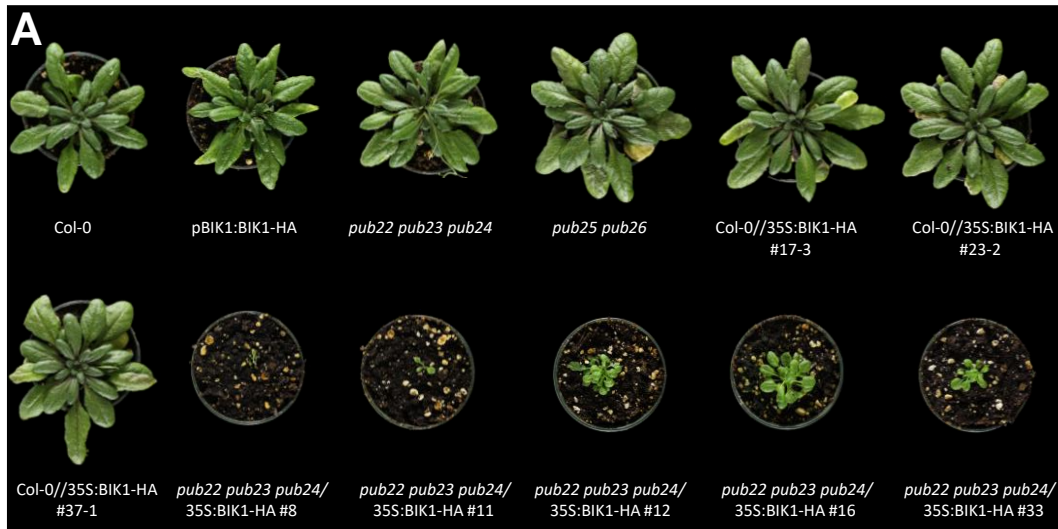


Figure 3A.6. Generation of *pub22 pub23 pub24*//35S:BIK1-HA lines. A) Rosette phenotype of 5- week old *Arabidopsis* of *pub22 pub23 pub24*//35S:BIK1-HA in comparison to Col-0 and *pub* mutant backgrounds. B) *pub22 pub23 pub24*//35S:BIK1-HA analysis of BIK1 accumulation in comparison to Col-0//35S:BIK1-HA. Seedlings were grown in 6-well plates for 10 days in liquid MS, total protein was extracted, normalized and anti-HA western blot was performed. This assay was performed 3 times on T3 homozygous plants with similar results. The CBB stain was used to indicate loading. Despite unequal loading, it is clear that all lines express BIK1-HA, however future experiments are required to determine BIK1 levels more accurately.

3B. IDENTIFICATION OF BIK1 UBIQUITINATION SITES

3B.1- Generation of a plasma membrane ubiquitome

Plant immune responses induce signaling cascades, which include many protein PTMs such as phosphorylation and ubiquitination. The ubiquitin-proteasome system is important for plants to maintain an optimal level of signaling output, with several known circumstances of ubiquitination of PRRs and intracellular R proteins (Cheng & Li, 2012; Dielen *et al.*, 2010; Marino *et al.*, 2012; Robatzek *et al.*, 2006). For example, the well-studied PRR FLS2 is ubiquitinated by the closely related PUB12 and PUB13, and is targeted for degradation (Lu *et al.*, 2011). PRRs and other host proteins can also be subject to ubiquitination by pathogen effectors, such as AvrPtoB, which ubiquitinates FLS2 and CERK1 via a C-terminal E3 ligase domain (Gimenez-Ibanez *et al.*, 2009; Göhre *et al.*, 2008). Thus, ubiquitination of proteins acting in early immune signaling plays an important role in modulating the strength of the immune response.

We sought to generate an *Arabidopsis* plasma membrane ubiquitome to determine plasma membrane proteins that are ubiquitinated under normal conditions with mock and elf18 treatment. This dataset can act as a snapshot of the dynamics of ubiquitination on plasma membrane associated proteins upon immune elicitation by elf18. It may lead to a finer understanding of the role of PTMs in modulating immune signaling strength. Previously, datasets of endogenous human protein ubiquitination sites for use in understanding diseases have been generated (Chen *et al.*, 2014; Shi *et al.*, 2011). Recently, studies involving ubiquitinated proteins in wheat, and rice proteins ubiquitinated upon pathogen infection have been published (Chen *et al.*, 2018; Zhang *et al.*, 2017). We adapted the Udeshi *et al.*, (2013) protocol using anti-K-ε-GG antibody, previously used for identification of ubiquitinated proteins in mammals, to identify

plasma membrane-resident ubiquitinated *Arabidopsis* proteins. It was hoped that these data would generate an *Arabidopsis* ‘ubiquitome’ that would be useful for several research purposes. To enhance our study, we set out to compare protein ubiquitination in unelicited and elicited tissues. Genotypes used were Col-0//pBIK1:BIK1-HA, CPK28-OE1//pBIK1:BIK1-HA, and *cpk28-1*/pBIK1:BIK1-HA, which express *BIK1* at 100 fold its protein expression in wild-type (Monaghan *et al.*, 2014). Seedlings were grown for 8 days with shaking prior to treatment with 50 μ M MG-132 for 1 h prior to elicitor treatment. Seedlings were then treated with MS or MS containing 1 μ M elf18, vacuum infiltrated for 1 min, then left to shake for up to 10 min prior to flash-freezing. Importantly, successful elf18 induction was confirmed in all background genotypes by analyzing activation of MAPK (Figure 3B.1), a well-defined immune signaling event (Asai *et al.*, 2002). Proteins were extracted, and microsomal fractions enriched prior to trypsin digestion. Anti K- ϵ -GG antibody beads enriched ubiquitinated peptides, which were detected using LC-MS/MS.

3B.2- Analysis of ubiquitinated proteins

In the Col-0/pBIK1:BIK1-HA *Arabidopsis* background, we identified a total of 411 ubiquitinated proteins across 3 repetitions using a false discovery rate (FDR) of 0.1, with 919 unique peptides identified (Appendix Table S10). The ubiquitinated peptides ranged in length from 8 to 44 amino acids. 46.2% of proteins showed only 1 ubiquitinated lysine, and 24.8%, 10.7%, 7.3% and 3.6% of proteins had 2, 3, 4, or 5 ubiquitinated lysines, respectively (Appendix Table S10). There were 8 proteins (1.9%) that showed 10 or more ubiquitinated lysines, and 3 proteins showing 15 or more, which were PENETRATION3 (PEN3), ARABIDOPSIS H(+)-ATPase1 (AHA1) and AHA2. Motif-X was used to identify the following enriched ubiquitination motifs among the ubiquitinated peptides: AXXK^{Ub}, K^{Ub}G, TK^{Ub}, AK^{Ub}, K^{Ub}A, AXXXXK^{Ub}, GK^{Ub} (Chou &

Schwartz, 2011; Schwartz & Gygi, 2005), where X is any amino acid. An analysis of the Gene Ontology (GO) terms using Search Tool for the Retrieval of Interacting Genes/Proteins (STRING) enrichment identified that the ubiquitinated proteins in both mock and elf18 treatment were involved in a multitude of processes, including those of “metabolism”, “localization”, “response to stimuli”, “cell communication”, “signal transduction” and “transport”, consistent with previous studies which looked at all *Arabidopsis* ubiquitinated proteins, or rice proteins following immune elicitor treatment (Chen *et al.*, 2018; Kim *et al.*, 2013). Upon elf18 treatment, there was an enrichment in terms including “biological regulation”, “negative regulation of cell death”, “positive regulation of proteasomal protein catabolism”, “negative regulation of biological processes”, and “immune response regulating signaling pathway” and “protein kinases” compared to the mock treated samples (Appendix Table S11-S12). These terms suggest the involvement of the *Arabidopsis* ubiquitination system in complex regulation of defence responses, further elucidating a role of maintenance of immune signaling proteins at optimal levels. Also, GO term analysis of cellular component confirms enrichment of membrane-localized proteins, indicating the efficacy of the microsomal enrichment (Appendix Table S11-S12).

There were several plasma membrane ubiquitinated proteins and receptor-like kinases involved in immunity that were previously found to be polyubiquitinated and degraded by the 26S proteasome. Interestingly, many protein kinases were also found to have ubiquitinated lysines, which indicates a role for mono- or polyubiquitination in mediating many different processes and signal transduction pathways that may be activated or inactivated by phosphorylation mediated by a protein kinase. The ubiquitinated lysines observed here were consistent with those found in previous studies such as ubiquitination of the rice homolog

OsCERK1. We observed ubiquitination of Lys452, which is consistent with ubiquitination of OsCERK1 on the conserved Lys453 (Chen *et al.*, 2018).

3B.3- Determination of ubiquitinated residues on BIK1

As described in Chapter 3, PUB25 and PUB26 were identified as the E3 ligases contributing to BIK1 polyubiquitination and turnover via the 26S proteasome. CPK28 contributes to BIK1 turnover via phosphorylation of PUB25 and PUB26 to enhance their activity (Wang *et al.*, 2018). The next step was to determine which lysine residues were polyubiquitinated to facilitate the turnover. Using the di-Gly-enriched peptides described in section 4.1, I determined which BIK1 lysine residues were ubiquitinated. The initial plan was to use CPK28 and PUB25 or PUB26 knockout and overexpression lines to determine which BIK1 sites were CPK28- and PUB25- or PUB26-mediated. However, I was unable to detect BIK1 in preliminary tests using Col-0, likely due to relatively low abundance of BIK1 protein. We thus used BIK1 over-expression lines (Col-0/pBIK1:BIK1-HA where BIK1 is 100-fold overexpressed; Monaghan *et al.*, 2014), and included CPK28-OE/pBIK1:BIK1-HA and *cpk28*/pBIK1:BIK1-HA, as these materials were already available (Monaghan *et al.*, 2014). Ubiquitinated lysine residues observed on BIK1 are listed in Table 3B.1; I focused only on sites observed more than once (K31, K41, K61, K337, K358, K366, K369, K370, K374, and K388). Spectra were manually inspected for quality control, and an increase of 114 kDa observed was indicative of the incorporation of a ubiquitin moiety (Figure 3B.2). Interestingly, these high-confidence ubiquitinated lysine residues were on the N- and C-terminal ends of the protein, outside of the kinase domain (Figure 3B.3a). We modeled these sites against the recently published BIK1 crystal structure (Lal *et al.*, 2018), and determined that they appeared accessible to the E3 ligase for ubiquitination (Figure 3B.3b).

It was difficult to determine an overall pattern in the ubiquitination sites on BIK1 between mock versus. elf18 treatment, as well as between the wild-type, CPK28-OE and *cpk28-1* backgrounds. Interestingly, in general the CPK28-OE line saw fewer overall ubiquitinated lysine residues, with the knockout *cpk28* showing more observed ubiquitinated lysines on BIK1. This may be due to the relative lower and higher abundance of BIK1 in these genotypes, respectively (Monaghan *et al.*, 2014). Further targeted examination and quantification of ubiquitination on these lysine residues is currently ongoing by our collaborator Frank Menke, using parallel reaction monitoring (PRM), which may serve to indicate a more defined pattern of ubiquitination to pinpoint precisely which lysine residues are ubiquitinated upon PAMP treatment.

3B.4- Site-directed mutagenesis and generation of *in planta* BIK1 mutants

It is important to note that the di-Gly enrichment method enriches all ubiquitinated peptides, which could include both mono-ubiquitination and polyubiquitination. We were interested in those residues that are polyubiquitinated, as this modification targets a protein for degradation by the 26S proteasome. To determine which BIK1 lysine residues are polyubiquitinated to contribute to CPK28-, PUB25- and PUB26- mediated turnover, site-directed mutagenesis was conducted to mutate the lysine residues determined by mass spectrometry to arginine residues. This amino acid conversion sought to prevent their ubiquitination, while still maintaining the positive amino acid charge and overall protein structure (Betts & Russell, 2003; Forget *et al.*, 2008). As part of a team effort, the lysine to arginine mutations were generated for each of the MS-determined lysines individually and in combinations. These mutants were first mutagenized in pENTR Gateway clones and shuttled into either pGWB14 vectors for plant expression (35S-driven, C-terminally tagged with 3x HA) or pGEX6p.1 or pET44a for *E. coli* expression and purification as indicated in Appendix Table S2. The BIK1 mutants were expressed and purified

from *E. coli*, and their autophosphorylation kinase activity was assessed *in vitro* (Jacqueline Monaghan and Danielle Ciren, BIOL 538 mentorship, unpublished data). Thus, BIK1 protein kinase activity is maintained at least in the single lysine mutants, which is important as it indicates that the overall protein structure is maintained, which may be necessary for it to associate and be ubiquitinated by its E3 ligases for turnover.

Plant expression vectors were used for *Agrobacterium*-mediated floral dip to produce stable transgenic *Arabidopsis* lines for *in vivo* analysis of the involvement of the BIK1 lysine residues on its proteasome-mediated turnover. The background genotypes used for dipping were Col-0, CPK28-OE, *bik1* and PUB25-OE. The *bik1* background served to assess the functionality of the lysine mutant both in development as well as immune signaling. The *bik1* mutant possess serrated leaves and a lodging phenotype, as well as early bolting and flowering (Veronese *et al.*, 2006). Thus, the transformation of the BIK1 K→R mutants into the *bik1* background should restore this phenotype back to wild-type if that particular lysine was not involved in these aspects of development. These lines may also be used to assess functionality of the BIK1^{mut} constructs in immunity through assessment of whether the ROS burst can be complemented, or possibly even higher based on 35S over-expression. The Col-0 mutant background was used to assess the immune or ROS burst phenotype of plants transformed with the BIK1 K→R mutants. If the lysine residues are involved in turnover of BIK1, their mutation to an arginine should prevent BIK1 polyubiquitination, and thus its turnover, potentiating a heightened immune response in comparison to Col-0/35S:BIK1-HA lines. The CPK28-OE and PUB25-OE backgrounds were dipped with the BIK1 K→R mutants to confirm that these lysines were indeed involved in the CPK28- or PUB25-mediated polyubiquitination and turnover of BIK1. As the BIK1 K→R mutants involved in polyubiquitination of BIK1 should prevent their turnover, the CPK28-OE

and PUB25-OE backgrounds should not be able to suppress the ROS burst in the same way that they do normally. Thus, any mutants shown to have a heightened immune response in the Col-0 background should also display a greater immune response in these backgrounds consistent with BIK1 accumulation in those mutants in which wild-type BIK1 would normally accumulate less. Together with summer student Mansuba Rana, these mutants have been dipped, and initial selection and testing has begun in the T1 generation, to be continued by a future student.

3B.5- Development of ubiquitination assays to test which BIK1 lysines are subject to regulation by the CPK28-PUB25/26 regulatory module

Having identified ubiquitinated lysine residues on BIK1, and with work ongoing on analyzing ubiquitin sites through *in vivo* stable expression in *Arabidopsis*, we sought to complement these assays with biochemical analysis of recombinant proteins. Due to time constraints, these assays are still in troubleshooting stages with preliminary work, thus in this thesis I present an analysis of optimization of the protocols using WT-BIK1.

3B.5.1- *In vitro* ubiquitination assays

The first assay we sought to use was an *in vitro* ubiquitination assay, which has been previously been performed in several plant immunity studies (Furlan *et al.*, 2017; Wang *et al.*, 2018). These assays involve the incubation of purified recombinant protein of interest in the presence of E1, and E2 and an E3 ligase, ubiquitin and ATP for 2 h in an incubator with shaking, as described in section 2.12. In my thesis, I was working with GST-BIK1 as my target protein, an unknown wheat E1, AtUBC8 as an E2, and PUB25 or PUB26 as my E3 ligase. The literature presented different concentrations of E1 and target protein, thus I began with the use of both to optimize the assay for my target protein. In lane 1, I used 12.5 ng E1 and 60 ng GST-BIK1, and in lane 2, used 50 ng E1 and 150 ng GST-BIK1 (Figure 3B.4a). I observed smearing that is

indicative of polyubiquitination in a α -GST immunoblot, and thus followed that up with a α -ubiquitin blot to confirm ubiquitination. To confirm that this was not an artifact of the purified BIK1, I ran an immunoblot of BIK1-WT with the BIK1 single mutants without incubation with E1, E2 and E3, and observed the same banding (data not shown), and thus it is possible that something is contributing to ubiquitination of BIK1, or that the antibody is showing unspecific binding. Thus, I decided to try a different ubiquitination assay with fewer individually purified components in order to observe more distinct patterns indicative of ubiquitination.

3B.5.2- Cell-free degradation assays

The next assay I tested for determination of ubiquitination and turnover of BIK1 were cell-free degradation assays. These assays have been performed in previous studies looking at components of the plant immune system (Wang *et al.*, 2018a; Wang *et al.*, 2018b). As BIK1 is degraded by the 26S proteasome mediated by CPK28, PUB25 and PUB26 we would expect to see degradation over time when BIK1 is incubated with these components. This assay involves incubating a recombinant protein (in our case GST-BIK1) with crude total protein extract as described in section 2.11. On first attempt, I used our protein extraction buffer (minus the protease inhibitors) for extraction of crude total protein (5 mM DTT, 1% (v/v) Igepal®, 2 mM Na₂MoO₄, 2.5 mM NaF, 1.5 mM activated Na₃VO₄, 50 mM Tris-HCl pH 7.5, 150 mM NaCl). We did not observe degradation of WT-BIK1 in initial tests (Figure 3B.4b), which may suggest that the components of this buffer are too harsh resulting in extraction of only membrane proteins, and if PUB25 and PUB26 do not intimately associate with the membrane, they may have been excluded. We next tried using a native extraction buffer as used in Wang *et al.*, (2018b), which consisted of 50 mM Tris-MES pH 8.0, 0.5 M sucrose, 10 mM EDTA, 5 mM DTT, 1 mM MgCl₂. This method proved more fruitful, and we were able to observe BIK1 degradation within 2 h,

with complete degradation at 4 h incubation at 28°C (Figure 3B.4b). We then begun testing the purified single GST-BIK1^{mut} constructs, and due to time constraints, only K31R is presented, and shows similar degradation in comparison to WT-BIK1 (Figure 3B.4c), suggesting it alone is not involved in BIK1 turnover by the 26S proteasome. These assays will be complemented using crude total protein from CPK28, PUB25 and PUB26 knockout and overexpression lines to verify that these lysine residues are indeed those that mediate turnover via CPK28, PUB25 and PUB26.

3B.5.3- *In vivo* transient ubiquitination assays in *N. benthamiana*

As the *in vitro* ubiquitination assays and cell-free degradation assays contain a number of different components and require functional purified protein, we decided to complement these assays with *in vitro* assays in *N. benthamiana* as described in Liu *et al.*, (2010). This involved transient expression in *N. benthamiana* of the BIK1^{mut} constructs in combination with CPK28 and PUB25 to catalyze ubiquitination, followed by extractions and α -HA IPs to immunoprecipitated BIK1-HA species with 50 μ M MG-132 to prevent proteasomal degradation for observation of ubiquitinated BIK1. We first tested that this would be feasible with WT-BIK1 (Figure 3B.5), performed two times with similar results, and preliminary tests with BIK1^{mut} have been done, but need to be repeated (data not shown), and will also be complemented with the other *in vitro* assays.

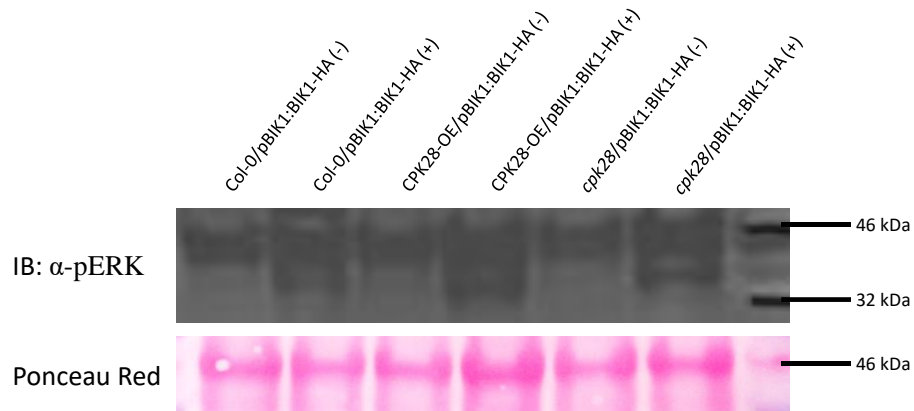


Figure 3B.1. MPK3, MPK4/11 and MPK6 are activated upon elf18 treatment. MAPK activation assays performed on extracted protein from microsomal preps to confirm elf18 induction in samples that were extracted from 8-day old seedlings. pMAPK44/42 (Cell Signaling) antibody was used for IB (immunoblot). Plants were treated with (+) or without (-) 1 μ M elf18 for 10 min. Ponceau Red staining was used to confirm equal sample loading and Rubisco can be seen at 46 kDa. This assay was performed for each of the 3 repetitions prior to analysis by LC-MS/MS.

Table 3B.1. BIK1 peptides identified by mass spectrometry. Breakdown of all ubiquitinated lysine residues seen in microsomal and di-Gly enriched samples. Lysines are organized into N-terminal domain, kinase domain and C-terminal domain. Total number of samples in which these peptides were observed as well as number of times seen in Col-0/pBIK1:BIK1-HA, CPK28-OE/pBIK1:BIK1-HA and *cpk28-1*/pBIK1:BIK1-HA mock and *elf18*-treated samples is presented as well as the peptide sequence observed. The ubiquitinated lysine residue is denoted by [K].

Residue	Peptide	Total # Samples Observed	Col-0 mock	Col-0 <i>elf18</i>	CPK28-OE mock	CPK28-OE <i>elf18</i>	<i>cpk28</i> mock	<i>cpk28</i> <i>elf18</i>
N-term								
K31	[K]SSSTVAAAQKTEGEILSS TPVK	2	0	1	0	0	0	1
K41	SSSTVAAAQ[K]TEGEILSS TPVK	11	2	2	2	0	3	2
K61	SFTFNEL[K]LATR	9	1	2	1	1	2	2
Kinase								
K83	NFRPDSVIGEGGFGcVF[K]	1	0	0	0	0	1	0
K106	[K]LNQEGFQGHR	1	1	0	0	0	0	0
K155	LLVYEFmQ[K]GSLENHLFR	2	1	1	0	0	0	0
K197	GLAFLHSDPV[K]VIYR	2	0	0	0	0	1	1
K286	RALDHNRPV[K]	1	0	0	0	1	0	0
K337	mASVAVQcLSFEP[K]SRPTm DQVVR	1	0	1	0	0	0	0
C-term								
K358	ALQQLQDNLG[K]PSQTNPV KDTK	9	1	2	0	2	2	2
K366	ALQQLQDNLGKPSQTNPV[K] DTK	7	1	1	0	1	2	2
K369	ALQQLQDNLGKPSQTNPVK DT[K]K	9	2	2	0	1	2	2
K370	[K]LGFKTGTTK/ ALQQLQDNLGKPSQTNPVK DTK[K]	7	2	0	0	0	3	2
K374	KLGF[K]TGTTK	6	1	1	0	0	2	2
K388	FTQ[K]PFGR	11	2	2	1	1	2	3

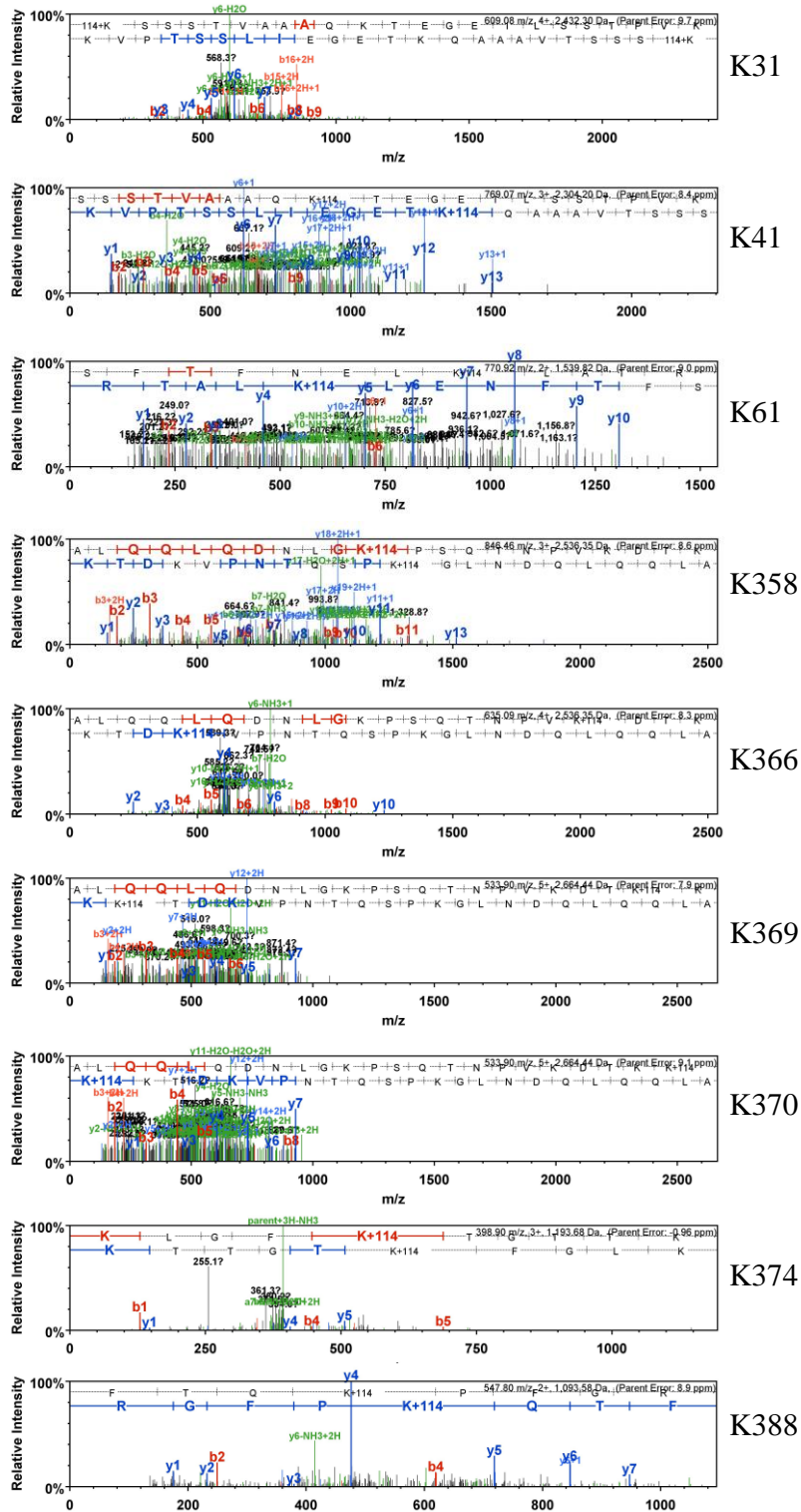


Figure 3B.2. Validation of BIK1 ubiquitination at residues K31, K41, K61, K358, K366, K369, K370, K374, and K388 by manual inspection of -MS/MS spectra. LC-MS/MS spectra of charged ions and mass over charge (m/z) are shown. A mass increment of 114 kDa indicate the covalent incorporation of a ubiquitin moiety.

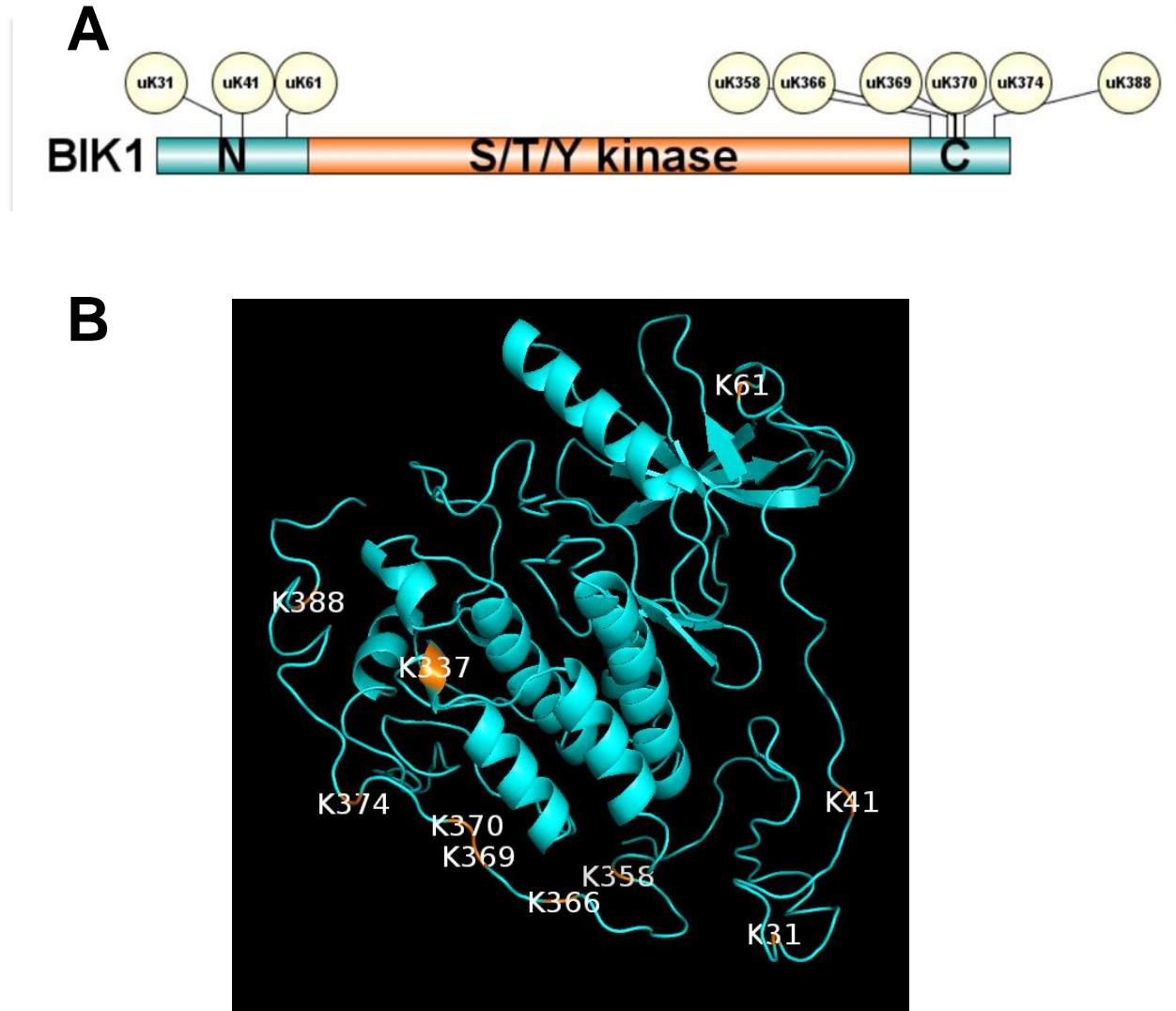


Figure 3B.3. Ubiquitinated lysine residues on BIK1. A) Several lysine residues of *in vivo* BIK1 were identified by mass spectrometry following trypsin digestion and probing with α K- ϵ -GG antibody. N; N-terminal, C; C-terminal, S/T/Y kinase; serine, threonine, and tyrosine kinase, u; ubiquitinated residue. Shown here are the 9 sites we chose to focus on as they were seen in more than one repetition. B) Mapping of ubiquitinated lysine residues on the crystal structure of BIK1 from Lal *et al.* (2018). Modeled in PyMol with protein structure retrieved from Phyre 2.0.

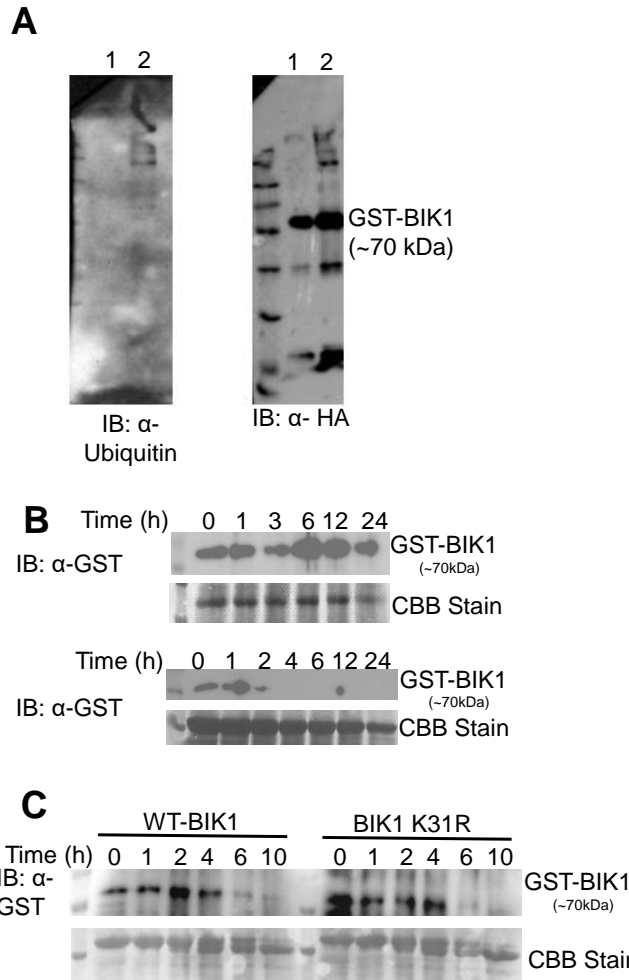


Figure 3B.4. Optimization of *in vitro* ubiquitination assays for determination of BIK1 lysines responsible for its CPK28-, PUB25- and PUB26-mediated degradation. A) *in vitro* ubiquitination assay with E1, E2 and PUB25 E3 ligase with WT-BIK1 to test for optimal polyubiquitination with different concentration of components as described in section 4.5. Lane 1 used 12.5 ng of E1 and 60 ng GST-BIK1. Lane 2 used 50 ng E1 and 150 ng GST-BIK1. B) Cell-free degradation assay to test for BIK1 lysine mutants that suppress BIK1 degradation. The purified recombinant GST-BIK1 was incubated with crude Col-0 protein extract for the indicated time course, and then α -GST immunoblotted. The blot shown in the upper panel used crude protein extract with the plasma-membrane specific protein extraction buffer, the lower blot was with native extraction buffer. C) Preliminary cell-free degradation assay α -GST blot with WT and BIK1-K31R. CBB stain is shown in degradation assays to indicate equal loading.

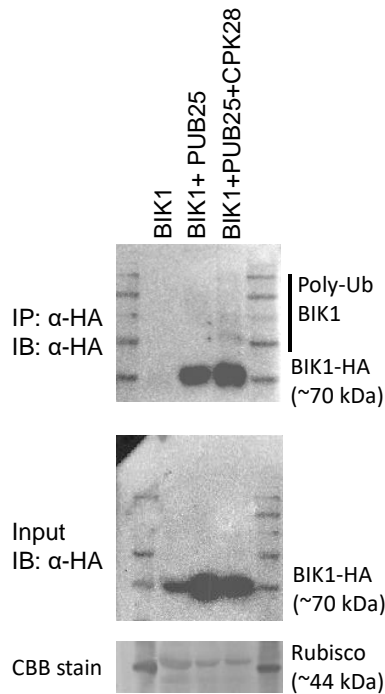


Figure 3B.5. Optimization of *in vivo* ubiquitination assays in *N. benthamiana*. 4-5 week old *N. benthamiana* were transformed with *A. tumefaciens* expressing the indicated protein constructs and tissue was collected at 3 dpi. Total protein was extracted with native protein extraction buffer and α -HA IPs were performed with 50 μ M MG-132 to enrich for BIK1 and prevent proteasome-mediated turnover. Immunoblots were performed using α -HA, and here both the IP and input samples are shown. CBB stain of Rubisco at ~ 46 kDa is included as a loading control to indicate equal sample concentration loading.

4. DISCUSSION

BIK1 is a key RLCK which was initially identified through its increase in transcript accumulation in response to *B. cinerea* (Veronese *et al.*, 2006). It is located downstream as a convergent substrate of many PRRs located at the plant plasma membrane (Zhang *et al.*, 2010). As well as its role in immune signaling, BIK1 is also required for normal plant growth and development, likely through its involvement in ethylene, BR, JA and SA signaling (Laluk *et al.*, 2011). In absence of ligand, it is part of a complex located at the plasma membrane with PRRs such as FLS2 and co-receptor such as BAK1 or related SERKs (Couto & Zipfel, 2016; Lu *et al.*, 2010a; J. Zhang *et al.*, 2010a). Upon PAMP perception, BIK1 is phosphorylated and released from the complex, where it may go on to transduce the signal through interaction with its downstream substrates (Lu *et al.*, 2010; Zhang *et al.*, 2010). One of these substrates that may be targeted by BIK1 following its release from the receptor complex is RBOHD, which is responsible for production of ROS upon pathogen perception (Kadota *et al.*, 2014a; Li *et al.*, 2014b). Additionally, BIK1 has been found to localize to the nucleus upon elf18 perception, where it interacts with WRKY transcription factors to regulate JA and SA signaling (Lal *et al.*, 2018). BIK1 is also required for stomatal closure and the increase in cytosolic Ca²⁺, which together act as part of the plant immune responses (Li *et al.*, 2014; Monaghan *et al.*, 2015; Ranf *et al.*, 2014). As further indication of the importance of BIK1 in immune signaling, it has been identified as the target of several different microbial effector proteins (Feng *et al.*, 2012b; Zhang *et al.*, 2010).

The overexpression of BIK1 can lead to greatly enhanced immune responses (Liang *et al.*, 2016; Monaghan *et al.*, 2014; Veronese *et al.*, 2006), however over-active immune responses prove detrimental to the overall fitness of the plant. Thus, BIK1 is subject to tight regulation to

ensure an optimal immune signaling response. To date, both positive regulation through G protein stabilization (Liang *et al.*, 2016), and negative regulation through a protein phosphatase PP2C38 (Couto *et al.*, 2016) and the calcium-dependent protein kinase CPK28 (Monaghan *et al.*, 2014) have been documented. CPK28 negative regulation and observed BIK1 laddering upon treatment with MG-132 indicated the presence of polyubiquitinated forms of BIK1 suggesting the action of an E3 ligase involved in proteasome-mediated turnover (Monaghan *et al.*, 2014). The Zhou lab in Beijing identified PUB25 and PUB26 as Plant U-box E3 ligases involved in destabilizing BIK1 through polyubiquitination (Wang *et al.*, 2018), and we collaborated on this work. Based on the association of CPK28 with BIK1, and lower accumulation of BIK1 upon CPK28 overexpression, we sought to determine further information about the mechanism of BIK1 turnover through CPK28, PUB25 and PUB26. Therefore, important goals of my thesis were (1) to determine which residues on BIK1 are ubiquitinated *in vivo* contributing to its turnover by the 26S proteasome, and (2) to determine how CPK28 contributes to this regulation.

4.1- CPK28, PUB25 and PUB26 contribute to BIK1 turnover

To assess CPK28 involvement in PUB25 or PUB26-mediated turnover of BIK1, I first tested that there is association between these proteins. Based on previous work indicating association between CPK28 with BIK1 (Monaghan *et al.*, 2014), and on the pull-down assay performed by our collaborators showing BIK1 association with PUB25 and PUB26 (Wang *et al.*, 2018), we used split-luciferase complementation assays and co-IP assays to confirm association of CPK28 with PUB25 and PUB26 (Figure 3A.1-3A.2a-c). We further performed a 3-way co-IP (Figure 3A.2d-e), which indicated the presence of a BIK1-CPK28-PUB25/26 regulatory complex.

With the observation that CPK28, BIK1 and PUB25 or PUB26 associate, the next step was to genetically assess the role of PUB25 and PUB26 in the plant. This began with an analysis

of rosette phenotype in *Arabidopsis* with *pub25-1 pub26-1* and PUB25-OE or PUB26-OE. While the *pub25-1 pub26-1* mutant did not differ from the rosette phenotype of Col-0, the PUB25-OE and PUB26-OE mutants showed a BR hypersensitive rosette phenotype (Figure 3A.4a). This was consistent with lower BIK1 accumulation, as BIK1 acts as a negative regulator of BR signaling (Lin *et al.*, 2013). Additionally, we observed a decreased ROS burst in PUB25-OE and PUB26-OE lines in comparison to wild-type (Figure 3A.4c), indicative of lower levels of BIK1 contributing to a suppressed immune response. Indeed, our collaborators raised antibodies to BIK1, and observed a lower BIK1 accumulation by western blot in these PUB25-OE and PUB26-OE lines, with higher BIK1 accumulation in *pub25-1 pub26-1* in comparison to wild-type (Wang *et al.*, 2018). Following elucidation of the role of PUB25 and PUB26 in negatively regulating BIK1 levels, we sought to determine the placement of CPK28 in the pathway through epistasis analysis. Through the observed suppression of the *cpk28-1* high ROS phenotype by PUB25-OE or PUB26-OE (Figure 3A.5c), we were able to place CPK28 upstream of PUB25 and PUB26 in this BIK1 regulatory pathway. Indeed, our collaborators determined that PUB25 and PUB26 are phosphorylated on T95 and T94, respectively, by CPK28, which enhances their polyubiquitination activity on BIK1 (Wang *et al.*, 2018). This poses a model for CPK28 phosphorylating PUB25 and PUB26 to activate them for facilitation of BIK1 polyubiquitination contributing to its turnover by the 26S proteasome. Interestingly, PUB25 and PUB26 were found to specifically polyubiquitinate non-activated underphosphorylated BIK1, with the BIK1 phosphomimetic mutant of flg22-induced S236/T237 residues showing insensitivity to PUB25- and PUB26-mediated degradation (Wang *et al.*, 2018). It is possible that this targeting of non-activated BIK1 for degradation serves as a mechanism to limit the active pool of BIK1, to mediate the strength of the immune response by preventing further BIK1 activation. It is possible

that the phosphorylation of BIK1 induces a conformational change that masks the polyubiquitination site, thus future structural studies could provide more insight.

Negative regulation by a PUB E3 ligase or a CDPK occurs in several pathways. The PUB25 or PUB26-mediated ubiquitination and turnover of BIK1 is reminiscent of PUB30 negatively regulating *Arabidopsis* salt tolerance through polyubiquitination of BRI1 KINASE INHIBITOR1 (BKI1), a central component in BR signaling (Zhang *et al.*, 2017). Upon BR perception the BRI1 receptor, BAK1 co-receptor, and BKI1 cytoplasmic kinase undergo a phosphorylation cascade resulting in dissociation of BKI1 from its association with downstream targets (Wang *et al.*, 2011), in a similar manner to the BIK1 dissociation from the FLS2-BAK1 receptor complex (Lu *et al.*, 2010; Zhang *et al.*, 2010).

In addition to our CPK28-PUB25/26 as negative regulators of BIK1, a homologous system has been observed in rice, *Oryza sativa* with the BIK1 ortholog OsRLCK176 negatively regulated by the CPK28 ortholog OsCPK4 (Wang *et al.*, 2018). An E3 ligase has not yet been identified, but other group III PUB homologs such as OsPUB31/32/33/34 and OsPUB38/43 have been suggested as possible candidates (Monaghan, 2018), which would point to similar systems of immune signaling regulation across the plant kingdom.

4.2- Analysis of PUB22, PUB23 and PUB24 as other factors in BIK1 turnover

PUB25 and PUB26 were identified as negative regulators of BIK1 accumulation, and thus immune signaling output. However, in our analysis of the PAMP-induced oxidative burst, the *pub25-1 pub26-1* double mutant was not significantly higher than wild-type (Figure 3A.4c). It would be expected that eliminating the E3 ligases involved in polyubiquitinating BIK1 to target it for degradation would result in increased BIK1 levels, and in turn a higher ROS burst through its increased activation of RBOHD. This lack of a statistically significant higher oxidative burst

in the double knockout, as well as the *cpk28-1* mutant having such a drastically increased immune response indicated the involvement of other E3 ligases in catalyzing BIK1 turnover. The analysis of knockout lines can be difficult due to functional redundancy present in large gene families, thus the examination of our dominant PUB25-OE and PUB26-OE lines had more easily interpreted results.

A second line of evidence of involvement of other regulators came from our epistasis analysis in section 3.4. In the CPK28-OE/ *pub25 pub26* lines, if our pathway analysis is correct we would expect that knocking out the E3 ligases would result in higher levels of BIK1 regardless of CPK28 levels. However, we observed a ROS burst that was lower than wild-type, but seemed to partially complement the low ROS burst of the CPK28-OE mutant (Figure 3A.5b). This indicates either the presence of other E3 ligases in BIK1 turnover, or perhaps direct regulation of CPK28 on BIK1. Phosphorylation of BIK1 by CPK28 has previously been observed *in vitro* (Monaghan *et al.*, 2014); however, the nature of this regulation is not currently known.

PUB25 and PUB26 are *Arabidopsis* group III PUBs (Azevedo *et al.*, 2001), closely related PUB22, PUB23 and PUB24, which have previously been shown to redundantly contribute to negatively regulating immune signaling (Trujillo *et al.*, 2008). Consistent with this, PUB22 and PUB23 were shown to strongly destabilize BIK1 in protoplasts, and contain the conserved CPK phosphorylation motif ϕ XXXTXB, where ϕ , X, T and B represent a hydrophobic residue, any residue, threonine and basic residue, respectively (Wang *et al.*, 2018), suggesting that they also play a role in BIK1 degradation by the 26S proteasome. This is further substantiated by our preliminary analyses of *pub22 pub23 pub24/35S:BIK1-HA* lines, where we observed higher BIK1 accumulation (Figure 3A.6b). We additionally performed genetic crosses

to generate a *pub22 pub23 pub24 pub25 pub26* quintuple mutant, and it will be interesting to test whether they play a redundant role in negatively regulating BIK1 accumulation and PAMP-triggered immunity, indicative of functional redundancy. Several other studies have found PUB22 and PUB23 involvement in ubiquitination to regulate both immune responses and drought responses through interaction with different target substrates. The Exo70B2 subunit of the exocyst complex, known for its role in mediating vesicle tethering during exocytosis (He & Guo, 2009), was identified as a target of PUB22 (Stegmann *et al.*, 2012). Involvement of the Exo70B2 subunit has previously been demonstrated to be involved in plant-pathogen interactions (Pečenková *et al.*, 2011). Its degradation was found to be regulated by the PAMP-induced stabilization of PUB22 autocatalytic turnover, which normally autoubiquitinates to catalyze its own proteasome-mediated turnover, and thus PUB22 may contribute to attenuation of PAMP-induced signaling through degradation of Exo70B2 (Stegmann *et al.*, 2012). In addition, PUB22 has also been found to play a role in attenuating PAMP-induced responses through its degradation of MPK3 through a negative feedback loop (Furlan *et al.*, 2017). This negative feedback loop consists of the phosphorylation of PUB22 at sites in and adjacent to the E2 docking domain, resulting in inhibition of PUB22 oligomerization, and thus its autoubiquitination. These studies both present interesting findings where PUB22 autoubiquitination is stabilized upon pathogen infection, acting as a switch to control the level of immune activation. Interestingly, PUB22 and PUB23 play roles in negatively regulating drought tolerance through the ubiquitination of RPN12a and RPN6, which are subunits of the 19S regulatory particle in the 26S proteasome (Cho *et al.*, 2015; Cho *et al.*, 2008), presenting direct regulation of the 26S proteasome by PUB22 and PUB23 response to drought stress.

These results and other studies suggest that group III PUB E3 ubiquitin ligases play many roles and show quite a bit of functional redundancy. Our results indicate regulation of BIK1 by 5 different closely-related PUBs, PUB22, PUB23, PUB24, PUB25 and PUB26. This further indicates the importance of BIK1 in immune responses as a downstream convergent substrate in perception of several different PAMPs (Zhang *et al.*, 2010). The functional redundancy may serve to ensure that BIK1 levels are under constant regulatory control to prevent too drastic an immune response upon PAMP perception, maintaining an immune homeostasis so that the plant can still function in other responses. It is also interesting to note the number of targets for these group III PUBs, associating with and ubiquitinating multiple substrates involved in both immunity and drought stress. This may suggest a complicated mechanism by which these responses are coupled to ensure that the plant is able to respond appropriately by ubiquitinating different targets dependent on the perceived environmental cue, to prevent antagonism between pathways and allow the plant to maintain homeostasis between its responses. Thus, future work may be interesting in determining interplay between these responses and multiple pathways in which the PUB E3 ligases play a role.

4.3- Identifying BIK1 ubiquitination sites

Di-gly enrichment from microsomal fractions followed by LC-MS/MS identified 15 ubiquitinated lysine residues on BIK1, and we chose to focus on 9 which were observed in more than one repetition (K31, K41, K61, K358, K366, K369, K370, K374 and K388). These lysine residues were located on either the N- or C-terminus of BIK1, outside of the kinase domain (Figure 3B.3, Table 3B.1) on accessible parts of the protein when modeled onto the crystal structure from Lal *et al.*, (2018). Our initial attempts at using wild-type tissue were unsuccessful and we speculated that BIK1 was expressed at too low levels. Thus we utilized Col-

0/pBIK1:BIK1-HA lines, which express BIK1 at 100-fold higher levels than wild-type (Monaghan *et al.*, 2014), and included CPK28-OE/pBIK1:BIK1-HA and *cpk28*/pBIK1:BIK1-HA to determine CPK28-mediated ubiquitination sites. Following our mass spectrometry, published work reported that BIK1 is localized to the nucleus upon elf18 treatment where it interacts with WRKY transcription factors to regulate JA/SA signaling (Lal *et al.*, 2018). However, this has never been observed before, and was not reported in an earlier study on immune protein subcellular dynamics (Bücherl *et al.*, 2017). It is possible that our elf18 treatment induced BIK1 localization to the nucleus, and thus by enriching for microsome we may have eliminated a pool of modified BIK1 from our analyses. However, as we are looking at polyubiquitination sites of PUB25 and PUB26, which have not been shown to localize to the nucleus, then this may not be an issue. In addition, the overexpression of BIK1 in these lines may have induced false positives in our identification of ubiquitinated lysine residues. As *A. tumefaciens*-mediated transformation can lead to gene insertion anywhere in the genome, it may have been inserted behind a strong promoter, or in a highly-transcribed region, leading to its overexpression despite the specific pBIK1 promoter. In general, it was difficult to identify patterns in our Col-0/pBIK1:BIK1-HA vs. CPK28-OE/pBIK1:BIK1-HA and *cpk28*/pBIK1:BIK1-HA lines, so parallel reaction monitoring to quantify changes in ubiquitination on these lysine residues is ongoing by our collaborator Dr. Frank Menke. Following performance of these experiments, it was determined that it is non-activated (non-phosphorylated) BIK1 that is ubiquitinated and targeted for degradation by the 26S proteasome (Wang *et al.*, 2018). Thus, the elf18 treatment may not have provided us with the information we were looking for as BIK1 becomes hyperphosphorylated upon elicitor treatment, and thus this treatment may indeed have masked the lysines that are ubiquitinated on non-activated BIK1 due

to a larger activated pool. However, with the use of the unelicited samples, we can still determine sites that may be ubiquitinated, or sites that are ubiquitinated upon elf18 treatment on both BIK1 and within our ubiquitome. In addition, due to possible false positives, the difficulty of distinguishing monoubiquitinated residues from polyubiquitinated residues, and the possibility of multiple sites playing a role, we created site-directed mutants to further test these sites both *in vitro* and *in planta*, and these observations will help to further elucidate the mechanism of BIK1 regulation.

4.4- Troubleshooting ideas for ubiquitination assays

Following generation of the site-directed mutants, I have been examining ubiquitination and degradation of purified recombinant BIK1 through a variety of ubiquitination techniques, including cell-free degradation assays and *in vitro* ubiquitination assays. Optimization of these assays is ongoing, with the cell-free degradation assays beginning to look promising, but no definitive polyubiquitination observed in the *in vitro* ubiquitination assays, so here I present a discussion of possible issues associated with these methods, as well as suggestions for their further optimization. Few plant studies have reported specific ubiquitination sites for proteasome-mediated turnover of individual proteins, instead opting for broad-range mass spectrometry analyses of global ubiquitination sites (Chen *et al.*, 2018; Manzano *et al.*, 2008; Wang *et al.*, 2018). There are mammalian studies that used mutagenesis to mutate conserved lysine residues to arginines to determine which lysine was involved (An *et al.*, 2013; Heras *et al.*, 2018). Each of these pointed to the involvement of one lysine residue, which, along with their quick generation and purification, led me to focus on the single mutants. Increasingly, studies have observed that even when all the lysines on their target protein were mutated to arginine that there was still polyubiquitination and turnover, such as in the case of the major

histocompatibility complex (MHC) (Wang *et al.*, 2007). Interestingly, the authors of this study observed ubiquitination on not only Lys, but also Ser and Cys residues. The α -K- ϵ -GG antibodies that we used enrich for ubiquitinated lysine residues, and thus we may have missed any Cys, Thr, or Ser residues if they were ubiquitinated instead of the classical lysine residues. The ubiquitin-proteasome system is also quite complex, requiring the action of an E1, an E2 and an E3 ligase, as well as ubiquitin and the target protein. Another study has shown that monoubiquitination may also be recognized by the proteasome to initiate protein degradation (Livneh *et al.*, 2017). Thus, ubiquitination and proteasome-mediated turnover of proteins are increasingly complex.

Issues arising with the lack of observed turnover of BIK1 in the degradation assays could be related to deubiquitinating enzymes (DUBs). It has been suggested that DUB activity must be blocked to be more likely to observe ubiquitination, and that EDTA or IAA should be added to the lysis buffer when purifying protein to inhibit DUBs that are metallo-proteases or cysteine proteinases by removing heavy metal ions and alkylate active site cysteine residues of DUBs (Emmerich & Cohen, 2015). Depending on the assay, these DUB inhibitors could also be added to the crude protein extract in which the degradation assays occur, or in extraction buffer for the *in vivo* assays in *N. benthamiana*. Thus, we could prevent any deubiquitinating activity, and thus view ubiquitinated BIK1 species without it being masked by deubiquitination by DUBS. Furthermore, these authors also determined that polyubiquitinated species may not transfer as efficiently in typical western blot transfer conditions, thus suggesting performing the transfer at a lower voltage such as 30 V for 2.5 hr to overnight. This may explain my failure to observe polyubiquitination through the *in vitro* assays as I typically would perform transfers at 90 V for 1.5-2 h.

Finally, as PUB25 and PUB26 were His tagged, I used GST-BIK1 for the *in vitro* ubiquitination assays. GST has been known to form dimers (Fabrini *et al.*, 2009). This dimerization may have prevented proper interaction of BIK1 with PUB25 and PUB26 in these assays, eliminating their ability to polyubiquitinate and contribute to its turnover. For the degradation assays, we were able to use BIK1-His proteins, however for the *in vitro* ubiquitination assays, it may prove useful to use a different protein tag in future. The GST-BIK1 constructs worked for *in vitro* ubiquitination assays in Wang *et al.*, (2018), and as such there may have been an issue with my purified recombinant protein. Furlan *et al.*, (2017) reported the purification of PUB22 in the same day as performing the *in vitro* ubiquitination assays, thus it is possible that freeze-thaw could drastically affect PUB activity, necessitating the use of fresh protein.

4.5- Identification of ubiquitinated proteins upon elf18 treatment

As part of my thesis, I generated a list of proteins that are ubiquitinated through LC-MS/MS analysis following enrichment for ubiquitinated lysine residues from microsomal fractionation. We observed protein ubiquitination with mock or elf18 elicitor treatment, and identified proteins involved in many different pathways. Interestingly, treatment with elf18 enriched for proteins involved in defence responses (FDR <0.05), and both positive and negative regulation of these defence responses. It also enriched for protein kinases. Our dataset of ubiquitinated proteins pulled out many protein kinases, including receptor-like kinases, receptor-like cytoplasmic kinases, calcium-dependent protein kinases, and a variety of other types of kinases (Appendix Table S10). Many of the RLKs and RLCKs included cysteine-rich and leucine-rich repeat domains. Importantly, we observed several RLKs and RLCKs already known to be involved in immunity, such as FLS2, EFR, CERK1, BIK1, FER, BAK1, and PBS1. Observation of FLS2 in

our dataset as a ubiquitinated protein is of interest as it has been found to be ubiquitinated by PUB E3 ligases, PUB12 and PUB13 to facilitate its receptor internalization through endocytosis following flg22 treatment (Lu *et al.*, 2011; Spallek *et al.*, 2013). It has been proposed that this receptor degradation acts as a desensitizing mechanism, to prevent too great an immune response (Smith *et al.*, 2014), similar to the system we propose with maintenance of BIK1 at optimal levels by PUB25 and PUB26. Additionally, our dataset contains many other proteins previously found in immune signaling. These include the NADPH oxidase RBOHD, and HIR1/2, which are induced upon infection with *Pto* DC3000 (Qi *et al.*, 2011), RPS6, which is a NBS-LRR protein that is required for resistance to *P. syringae* (Kim *et al.*, 2009), AHA1, involved in stomatal responses to pathogen perception (Liu *et al.*, 2009), and many more. Also, we found many plasma membrane proteins in our dataset (Appendix Table S11-S12), as well as proteins involved in the ubiquitin-proteasome system, validating the efficiency of our method of plasma membrane and di-Gly enrichment. Additional confirmation comes from the recent rice ubiquitome paper, which identified many orthologs with conserved ubiquitinated lysines to our study (Chen *et al.*, 2018). The involvement of so many protein kinases in ubiquitination processes is interesting as my work looks at interplay between CPK28 and U-box E3 ligases. A number of PUB-interacting kinases have been reported, including in self-incompatibility involving an S-domain receptor kinase and AtPUB9 (Samuel *et al.*, 2008), and in immune signaling, including the *Medicago trunculata* symbiotic receptor-like kinase LYK3 negative regulation by PUB1 (Mbengue *et al.*, 2010), and MPK3 interaction with PUB22 (Furlan *et al.*, 2017). In these cases, the PUB is also phosphorylated by the kinase resulting in feedback loops. Thus, PUBs appear to be central players in mediating a variety of key plant signal transduction pathways, and a role for interplay between phosphorylation and ubiquitination presents itself as a

common theme for regulating activity in immune signaling pathways. Overall, the generation of this dataset provides a tool for future research into a whole host of proteins, and act as a base for elucidating complex regulatory mechanisms in a variety of different pathways, including those involved in immune signaling.

4.6- Future directions

Many further questions have arisen based on the results of this thesis. Most importantly, my work has begun to pinpoint a regulatory mechanism for maintaining optimal levels of BIK1 by the PUB E3 ligases, PUB25 and PUB26, CPK28, and possibly other E3 ligases, with PUB22, PUB23, and PUB24 as promising candidates. Further work is required to understand the specific sites involved in BIK1 regulation and turnover. For example, CPK28 has been found to phosphorylate BIK1 *in vitro* (Monaghan *et al.*, 2014), however this still needs to be verified through a combination of *in vitro* and site-directed mutagenesis assays. This analysis may provide further information on whether CPK28 may bypass PUB25 and PUB26 to exert regulatory effects on BIK1, as indicated in section 3.3 and 3.4, that other proteins may play a role in regulating BIK1 levels, with the possibility of CPK28, BIK1 and PUB25/26 acting as a module on each other. Further work is also required for confirmation of the role of PUB22, PUB23 and PUB24 on BIK1 accumulation. Identification of the lysine residues involved in PUB25/26- and CPK28-mediated turnover will also add to the knowledge of BIK1 regulation, and those maintenance of optimal levels of immune signaling through this pathway. The identification of the residue responsible for turnover may allow future researchers to maintain high levels of BIK1 in crop species to engineer more resistant crops, and further work into the mechanism at which BIK1 is involved in immunity and not development, and vice versa, may help to generate resistant crops that do not show an immunity-growth trade-off. These data will

allow us to understand how PTMs interact, and this could be used to add to knowledge that could lead to engineering crop plants that are resistant without affecting the plant development. It is also important to understand how CPK28 is regulated, as it also plays a role in both immune signaling and development (Matschi *et al.*, 2013; Monaghan *et al.*, 2014).

4.7- Concluding remarks

The work presented in this thesis has further elucidated the mechanism by which BIK1 is maintained at optimal levels, thereby promoting appropriate strength of plant immune signaling in response to pathogen stress. Previously, BIK1 was known to be negatively regulated by CPK28 through regulation and turnover by the 26S proteasome (Monaghan *et al.*, 2014), however the E3 ligase involved in this turnover was unknown as well as the precise mechanism of CPK28 involvement in this turnover. We have confirmed the role of a CPK28-PUB25/26-BIK1 signaling module downstream of multiple PRRs involved in several immune responses, and together with our collaborators in the Zhou Lab, have determined a mechanism by which CPK28 phosphorylates PUB25 or PUB26 to activate them and promote their activity in polyubiquitinating BIK1, targeting it for turnover by the 26S proteasome. This work has also identified lysine residues that are ubiquitinated on BIK1, and work is ongoing to determine which sites are ubiquitinated in a CPK28- and PUB25- or PUB26-mediated fashion. Work on quantification of these substrates stemming from initial tests to determine the sites for targeting by PRM will lead to determination of a dynamic network by which the BIK1 ubiquitination occurs in response to pathogen elicitor treatment. Furthermore, this work also provides a plasma membrane ubiquitome, which represents a technical success and will be broadly useful to researchers interested in ubiquitination. Through generation of this ubiquitome dataset, we also identified several motifs that were commonly found to be ubiquitinated.

Finally, this work leads to an increased understanding of the mechanisms by which plants regulate their immune system to maintain a balance between defence signaling and optimal growth and development. Knowledge gained by this thesis, along with further elucidation of how plants maintain immune homeostasis, may lead to engineering of crops that are more resistant to pathogens, without compromising yield.

SUMMARY

1) CPK28 associates with PUB25 and PUB26, and both BIK1 and PUB25/26 were pulled down in a 3-way co-IP, indicating a regulatory CPK28-PUB25/26-BIK1 complex. This is consistent with work that showed CPK28 interaction with BIK1 (Monaghan *et al.*, 2014), and of BIK1 association with PUB25 and PUB26 (Wang *et al.*, 2018), which are plant U-box E3 ubiquitin ligases.

2) Genetic analyses showed that PUB25 and PUB26 are involved in BIK1 destabilization, with their overexpression and knockout lines contributing to heightened and suppressed ROS burst immune responses, respectively.

3) Epistasis analyses using double mutant combinations of PUB25 or PUB26 and CPK28 knockout and overexpression lines indicated an order for CPK28 acting upstream of PUB25 or PUB26, which are upstream of BIK1. Indeed, Wang *et al.*, (2018) determined that CPK28 phosphorylates PUB25 and PUB26 to activate them and promote their polyubiquitination of BIK1, targeting it for degradation by the 26S proteasome.

4) PUB22, PUB23 and PUB24 may also contribute to BIK1 turnover, with their *pub22 pub23 pub24//35S:BIK1-HA* lines showing higher BIK1 accumulation than *Col-0//35S:BIK1-HA* lines. They also showed greater sensitivity to peptide elicitor in seedling growth inhibition assays, indicative of a hyperactive immune response. Wang *et al.*, (2018) also provided evidence for PUB22 and PUB23 contributing to lower BIK1 accumulation when overexpressed.

5) LC-MS/MS was used to determine ubiquitinated lysine residues on BIK1, and work is ongoing to determine which lysines are ubiquitinated in a CPK28- and PUB25 or PUB26-mediated fashion. Preliminary *in vitro* and *in vivo* ubiquitination assays are presented.

6) This thesis also generated a dataset of plasma membrane ubiquitinated proteins in mock and elf18 treatment, providing a plasma membrane ‘ubiquitome’ for further elucidation of the complex ubiquitin network under resting conditions and upon PAMP perception.

LITERATURE CITED

- Abuqamar, S., Chai, M.-F., Luo, H., Song, F., & Mengiste, T. (2008). Tomato protein kinase 1b mediates signaling of plant responses to necrotrophic fungi and insect herbivory. *The Plant Cell*, 20(7), 1964–83.
- Adams, E. H. G., & Spoel, S. H. (2018). The ubiquitin–proteasome system as a transcriptional regulator of plant immunity. *Journal of Experimental Botany*, 69(19), 4529–4537.
- Akimoto-Tomiyama, C., Tanabe, S., Kajiwara, H., Minami, E., & Ochiai, H. (2018). Loss of chloroplast-localized protein phosphatase 2Cs in *Arabidopsis thaliana* leads to enhancement of plant immunity and resistance to *Xanthomonas campestris* pv. *campestris* infection. *Molecular Plant Pathology*, 19(5), 1184–1195.
- An, L., Jia, W., Yu, Y., Zou, N., Liang, L., Zhao, Y., Fan, Y., Cheng, J., Shi, Z., Xu, G., Li, G., Yang, J., & Zhang, H. (2013). Lys63-linked polyubiquitination of BRAF at lysine 578 is required for BRAF-mediated signaling. *Scientific Reports*, 3(1), 2344.
- Asai, T., Tena, G., Plotnikova, J., Willmann, M. R., Chiu, W.-L., Gomez-Gomez, L., Boller, T., Ausubel, F.M., & Sheen, J. (2002). MAP kinase signalling cascade in *Arabidopsis* innate immunity. *Nature*, 415(28), 977–983.
- Ausubel, F. M. (2005). Are innate immune signaling pathways in plants and animals conserved? *Nature Immunology*, 6(10), 973–979.
- Azevedo, C., Santos-Rosa, M. J., & Shirasu, K. (2001). The U-box protein family in plants. *Trends in Plant Science*, 6(8), 354–8.
- Beck, M., Zhou, J., Faulkner, C., MacLean, D., & Robatzek, S. (2012). Spatio-temporal cellular dynamics of the *Arabidopsis* flagellin receptor reveal activation status-dependent endosomal sorting. *The Plant Cell*, 24(10), 4205–4219.
- Benschop, J. J., Mohammed, S., O’Flaherty, M., Heck, A. J. R., Slijper, M., & Menke, F. L. H. (2007). Quantitative phosphoproteomics of early elicitor signaling in *Arabidopsis*. *Molecular & Cellular Proteomics*, 6(7), 1198–1214.
- Bent, A. (2006). *Arabidopsis thaliana* floral dip transformation method. *Methods of Molecular Biology* 343, 87–103.
- Betts, M. J., & Russell, R. B. (2003). Amino acid properties and consequences of substitutions. *Bioinformatics for Geneticists*. New York Wiley.
- Blume, B., Nürnberger, T., Nass, N., & Scheel, D. (2000). Receptor-mediated increase in cytoplasmic free calcium required for activation of pathogen defense in parsley. *The Plant Cell*, 12(8), 1425–40.
- Boehm, T., & Swann, J. B. (2014). Origin and evolution of adaptive immunity. *Annual Review of Animal Biosciences*, 2(1), 259–283.
- Boller, T., & Felix, G. (2009). A renaissance of elicitors: perception of microbe-associated molecular patterns and danger signals by pattern-recognition receptors. *Annual Review of Plant Biology*, 60, 379–406.
- Bommert, P., Je, B. Il, Goldshmidt, A., & Jackson, D. (2013). The maize $G\alpha$ gene COMPACT PLANT2 functions in CLAVATA signalling to control shoot meristem size. *Nature*, 502(7472), 555–8.
- Boudsocq, M., & Sheen, J. (2013). CDPKs in immune and stress signaling. *Trends in Plant Science*, 18(1), 30–40.
- Boutrot, F., Segonzac, C., Chang, K. N., Qiao, H., Ecker, J. R., Zipfel, C., & Rathjen, J. P. (2010). Direct transcriptional control of the *Arabidopsis* immune receptor FLS2 by the ethylene-dependent transcription factors EIN3 and EIL1. *Proceedings of the National Academy of Sciences of the United States of America*, 107(32), 14502–7.
- Bowling, S. A., Clarke, J. D., Liu, Y., Klessig, D. F., & Dong, X. (1997). The *cpr5* mutant of *Arabidopsis* expresses both NPR1-dependent and NPR1-independent resistance. *The Plant Cell Online*, 9(9), 1573–1584.
- Bücherl, C. A., Jarsch, I. K., Schudoma, C., Segonzac, C., Mbengue, M., Robatzek, S., MacLean, D., Ott,

- T., & Zipfel, C. (2017). Plant immune and growth receptors share common signalling components but localise to distinct plasma membrane nanodomains. *eLife*, 6.
- Callis, J. (2014). The ubiquitination machinery of the ubiquitin system. *The Arabidopsis Book*, 12, e0174.
- Cao, Y., Liang, Y., Tanaka, K., Nguyen, C. T., Jedrzejczak, R. P., Joachimiak, A., & Stacey, G. (2014). The kinase LYK5 is a major chitin receptor in *Arabidopsis* and forms a chitin-induced complex with related kinase CERK1. *eLife*, 3.
- Chen, J.-G., Ullah, H., Temple, B., Liang, J., Guo, J., Alonso, J. M., Ecker, J.R., & Jones, A. M. (2006). RACK1 mediates multiple hormone responsiveness and developmental processes in *Arabidopsis*. *Journal of Experimental Botany*, 57(11), 2697–2708.
- Chen, J.-G., Willard, F. S., Huang, J., Liang, J., Chasse, S. A., Jones, A. M., & Siderovski, D. P. (2003). A seven-transmembrane RGS protein that modulates plant cell proliferation. *Science*, 301(5640), 1728–1731.
- Chen, Q., Yang, X., & Xie, Q. (2016). Approaches to determine protein ubiquitination residue types. *Methods in Molecular Biology (Clifton, N.J.)*, 1450, 3–10.
- Chen, T., Zhou, T., He, B., Yu, H., Guo, X., Song, X., & Sha, J. (2014). mUbiSiDa: a comprehensive database for protein ubiquitination sites in mammals. *PLoS One*, 9(1), e85744.
- Chen, X.-L., Xie, X., Wu, L., Liu, C., Zeng, L., Zhou, X., Luo, F., Wang, G.L., & Liu, W. (2018). Proteomic analysis of ubiquitinated proteins in rice (*Oryza sativa*) after treatment with pathogen-associated molecular pattern (PAMP) elicitors. *Frontiers in Plant Science*, 9, 1064.
- Cheng, Y. T., & Li, X. (2012). Ubiquitination in NB-LRR-mediated immunity. *Current Opinion in Plant Biology*, 15(4), 392–399.
- Cheng, Z., Li, J.-F., Niu, Y., Zhang, X.-C., Woody, O. Z., Xiong, Y., Djonovic, S., Millet, Y., Bush, J., McConkey, B.J., Sheen, J., & Ausubel, F. M. (2015). Pathogen-secreted proteases activate a novel plant immune pathway. *Nature*, 521(7551), 213–216.
- Cho, S. K., Bae, H., Ryu, M. Y., Wook Yang, S., & Kim, W. T. (2015). PUB22 and PUB23 U-BOX E3 ligases directly ubiquitinate RPN6, a 26S proteasome lid subunit, for subsequent degradation in *Arabidopsis thaliana*. *Biochemical and Biophysical Research Communications*, 464(4), 994–999.
- Cho, S. K., Ryu, M. Y., Song, C., Kwak, J. M., & Kim, W. T. (2008). *Arabidopsis* PUB22 and PUB23 are homologous U-Box E3 ubiquitin ligases that play combinatorial roles in response to drought stress. *The Plant Cell*, 20(7), 1899–914.
- Choe, S., Fujioka, S., Noguchi, T., Takatsuto, S., Yoshida, S., & Feldmann, K. A. (2001). Overexpression of DWARF4 in the brassinosteroid biosynthetic pathway results in increased vegetative growth and seed yield in *Arabidopsis*. *The Plant Journal*, 26(6), 573–582.
- Chou, M. F., & Schwartz, D. (2011). Biological sequence motif discovery using motif-x. *Current Protocols in Bioinformatics, Chapter 13*, Unit 13.15-24.
- Christou, P., & Twyman, R. M. (2018). The potential of genetically enhanced plants to address food insecurity. *Nutrition Research Reviews*, 17, 23–42.
- Clarke, J. D., Volko, S. M., Ledford, H., Ausubel, F. M., & Dong, X. (2000). Roles of salicylic acid, jasmonic acid, and ethylene in cpr-induced resistance in *Arabidopsis*. *The Plant Cell*, 12(11), 2175–90.
- Clough, S. J., & Bent, A. F. (1998). Floral dip: a simplified method for *Agrobacterium*-mediated transformation of *Arabidopsis thaliana*. *The Plant Journal: For Cell and Molecular Biology*, 16(6), 735–43.
- Couto, D., Niebergall, R., Liang, X., Bücherl, C. A., Sklenar, J., Macho, A. P., Ntoukakis, V., Derbyshire, P., Altenbach, D., Maclean, D., Robatzek, S., Uhrig, J., Menke, F.M., Zhou, J.M., & Zipfel, C. (2016). The *Arabidopsis* protein phosphatase PP2C38 negatively regulates the central immune kinase BIK1. *PLoS Pathogens*, 12(8), e1005811.
- Couto, D., & Zipfel, C. (2016). Regulation of pattern recognition receptor signalling in plants. *Nature Reviews Immunology*, 16(9), 537–552.
- Dangl, J. L., Dietrich, R. A., & Richberg, M. H. (1996). Death don't have no mercy: cell death programs in plant-microbe interactions. *The Plant Cell*, 8(10), 1793–1807.

- Dielen, A.S., Badaoui, S., Candresse, T., & German-Retana, S. (2010). The ubiquitin/26S proteasome system in plant-pathogen interactions: a never-ending hide-and-see game. *Molecular Plant Pathology*, *11*(2), 293–308.
- Ding, L., Pandey, S., & Assmann, S. M. (2007). *Arabidopsis* extra-large G proteins (XLGs) regulate root morphogenesis. *The Plant Journal*, *53*(2), 248–263.
- Du, C., Li, X., Chen, J., Chen, W., Li, B., Li, C., Wang, L., Li, J., Zhao, X., Lin, J., Liu, X., Luan, S., & Yu, F. (2016). Receptor kinase complex transmits RALF peptide signal to inhibit root growth in *Arabidopsis*. *Proceedings of the National Academy of Sciences of the United States of America*, *113*(51), 8326–8334.
- Emmerich, C. H., & Cohen, P. (2015). Optimising methods for the preservation, capture and identification of ubiquitin chains and ubiquitylated proteins by immunoblotting. *Biochemical and Biophysical Research Communications*, *466*(1), 1–14.
- Escudero, V., Jordá, L., Sopenña-Torres, S., Mélida, H., Miedes, E., Muñoz-Barríos, A., Swami, S., Alexander, D., McKee, L.S., Sanchez-Vallet, A., Bulone, V., Jones, A.M., & Molina, A. (2017). Alteration of cell wall xylan acetylation triggers defense responses that counterbalance the immune deficiencies of plants impaired in the β -subunit of the heterotrimeric G-protein. *The Plant Journal*, *92*(3), 386–399.
- Fabrini, R., De Luca, A., Stella, L., Mei, G., Orioni, B., Ciccone, S., Federici, G., Lo Bello, M., & Ricci, G. (2009). Monomer–dimer equilibrium in glutathione transferases: a critical re-examination. *Biochemistry*, *48*(43), 10473–10482.
- Feng, F., Yang, F., Rong, W., Wu, X., Zhang, J., Chen, S., He, C., & Zhou, J.-M. (2012a). A *Xanthomonas* uridine 5'-monophosphate transferase inhibits plant immune kinases. *Nature*, *485*(7396), 114–8.
- Forget, A., Ayrault, O., Den Besten, W., Kuo, M.-L., Sherr, C. J., & Roussel, M. F. (2008). Differential post-transcriptional regulation of two Ink4 proteins, p18 Ink4c and p19 Ink4d. *Cell Cycle*, *7*(23), 3737–3746.
- Friso, G., & van Wijk, K. J. (2015). Post-translational protein modifications in plant metabolism. *Plant Physiology*, *169*(3), pp.01378.2015.
- Furlan, G., Nakagami, H., Eschen-Lippold, L., Jiang, X., Majovsky, P., Kowarschik, K., Hoehenwarter, W., Lee, J., & Trujillo, M. (2017). Changes in PUB22 ubiquitination modes triggered by MITOGEN-ACTIVATED PROTEIN KINASE3 dampen the immune response. *The Plant Cell*, *29*(4), 726–745.
- Gibson, D. G., Young, L., Chuang, R.-Y., Venter, J. C., Hutchison, C. A., & Smith, H. O. (2009). Enzymatic assembly of DNA molecules up to several hundred kilobases. *Nature Methods*, *6*(5), 343–345.
- Gimenez-Ibanez, S., Hann, D. R., Ntoukakis, V., Petutschnig, E., Lipka, V., & Rathjen, J. P. (2009). AvrPtoB targets the LysM receptor kinase CERK1 to promote bacterial virulence on plants. *Current Biology*, *19*(5), 423–429.
- Göhre, V., Spallek, T., Häweker, H., Mersmann, S., Mentzel, T., Boller, T., de Torres, M., Mansfield, J.W., & Robatzek, S. (2008). Plant pattern-recognition receptor FLS2 is directed for degradation by the bacterial ubiquitin ligase AvrPtoB. *Current Biology*, *18*(23), 1824–1832.
- Gómez-Gómez, L., & Boller, T. (2000). FLS2: an LRR receptor-like kinase involved in the perception of the bacterial elicitor flagellin in *Arabidopsis*. *Molecular Cell*, *5*(6), 1003–11.
- Gómez-Gómez, L., Felix, G., & Boller, T. (1999). A single locus determines sensitivity to bacterial flagellin in *Arabidopsis thaliana*. *The Plant Journal : For Cell and Molecular Biology*, *18*(3), 277–84.
- Gonzalez-Lamothe, R., Tsitsigiannis, D. I., Ludwig, A. A., Panicot, M., Shirasu, K., & Jones, J. D. G. (2006). The U-box protein CMPG1 is required for efficient activation of defense mechanisms triggered by multiple resistance genes in tobacco and tomato. *The Plant Cell Online*, *18*(4), 1067–1083.
- Gust, A. A., Pruitt, R., & Nürnberger, T. (2017). Sensing danger: key to activating plant immunity.

- Trends in Plant Science*, 22(9), 779–791.
- Guy, E., Lautier, M., Chabannes, M., Roux, B., Lauber, E., Arlat, M., & Noël, L. D. (2013). xopAC-triggered immunity against *Xanthomonas* depends on *Arabidopsis* receptor-like cytoplasmic kinase genes PBL2 and RIPK. *PLoS One*, 8(8), e73469.
- Haas, A. L., Warms, J. V., Hershko, A., & Rose, I. A. (1982). Ubiquitin-activating enzyme. Mechanism and role in protein-ubiquitin conjugation. *The Journal of Biological Chemistry*, 257(5), 2543–8.
- Hamel, L.-P., Sheen, J., & Séguin, A. (2014). Ancient signals: comparative genomics of green plant CDPKs. *Trends in Plant Science*, 19(2), 79–89.
- Hashiguchi, A., & Komatsu, S. (2016). Impact of post-translational modifications of crop proteins under abiotic stress. *Proteomes*, 4(4), 42.
- Hatfield, P. M., Gosink, M. M., Carpenter, T. B., & Vierstra, R. D. (1997). The ubiquitin-activating enzyme (E1) gene family in *Arabidopsis thaliana*. *The Plant Journal : For Cell and Molecular Biology*, 11(2), 213–26.
- He, B., & Guo, W. (2009). The exocyst complex in polarized exocytosis. *Current Opinion in Cell Biology*, 21(4), 537–542.
- Heise, A., Lippok, B., Kirsch, C., & Hahlbrock, K. (2002). Two immediate-early pathogen-responsive members of the AtCMPG gene family in *Arabidopsis thaliana* and the W-box-containing elicitor-response element of AtCMPG1. *Proceedings of the National Academy of Sciences of the United States of America*, 99(13), 9049–54.
- Henty-Ridilla, J. L., Shimono, M., Li, J., Chang, J. H., Day, B., & Staiger, C. J. (2013). The plant actin cytoskeleton responds to signals from microbe-associated molecular patterns. *PLoS Pathogens*, 9(4), e1003290.
- Heras, G., Namuduri, A. V., Traini, L., Shevchenko, G., Falk, A., Bergström Lind, S., Mi, J., Tian, G., & Gastaldello, S. (2018). Muscle RING-finger protein-1 (MuRF1) functions and cellular localization are regulated by SUMO1 post-translational modification. *Journal of Molecular Cell Biology*, doi: 10.1093/jmcb/mjy036.
- Huffaker, A., & Ryan, C. A. (2007). Endogenous peptide defense signals in *Arabidopsis* differentially amplify signaling for the innate immune response. *Proceedings of the National Academy of Sciences*, 104(25), 10732–10736.
- Huot, B., Yao, J., Montgomery, B. L., & He, S. Y. (2014). Growth–defense tradeoffs in plants: a balancing act to optimize fitness. *Molecular Plant*, 7(8), 1267–1287.
- Indriolo, E., Safavian, D., & Goring, D. R. (2014). The ARC1 E3 ligase promotes two different self-pollen avoidance traits in *Arabidopsis*. *The Plant Cell*, 26(4), 1525–1543.
- Ishikawa, A. (2009). The *Arabidopsis* G-protein β -subunit is required for defense response against *Agrobacterium tumefaciens*. *Bioscience, Biotechnology, and Biochemistry*, 73(1), 47–52.
- Ishikura, S., Weissman, A. M., & Bonifacino, J. S. (2010). Serine residues in the cytosolic tail of the T-cell antigen receptor alpha-chain mediate ubiquitination and endoplasmic reticulum-associated degradation of the unassembled protein. *The Journal of Biological Chemistry*, 285(31), 23916–24.
- Isono, E., Katsiarimpa, A., Müller, I. K., Anzenberger, F., Stierhof, Y.-D., Geldner, N., Chory, J., & Schwechheimer, C. (2010). The deubiquitinating enzyme AMSH3 is required for intracellular trafficking and vacuole biogenesis in *Arabidopsis thaliana*. *The Plant Cell*, 22(6), 1826–1837.
- Kadota, Y., Sklenar, J., Derbyshire, P., Stransfeld, L., Asai, S., Ntoukakis, V., Jones, J.D., Shirasu, K., Menke, F.L.H., Jones, A., & Zipfel, C. (2014). Direct regulation of the NADPH oxidase RBOHD by the PRR-associated kinase BIK1 during plant immunity. *Molecular Cell*, 54(1), 43–55.
- Karimi, M., Inzé, D., & Depicker, A. (2002). GATEWAY vectors for *Agrobacterium*-mediated plant transformation. *Trends in Plant Science*, 7(5), 193–5.
- Kim, D.-Y., Scalf, M., Smith, L. M., & Vierstra, R. D. (2013). Advanced proteomic analyses yield a deep catalog of ubiquitylation targets in *Arabidopsis*. *The Plant Cell*, 25(5), 1523–1540.
- Kim, S. H., Kwon, S. Il, Saha, D., Anyanwu, N. C., & Gassmann, W. (2009). Resistance to the *Pseudomonas syringae* effector HopA1 is governed by the TIR-NBS-LRR protein RPS6 and is enhanced by mutations in SRFR1. *Plant Physiology*, 150(4), 1723–32.

- Kim, T.-W., Guan, S., Burlingame, A. L., & Wang, Z.-Y. (2011). The CDG1 kinase mediates brassinosteroid signal transduction from BRI1 receptor kinase to BSU1 phosphatase and GSK3-like kinase BIN2. *Molecular Cell*, *43*(4), 561–71.
- Kimura, Y., & Tanaka, K. (2010). Regulatory mechanisms involved in the control of ubiquitin homeostasis. *Journal of Biochemistry*, *147*(6), 793–798.
- Kirsch, C., Logemann, E., Lippok, B., Schmelzer, E., & Hahlbrock, K. (2001). A highly specific pathogen-responsive promoter element from the immediate-early activated CMPG1 gene in *Petroselinum crispum*. *The Plant Journal : For Cell and Molecular Biology*, *26*(2), 217–27.
- Kong, L., Cheng, J., Zhu, Y., Ding, Y., Meng, J., Chen, Z., Xie, Q., Guo, Y., Li, J., Yang, S., & Gong, Z. (2015). Degradation of the ABA co-receptor ABI1 by PUB12/13 U-box E3 ligases. *Nature Communications*, *6*(1), 8630.
- Kunze, G., Zipfel, C., Robatzek, S., Niehaus, K., Boller, T., & Felix, G. (2004). The N terminus of bacterial elongation factor Tu elicits innate immunity in *Arabidopsis* plants. *The Plant Cell*, *16*(12), 3496–507.
- Kurepa, J., & Smalle, J. A. (2008). To misfold or to lose structure?: Detection and degradation of oxidized proteins by the 20S proteasome. *Plant Signaling & Behavior*, *3*(6), 386–8.
- Lakatos, L., Szittyá, G., Silhavy, D., & Burgyán, J. (2004). Molecular mechanism of RNA silencing suppression mediated by p19 protein of tombusviruses. *The EMBO Journal*, *23*(4), 876–84.
- Lal, N. K., Nagalakshmi, U., Hurlburt, N. K., Flores, R., Bak, A., Sone, P., Ma, X., Song, G., Walley, J., Shan, L., He, P., Casteel, C., Fisher, A.J., & Dinesh-Kumar, S. P. (2018). The receptor-like cytoplasmic kinase BIK1 localizes to the nucleus and regulates defense hormone expression during plant innate immunity. *Cell Host & Microbe*, *23*(4), 485–497.
- Laluk, K., Luo, H., Chai, M., Dhawan, R., Lai, Z., & Mengiste, T. (2011). Biochemical and genetic requirements for function of the immune response regulator BOTRYTIS-INDUCED KINASE1 in plant growth, ethylene signaling, and PAMP-triggered immunity in *Arabidopsis*. *The Plant Cell*, *23*(8), 2831–2849.
- Lei, J. X., Finlayson, S. a, Salzman, R. a, Shan, L. B., & Zhu-Salzman, K. (2014). BOTRYTIS-INDUCED KINASE1 modulates *Arabidopsis* resistance to green peach aphids via PHYTOALEXIN DEFICIENT4. *Plant Physiology*, *165*(4), 1657–1670.
- Li, L., Li, M., Yu, L., Zhou, Z., Liang, X., Liu, Z., Cai, G., Gao, L., Zhang, X., Wang, Y., Chen, S., & Zhou, J. M. (2014). The FLS2-associated kinase BIK1 directly phosphorylates the NADPH oxidase RbohD to control plant immunity. *Cell Host and Microbe*, *15*(3), 329–338.
- Li, L., Yu, Y., Zhou, Z., & Zhou, J.-M. (2016). Plant pattern-recognition receptors controlling innate immunity. *Science China Life Sciences*, *59*(9), 878–888.
- Liang, X., Ding, P., Lian, K., Wang, J., Ma, M., Li, L., Li, M., Zhang, X., Chen, S., Zhang, Y., & Zhou, J.-M. (2016). *Arabidopsis* heterotrimeric G proteins regulate immunity by directly coupling to the FLS2 receptor. *eLife*, *5*, 1–18.
- Liao, D., Cao, Y., Sun, X., Espinoza, C., Nguyen, C. T., Liang, Y., & Stacey, G. (2017). *Arabidopsis* E3 ubiquitin ligase PLANT U-BOX13 (PUB13) regulates chitin receptor LYSIN MOTIF RECEPTOR KINASE5 (LYK5) protein abundance. *The New Phytologist*, *214*(4), 1646–1656.
- Lin, W., Li, B., Lu, D., Chen, S., Zhu, N., He, P., & Shan, L. (2014). Tyrosine phosphorylation of protein kinase complex BAK1/BIK1 mediates *Arabidopsis* innate immunity. *Proceedings of the National Academy of Sciences of the United States of America*, *111*(9), 3632–7.
- Lin, W., Lu, D., Gao, X., Jiang, S., Ma, X., Wang, Z., Mengiste, T., He, P., & Shan, L. (2013). Inverse modulation of plant immune and brassinosteroid signaling pathways by the receptor-like cytoplasmic kinase BIK1. *Proceedings of the National Academy of Sciences*, *110*(29), 12114–12119.
- Lin, Z.-J. D., Liebrand, T. W. H., Yadeta, K. A., & Coaker, G. (2015). PBL13 is a serine/threonine protein kinase that negatively regulates *Arabidopsis* immune responses. *Plant Physiology*, *169*(4), 2950–62.
- Liu, C., Shen, W., Yang, C., Zeng, L., & Gao, C. (2018). Knowns and unknowns of plasma membrane

- protein degradation in plants. *Plant Science*, 272, 55–61.
- Liu, J., Ding, P., Sun, T., Nitta, Y., Dong, O., Huang, X., Yang, W., Li, X., Botella, B.R., & Zhang, Y. (2013). Heterotrimeric G proteins serve as a converging point in plant defense signaling activated by multiple receptor-like kinases. *Plant Physiology*, 161(4), 2146–2158.
- Liu, J., Elmore, J. M., Fuglsang, A. T., Palmgren, M. G., Staskawicz, B. J., & Coaker, G. (2009). RIN4 functions with plasma membrane H⁺-ATPases to regulate stomatal apertures during pathogen attack. *PLoS Biology*, 7(6), e1000139.
- Liu, J., Zhong, S., Guo, X., Hao, L., Wei, X., Huang, Q., Hou, Y., Shi, J., Wang, C., Gu, H., & Qu, L.-J. (2013). Membrane-bound RLCKs LIP1 and LIP2 are essential male factors controlling male-female attraction in *Arabidopsis*. *Current Biology*, 23(11), 993–998.
- Liu, L., Zhang, Y., Tang, S., Zhao, Q., Zhang, Z., Zhang, H., Dong, L., Guo, H., & Xie, Q. (2010). An efficient system to detect protein ubiquitination by agroinfiltration in *Nicotiana benthamiana*. *The Plant Journal*, 61(5), 893–903.
- Liu, Z., Wu, Y., Yang, F., Zhang, Y., Chen, S., Xie, Q., Tian, X., & Zhou, J.-M. (2013). BIK1 interacts with PEPRs to mediate ethylene-induced immunity. *Proceedings of the National Academy of Sciences of the United States of America*, 110(15), 6205–10.
- Livneh, I., Kravtsova-Ivantsiv, Y., Braten, O., Kwon, Y. T., & Ciechanover, A. (2017). Monoubiquitination joins polyubiquitination as an esteemed proteasomal targeting signal. *BioEssays*, 39(6), 1700027.
- Llorente, F., Alonso-Blanco, C., Sánchez-Rodríguez, C., Jorda, L., & Molina, A. (2005). ERECTA receptor-like kinase and heterotrimeric G protein from *Arabidopsis* are required for resistance to the necrotrophic fungus *Plectosphaerella cucumerina*. *The Plant Journal : For Cell and Molecular Biology*, 43(2), 165–80.
- Lorek, J., Griebel, T., Jones, A. M., Kuhn, H., & Panstruga, R. (2013). The role of *Arabidopsis* heterotrimeric G-protein subunits in MLO2 function and MAMP-triggered immunity. *Molecular Plant-Microbe Interactions : MPMI*, 26(9), 991–1003.
- Lozano-Durán, R., & Zipfel, C. (2015). Trade-off between growth and immunity: role of brassinosteroids. *Trends in Plant Science*, 20(1), 12–19.
- Lu, D., Lin, W., Gao, X., Wu, S., Cheng, C., Avila, J., Heese, A., Devarenne, T.P., He, P., & Shan, L. (2011). Direct ubiquitination of pattern recognition receptor FLS2 attenuates plant innate immunity. *Science (New York, N.Y.)*, 332(6036), 1439–42.
- Lu, D., Wu, S., Gao, X., Zhang, Y., Shan, L., & He, P. (2010). A receptor-like cytoplasmic kinase, BIK1, associates with a flagellin receptor complex to initiate plant innate immunity. *Proceedings of the National Academy of Sciences of the United States of America*, 107(1), 496–501.
- Lu, D., Wu, S., He, P., & Shan, L. (2010). Phosphorylation of receptor-like cytoplasmic kinases by bacterial flagellin. *Plant Signaling & Behavior*, 5(5), 598–600.
- Ma, Y., Dai, X., Xu, Y., Luo, W., Zheng, X., Zeng, D., Pan, Y., Lin, X., Liu, H., Zhang, D., Xiao, J., Guo, X., Xu, S., Niu, Y., Jin, J., Zhang, H., Xu, X., Li, L., Wang, W., Qian, Q., Ge, S., & Chong, K. (2015). COLD1 confers chilling tolerance in rice. *Cell*, 160(6), 1209–1221.
- Macho, A. P., & Zipfel, C. (2014). Plant PRRs and the activation of innate immune signaling. *Molecular Cell*, 54(2), 263–272.
- Macho, A. P., & Zipfel, C. (2015). Targeting of plant pattern recognition receptor-triggered immunity by bacterial type-III secretion system effectors. *Current Opinion in Microbiology*, 23, 14–22.
- Manzano, C., Abraham, Z., López-Torrejón, G., & Del Pozo, J. C. (2008). Identification of ubiquitinated proteins in *Arabidopsis*. *Plant Molecular Biology*, 68(1–2), 145–158.
- Maor, R., Jones, A., Nühse, T. S., Studholme, D. J., Peck, S. C., & Shirasu, K. (2007). Multidimensional protein identification technology (MudPIT) analysis of ubiquitinated proteins in plants. *Molecular & Cellular Proteomics : MCP*, 6(4), 601–10.
- Marino, D., Peeters, N., & Rivas, S. (2012). Ubiquitination during plant immune signaling. *Plant Physiology*, 160(1), 15–27.
- Maruta, N., Trusov, Y., Brenya, E., Parekh, U., & Botella, J. R. (2015). Membrane-localized extra-large

- G proteins and G $\beta\gamma$ of the heterotrimeric G proteins form functional complexes engaged in plant immunity in *Arabidopsis*. *Plant Physiology*, 167(3), 1004–1016.
- Matschi, S., Werner, S., Schulze, W. X., Legen, J., Hilger, H. H., & Romeis, T. (2013). Function of calcium-dependent protein kinase CPK28 of *Arabidopsis thaliana* in plant stem elongation and vascular development. *The Plant Journal*, 73(6), 883–896.
- Mbengue, M., Bourdais, G., Gervasi, F., Beck, M., Zhou, J., Spallek, T., Bartels, S., Boller, T., Ueda, T., Kuhn, H., & Robatzek, S. (2016). Clathrin-dependent endocytosis is required for immunity mediated by pattern recognition receptor kinases. *Proceedings of the National Academy of Sciences*, 113(39), 11034–11039.
- Mbengue, M., Camut, S., de Carvalho-Niebel, F., Deslandes, L., Froidure, S., Klaus-Heisen, D., Moreau, S., Rivas, S., Timmers, T., Herve, C., Cullimore, J., & Lefebvre, B. (2010). The *Medicago truncatula* E3 ubiquitin ligase PUB1 interacts with the LYK3 symbiotic receptor and negatively regulates infection and nodulation. *The Plant Cell*, 22(10), 3474–3488.
- Mersmann, S., Bourdais, G., Rietz, S., & Robatzek, S. (2010). Ethylene signaling regulates accumulation of the FLS2 receptor and is required for the oxidative burst contributing to plant immunity. *Plant Physiology*, 154(1), 391–400.
- Miya, A., Albert, P., Shinya, T., Desaki, Y., Ichimura, K., Shirasu, K., Narusaka, Y., Kawakami, N., Kaku, H., & Shibuya, N. (2007). CERK1, a LysM receptor kinase, is essential for chitin elicitor signaling in *Arabidopsis*. *Proceedings of the National Academy of Sciences of the United States of America*, 104(49), 19613–8.
- Monaghan, J. (2018). Conserved degradation of orthologous RLCKs regulates immune homeostasis. *Trends in Plant Science*, 23(7), 554–557.
- Monaghan, J., Matschi, S., Romeis, T., & Zipfel, C. (2015). The calcium-dependent protein kinase CPK28 negatively regulates the BIK1-mediated PAMP-induced calcium burst. *Plant Signaling & Behavior*, 10(5), e1018497.
- Monaghan, J., Matschi, S., Shorinola, O., Rovenich, H., Matei, A., Segonzac, C., Malinovsky, F.G., Rathjen, J.P., MacLean, D., Romeis, T., & Zipfel, C. (2014). The calcium-dependent protein kinase CPK28 buffers plant immunity and regulates BIK1 turnover. *Cell Host and Microbe*, 16(5), 605–615.
- Mudgil, Y., Shiu, S.-H., Stone, S. L., Salt, J. N., & Goring, D. R. (2004). A large complement of the predicted *Arabidopsis* ARM repeat proteins are members of the U-box E3 ubiquitin ligase family. *Plant Physiology*, 134(1), 59–66.
- Navarro, L., Zipfel, C., Rowland, O., Keller, I., Robatzek, S., Boller, T., & Jones, J. D. G. (2004). The transcriptional innate immune response to flg22. Interplay and overlap with Avr gene-dependent defense responses and bacterial pathogenesis. *Plant Physiology*, 135(2), 1113–1128.
- Nolen, B., Taylor, S., & Ghosh, G. (2004). Regulation of protein kinases. *Molecular Cell*, 15(5), 661–675.
- Nühse, T. S., Bottrill, A. R., Jones, A. M. E., & Peck, S. C. (2007). Quantitative phosphoproteomic analysis of plasma membrane proteins reveals regulatory mechanisms of plant innate immune responses. *The Plant Journal*, 51(5), 931–940.
- Nühse, T. S., Peck, S. C., Hirt, H., & Boller, T. (2000). Microbial elicitors induce activation and dual phosphorylation of the *Arabidopsis thaliana* MAPK 6. *The Journal of Biological Chemistry*, 275(11), 7521–6.
- Nürnberg, T., Brunner, F., Kemmerling, B., & Piater, L. (2004). Innate immunity in plants and animals: striking similarities and obvious differences. *Immunological Reviews*, 198, 249–66.
- Pandey, S., Chen, J.-G., Jones, A. M., & Assmann, S. M. (2006). G-protein complex mutants are hypersensitive to abscisic acid regulation of germination and postgermination development. *Plant Physiology*, 141(1), 243–56.
- Pečenková, T., Hála, M., Kulich, I., Kocourková, D., Drdová, E., Fendrych, M., Toupalova, H., & Žárský, V. (2011). The role for the exocyst complex subunits Exo70B2 and Exo70H1 in the plant–pathogen interaction. *Journal of Experimental Botany*, 62(6), 2107–2116.

- Qi, Y., Tsuda, K., Nguyen, L. V., Wang, X., Lin, J., Murphy, A. S., Glazebrook, J., Thordal-Christensen, H., & Katagiri, F. (2011). Physical association of *Arabidopsis* hypersensitive induced reaction proteins (HIRs) with the immune receptor RPS2. *The Journal of Biological Chemistry*, 286(36), 31297–307.
- Rafiqi, M., Bernoux, M., Ellis, J. G., & Dodds, P. N. (2009). In the trenches of plant pathogen recognition: Role of NB-LRR proteins. *Seminars in Cell & Developmental Biology*, 20(9), 1017–1024.
- Ranf, S., Eschen-Lippold, L., Fröhlich, K., Westphal, L., Scheel, D., & Lee, J. (2014a). Microbe-associated molecular pattern-induced calcium signaling requires the receptor-like cytoplasmic kinases, PBL1 and BIK1. *BMC Plant Biology*, 14(1), 374.
- Rao, S., Zhou, Z., Miao, P., Bi, G., Hu, M., Wu, Y., Feng, F., Zhang, X., & Zhou, J.-M. (2018). Roles of receptor-like cytoplasmic kinase VII members in pattern-triggered immune signaling. *Plant Physiology*, pp.00486.2018.
- Robatzek, S., Chinchilla, D., & Boller, T. (2006). Ligand-induced endocytosis of the pattern recognition receptor FLS2 in *Arabidopsis*. *Genes & Development*, 20(5), 537–542.
- Rubinfeld, H., & Seger, R. (2005). The ERK cascade: a prototype of MAPK signaling. *Molecular Biotechnology*, 31(2), 151–174.
- Sadowski, M., Suryadinata, R., Tan, A. R., Roesley, S. N. A., & Sarcevic, B. (2012). Protein monoubiquitination and polyubiquitination generate structural diversity to control distinct biological processes. *IUBMB Life*, 64(2), 136–142.
- Safavian, D., Zayed, Y., Indriolo, E., Chapman, L., Ahmed, A., & Goring, D. (2015). RNA silencing of exocyst genes in the stigma impairs the acceptance of compatible pollen in *Arabidopsis*. *Plant Physiology*, 169(4), pp.00635.2015.
- Saijo, Y., Loo, E. P.-I., & Yasuda, S. (2018). Pattern recognition receptors and signaling in plant-microbe interactions. *The Plant Journal : For Cell and Molecular Biology*, 93(4), 592–613.
- Samuel, M. A., Chong, Y. T., Haasen, K. E., Aldea-Brydges, M. G., Stone, S. L., & Goring, D. R. (2009). Cellular pathways regulating responses to compatible and self-incompatible pollen in Brassica and *Arabidopsis* stigmas intersect at Exo70A1, a putative component of the exocyst complex. *The Plant Cell*, 21(9), 2655–71.
- Samuel, M. A., Mudgil, Y., Salt, J. N., Delmas, F., Ramachandran, S., Chillelli, A., & Goring, D. R. (2008). Interactions between the S-domain receptor kinases and AtPUB-ARM E3 ubiquitin ligases suggest a conserved signaling pathway in *Arabidopsis*. *Plant Physiology*, 147(4), 2084–2095.
- Samuel, M. A., Salt, J. N., Shiu, S., & Goring, D. R. (2006). Multifunctional ARM repeat domains in plants. In *International review of cytology*, 253, 1–26.
- Schlesinger, D. H., Goldstein, G., & Niall, H. D. (1975). The complete amino acid sequence of ubiquitin, an adenylate cyclase stimulating polypeptide probably universal in living cells. *Biochemistry*, 14(10), 2214–8.
- Schwartz, D., & Gygi, S. P. (2005). An iterative statistical approach to the identification of protein phosphorylation motifs from large-scale data sets. *Nature Biotechnology*, 23(11), 1391–1398.
- Shi, Y., Chan, D. W., Jung, S. Y., Malovannaya, A., Wang, Y., & Qin, J. (2011). A data set of human endogenous protein ubiquitination sites. *Molecular & Cellular Proteomics : MCP*, 10(5), M110.002089.
- Shimizu, Y., Okuda-Shimizu, Y., & Hendershot, L. M. (2010). Ubiquitylation of an ERAD substrate occurs on multiple types of amino acids. *Molecular Cell*, 40(6), 917–926.
- Shiu, S.-H., & Bleecker, A. B. (2001). Receptor-like kinases from *Arabidopsis* form a monophyletic gene family related to animal receptor kinases. *Proceedings of the National Academy of Sciences*, 98(19), 10763–10768.
- Shiu, S. H., & Bleecker, A. B. (2003). Expansion of the receptor-like kinase/Pelle gene family and receptor-like proteins in *Arabidopsis*. *Plant Physiology*, 132(2), 530–43.
- Shu, K., & Yang, W. (2017). E3 ubiquitin ligases: ubiquitous actors in plant development and abiotic stress responses. *Plant & Cell Physiology*, 58(9), 1461–1476.

- Shubchynskyy, V., Boniecka, J., Schweighofer, A., Simulis, J., Kvederaviciute, K., Stumpe, M., Mauch, F., Balazadeh, S., Mueller-Roeber, B., Boutrot, F., Zipfel, C., & Meskiene, I. (2017). Protein phosphatase AP2C1 negatively regulates basal resistance and defense responses to *Pseudomonas syringae*. *Journal of Experimental Botany*, *68*(5), erw485.
- Smalle, J., & Vierstra, R. D. (2004). The ubiquitin 26S proteasome proteolytic pathway. *Annual Review of Plant Biology*, *55*(1), 555–590.
- Smith, J. M., Salamango, D. J., Leslie, M. E., Collins, C. A., & Heese, A. (2014). Sensitivity to Flg22 is modulated by ligand-induced degradation and de novo synthesis of the endogenous flagellin-receptor FLAGELLIN-SENSING2. *Plant Physiology*, *164*(1), 440–54.
- Spallek, T., Beck, M., Ben Khaled, S., Salomon, S., Bourdais, G., Schellmann, S., & Robatzek, S. (2013). ESCRT-I mediates FLS2 endosomal sorting and plant immunity. *PLoS Genetics*, *9*(12), e1004035.
- Stegmann, M., Anderson, R. G., Ichimura, K., Pecenkova, T., Reuter, P., Žársky, V., McDowell, J.M., Shirasu, K., & Trujillo, M. (2012). The ubiquitin ligase PUB22 targets a subunit of the exocyst complex required for PAMP-triggered responses in *Arabidopsis*. *The Plant Cell*, *24*(11), 4703–16.
- Stone, S. L., Anderson, E. M., Mullen, R. T., & Goring, D. R. (2003). ARC1 is an E3 ubiquitin ligase and promotes the ubiquitination of proteins during the rejection of self-incompatible *Brassica* pollen. *The Plant Cell*, *15*(4), 885–98.
- Stone, S. L., Arnoldo, M., & Goring, D. R. (1999). A breakdown of *Brassica* self-incompatibility in ARC1 antisense transgenic plants. *Science*, *286*(5445), 1729–31.
- Strange, R. N., & Scott, P. R. (2005). Plant disease: a threat to global food security. *Annual Review of Phytopathology*, *43*(1), 83–116.
- Sun, H., Qian, Q., Wu, K., Luo, J., Wang, S., Zhang, C., Ma, Y., Liu, Q., Huang, X., Yuan, Q., Han, R., Zhao, M., Dong, G., Guo, L., Zhu, X., Gou, Z., Wang, W., Wu, Y., Lin, H., & Fu, X. (2014). Heterotrimeric G proteins regulate nitrogen-use efficiency in rice. *Nature Genetics*, *46*(6), 652–656.
- Tang, D., Wang, G., & Zhou, J.-M. (2017). Receptor kinases in plant-pathogen interactions: more than pattern recognition. *The Plant Cell*, *29*(4), 618–637.
- Torres, M. A., Morales, J., Sánchez-Rodríguez, C., Molina, A., & Dangl, J. L. (2013). Functional interplay between *Arabidopsis* NADPH oxidases and heterotrimeric G protein. *Molecular Plant-Microbe Interactions : MPMI*, *26*(6), 686–94.
- Trujillo, M. (2018). News from the PUB: plant U-box type E3 ubiquitin ligases. *Journal of Experimental Botany*, *69*(3), 371–384.
- Trujillo, M., Ichimura, K., Casais, C., & Shirasu, K. (2008). Negative regulation of PAMP-triggered immunity by an E3 ubiquitin ligase triplet in *Arabidopsis*. *Current Biology*, *18*(18), 1396–1401.
- Trusov, Y., Rookes, J. E., Chakravorty, D., Armour, D., Schenk, P. M., & Botella, J. R. (2006). Heterotrimeric G proteins facilitate *Arabidopsis* resistance to necrotrophic pathogens and are involved in jasmonate signaling. *Plant Physiology*, *140*(1), 210–20.
- Udeshi, N. D., Svinkina, T., Mertins, P., Kuhn, E., Mani, D. R., Qiao, J. W., & Carr, S. A. (2013). Refined preparation and use of anti-diglycine remnant (K-ε-GG) antibody enables routine quantification of 10,000s of ubiquitination sites in single proteomics experiments. *Molecular & Cellular Proteomics : MCP*, *12*(3), 825–31.
- Ullah, H., Chen, J.-G., Temple, B., Boyes, D. C., Alonso, J. M., Davis, K. R., Ecker, J.R., & Jones, A. M. (2003). The beta-subunit of the *Arabidopsis* G protein negatively regulates auxin-induced cell division and affects multiple developmental processes. *The Plant Cell*, *15*(2), 393–409.
- Ullah, H., Chen, J. G., Young, J. C., Im, K. H., Sussman, M. R., & Jones, A. M. (2001). Modulation of cell proliferation by heterotrimeric G protein in *Arabidopsis*. *Science*, *292*(5524), 2066–2069.
- Veronese, P., Nakagami, H., Bluhm, B., Abuqamar, S., Chen, X., Salmeron, J., Dietrich, R.A., Hirt, H., & Mengiste, T. (2006). The membrane-anchored BOTRYTIS-INDUCED KINASE1 plays distinct roles in *Arabidopsis* resistance to necrotrophic and biotrophic pathogens. *The Plant Cell*, *18*(1), 257–73.
- Vierstra, R. D. (2009). The ubiquitin–26S proteasome system at the nexus of plant biology. *Nature Reviews Molecular Cell Biology*, *10*(6), 385–397.

- Vierstra, R. D. (2012). The expanding universe of ubiquitin and ubiquitin-like modifiers. *Plant Physiology*, 160(1), 2–14.
- Wang, H., Yang, C., Zhang, C., Wang, N., Lu, D., Wang, J., Zhang, S., Wang, Z.X., Ma, H., & Wang, X. (2011). Dual role of BKII and 14-3-3 s in brassinosteroid signaling to link receptor with transcription factors. *Developmental Cell*, 21(5), 825–34.
- Wang, J., Grubb, L. E., Wang, J., Liang, X., Li, L., Gao, C., Ma, M., Feng, F., Li, M., Li, L., Zhang, X., Yu, F., Xie, Q., Chen, S., Zipfel, C., Monaghan, J., & Zhou, J.-M. (2018). A regulatory module controlling homeostasis of a plant immune kinase. *Molecular Cell*, 69(3), 493–504.e6.
- Wang, J., Wang, S., Hu, K., Yang, J., Xin, X., Zhou, W., Fan, J., Cui, F., Mou, B., Zhang, S., Wang, G., & Sun, W. (2018). The kinase OsCPK4 regulates a buffering mechanism that fine-tunes innate immunity. *Plant Physiology*, 176(2), 1835–1849.
- Wang, N., Liu, Y., Cong, Y., Wang, T., Zhong, X., Yang, S., Li, Y., & Gai, J. (2016). Genome-wide identification of soybean U-box E3 ubiquitin ligases and roles of GmPUB8 in negative regulation of drought stress response in *Arabidopsis*. *Plant and Cell Physiology*, 57(6), 1189–1209.
- Wang, S., Sun, J., Fan, F., Tan, Z., Zou, Y., & Lu, D. (2016). A *Xanthomonas oryzae* pv. *oryzae* effector, XopR, associates with receptor-like cytoplasmic kinases and suppresses PAMP-triggered stomatal closure. *Science China Life Sciences*, 59(9), 897–905.
- Wang, X.-Q., Ullah, H., Jones, A. M., & Assmann, S. M. (2001). G protein regulation of ion channels and abscisic acid signaling in *Arabidopsis* guard cells. *Science*, 292(5524), 2070–2072.
- Wang, X., Herr, R. A., Chua, W.-J., Lybarger, L., Wiertz, E. J. H. J., & Hansen, T. H. (2007). Ubiquitination of serine, threonine, or lysine residues on the cytoplasmic tail can induce ERAD of MHC-I by viral E3 ligase mK3. *The Journal of Cell Biology*, 177(4), 613–624.
- Wang, Z. Y., Seto, H., Fujioka, S., Yoshida, S., & Chory, J. (2001). BRI1 is a critical component of a plasma-membrane receptor for plant steroids. *Nature*, 410(6826), 380–3.
- Warpeha, K. M., Lateef, S. S., Lapik, Y., Anderson, M., Lee, B.-S., & Kaufman, L. S. (2006). G-protein-coupled receptor 1, G-protein Galpha-subunit 1, and prephenate dehydratase 1 are required for blue light-induced production of phenylalanine in etiolated *Arabidopsis*. *Plant Physiology*, 140(3), 844–55.
- Wiborg, J., O’Shea, C., & Skriver, K. (2008). Biochemical function of typical and variant *Arabidopsis thaliana* U-box E3 ubiquitin-protein ligases. *The Biochemical Journal*, 413(3), 447–57.
- Withers, J., & Dong, X. (2017). Post-translational regulation of plant immunity. *Current Opinion in Plant Biology*, 38, 124–132.
- Wu, Y., & Zhou, J.-M. (2013). Receptor-like kinases in plant innate immunity. *Journal of Integrative Plant Biology*, 55(12), 1271–1286.
- Xu, J., Wei, X., Yan, L., Liu, D., Ma, Y., Guo, Y., Peng, C., Zhou, H., Yang, C., Lou, Z., & Shui, W. (2013). Identification and functional analysis of phosphorylation residues of the *Arabidopsis* BOTRYTIS-INDUCED KINASE1. *Protein and Cell*, 4(10), 771–781.
- Yamaguchi, Y., Huffaker, A., Bryan, A. C., Tax, F. E., & Ryan, C. A. (2010). PEPR2 is a second receptor for the Pep1 and Pep2 peptides and contributes to defense responses in *Arabidopsis*. *The Plant Cell*, 22(2), 508–522.
- Yamaguchi, Y., Pearce, G., & Ryan, C. A. (2006). The cell surface leucine-rich repeat receptor for AtPep1, an endogenous peptide elicitor in *Arabidopsis*, is functional in transgenic tobacco cells. *Proceedings of the National Academy of Sciences*, 103(26), 10104–10109.
- Yang, C.-W., González-Lamothe, R., Ewan, R. A., Rowland, O., Yoshioka, H., Shenton, M., Ye, H., O’Donnell, E., Jones, J.D., & Sadanandom, A. (2006). The E3 ubiquitin ligase activity of *Arabidopsis* PLANT U-BOX17 and its functional tobacco homolog ACRE276 are required for cell death and defense. *The Plant Cell Online*, 18(4), 1084–1098.
- Yee, D., & Goring, D. R. (2009). The diversity of plant U-box E3 ubiquitin ligases: from upstream activators to downstream target substrates. *Journal of Experimental Botany*, 60(4), 1109–21.
- Yu, F., Wu, Y., & Xie, Q. (2016). Ubiquitin–proteasome system in ABA signaling: from perception to action. *Molecular Plant*, 9(1), 21–33.

- Zeng, L.-R., Park, C. H., Venu, R. C., Gough, J., & Wang, G.-L. (2008). Classification, expression pattern, and E3 ligase activity assay of rice U-box-containing proteins. *Molecular Plant*, *1*(5), 800–15.
- Zhang, J., Li, W., Xiang, T., Liu, Z., Laluk, K., Ding, X., Zou, Y., Gao, M., Zhang, X., Chen, S., Mengiste, T., Zhang, Y., & Zhou, J.-M. (2010a). Receptor-like cytoplasmic kinases integrate signaling from multiple plant immune receptors and are targeted by a *Pseudomonas syringae* effector. *Cell Host & Microbe*, *7*(4), 290–301.
- Zhang, M., Zhao, J., Li, L., Gao, Y., Zhao, L., Patil, S. B., Fang, J., Zhang, W., Yang, Y., Li, M., & Li, X. (2017). The *Arabidopsis* U-box E3 ubiquitin ligase PUB30 negatively regulates salt tolerance by facilitating BRI1 kinase inhibitor 1 (BKI1) degradation. *Plant, Cell & Environment*, *40*(11), 2831–2843.
- Zhang, N., Zhang, L., Shi, C., Tian, Q., Lv, G., Wang, Y., Cui, D., & Chen, F. (2017). Comprehensive profiling of lysine ubiquitome reveals diverse functions of lysine ubiquitination in common wheat. *Scientific Reports*, *7*(1), 13601.
- Zhang, Y., Goritschnig, S., Dong, X., & Li, X. (2003). A gain-of-function mutation in a plant disease resistance gene leads to constitutive activation of downstream signal transduction pathways in suppressor of npr1-1, constitutive 1. *The Plant Cell Online* *15*(11), 2636–2646.
- Zhou, J., Lu, D., Xu, G., Finlayson, S. A., He, P., & Shan, L. (2015). The dominant negative ARM domain uncovers multiple functions of PUB13 in *Arabidopsis* immunity, flowering, and senescence. *Journal of Experimental Botany*, *66*(11), 3353–66.
- Zhu, H., Li, G.-J., Ding, L., Cui, X., Berg, H., Assmann, S. M., & Xia, Y. (2009). *Arabidopsis* extra large G-protein 2 (XLG2) interacts with the G β subunit of heterotrimeric G protein and functions in disease resistance. *Molecular Plant*, *2*(3), 513–525.
- Zipfel, C., Kunze, G., Chinchilla, D., Caniard, A., Jones, J. D. G., Boller, T., & Felix, G. (2006). Perception of the bacterial PAMP EF-Tu by the receptor EFR restricts *Agrobacterium*-mediated transformation. *Cell*, *125*(4), 749–60.

APPENDIX

Table S1. Germplasm used in this thesis

Genotype	Alias	Generated by	Resistance
Col-0/35S:CPK28-YFP	CPK28-OE	J Monaghan	Basta
<i>cpk28-1</i> (GABI_532308)	<i>cpk28</i>	S Matschi	none
Col-0/35S:BIK1-HA	BIK1-OE	J Monaghan	Kanamycin
<i>bik1</i> (SALK_005291; Veronese et al., 2006)	<i>bik1</i>	J Monaghan	none
<i>bik1 pbl1</i> (SALK_005291; SAIL_1236_D07; Zhang et al., 2010)	<i>bik1pbl1</i>	J Monaghan	none
<i>pub25-1</i> (SALK_147032)	<i>pub25-1</i>	JM Zhou	none
<i>pub26-1</i> (GABI_308D07)	<i>pub26-1</i>	JM Zhou	none
<i>pub25-1 pub26-1</i>	<i>pub25-1 pub26-1</i>	JM Zhou, L Grubb	none
Col-0/35S:PUB25-FLAG	PUB25-OE	JM Zhou, L Grubb	Hygromycin
Col-0/35S:PUB26-FLAG	PUB26-OE	JM Zhou, L Grubb	Hygromycin
<i>pub22 pub23 pub24</i> (SALK_072621; SALK_133841; SALK_041046, Trujillo et al., 2008)	<i>pub22 pub23 pub24</i>	M Trujillo	none
<i>cpk28-1</i> /PUB25-FLAG	<i>cpk28</i> /PUB25-OE	L Grubb, J Monaghan	Hygromycin
<i>cpk28-1</i> /PUB26-FLAG	<i>cpk28</i> /PUB26-OE	L Grubb, J Monaghan	Hygromycin
CPK28-YFP/ <i>pub25 pub26</i>	CPK28-OE/ <i>pub25 pub26</i>	L Grubb, J Monaghan	Basta
Col-0/pBIK1:BIK1-HA	BIK1-OE	J Monaghan	Hygromycin
Col-0/35S:BIK1-HA	Col-0//35S:BIK1-HA	L Grubb, J Monaghan	Kanamycin
<i>pub22 pub23 pub24</i> /35S:BIK1-HA	<i>pub22 pub23 pub24</i> /35S:BIK1-HA	L Grubb, J Monaghan	Kanamycin
CPK28-YFP/pBIK1:BIK1-HA	CPK28-OE/BIK1-OE	J Monaghan	Basta, Hygromycin
<i>cpk28-1</i> /pBIK1:BIK1-HA	<i>cpk28-1</i> /BIK1-OE	J Monaghan	Basta, Hygromycin

Table. S2. BIK1^{mut} constructs used for *Agrobacterium tumefaciens*-mediated transformation and expression and purification of recombinant protein from *E. coli*. Initials denote who was responsible for making which clones (LG= Lauren Grubb, DC= Danielle Ciren, HG= Heather Galley)

Mutation	pENTR glycerol stock in <i>E. coli</i> DB3.1	pGWB14 glycerol stock in <i>E. coli</i> DH5a	pGWB14 glycerol stock in <i>A. tumefaciens</i> GV3101	pGEX6p.1 glycerol stock in <i>E. coli</i> DH5a
SINGLES				
K31R	JMg45 (DC)	JMg178(HG)	JMg686(LG)	JMg85(DC/LG)
K41R	JMg674(LG)	JMg 677(LG)	JMg687(LG)	In progress
K61R	JMg27(DC)	JMg170(DC)	JMg688(LG)	JMg86(DC/LG)
K358R	JMg675(LG)	JMg678(LG)	JMg689(LG)	In progress
K366R	JMg28(DC)	JMg179(HG)	JMg690(LG)	JMg87(DC/LG)
K369R	JMg49(DC)	JMg169(DC)	JMg691(LG)	JMg88(DC/LG)
K370R	JMg29(DC)	JMg191(HG)	JMg191(HG)	JMg99(DC/LG)
K374R	JMg31(DC)	JMg180(HG)	JMg180(HG)	JMg90(DC/LG)
K388R	JMg32(DC)	JMg181(HG)	JMg181(HG)	JMg91(DC/LG)
DOUBLES				
31/61	JMg51(DC)	JMg182(HG)	JMg692(LG)	N/A
366/388	JMg50(DC)	JMg183(HG)	JMg183(HG)	N/A
366/369	JMg53(DC)	JMg184(HG)	JMg184(HG)	N/A
370/374	JMg48(DC)	JMg185(HG)	JMg185(HG)	N/A
370/388	JMg52(DC)	JMg186(HG)	JMg186(HG)	N/A
366/370	JMg64(DC)	JMg187(LG)	JMg719(LG)	N/A
374/388	JMg63(DC)	JMg188(HG)	JMg693(LG)	N/A
366/374	JMg62(DC)	JMg189(HG)	JMg696(LG)	N/A
369/370	JMg30(DC)	JMg190(HG)	JMg697(LG)	N/A
TRIPLES				

366/369/370	JMg61(DC)	JMg192(HG)	JMg699(LG)	N/A
366/370/388	JMg60(DC)	JMg193(HG)	JMg699(LG)	N/A
366/374/388	JMg59(DC)	JMg194(HG)	JMg695(LG)	N/A
370/374/388	JMg69(DC)	JMg195(HG)	JMg696(LG)	N/A
366/370/374	JMg67(DC)	JMg196(HG)	JMg697(LG)	N/A
369/370/388	JMg68(DC)	JMg197(HG)	JMg698(LG)	N/A
QUADS				
366/369/370/388	JMg65(DC)	JMg198(HG)	JMg722(LG)	N/A
366/370/374/388	JMg66(DC)	JMg199(HG)	JMg718(LG)	N/A
QUINTS				
366/369/370/388/31	JMg133(DC)	JMg200(HG)	JMg702(LG)	N/A
366/370/374/388/31	JMg136(DC)	JMg201(HG)	JMg201	N/A
366/370/374/388/61	JMg 676(DC)	JMg679(HG)	JMg700(LG)	N/A
SEXTUPLE				
366/370/374/388/61/31	JMg203(DC)	JMg202(HG)	JMg701(LG)	N/A

Table S3. Primers used in this thesis for site-directed mutagenesis and Gibson assembly

JMo Code FP	JMo Code RP	Forward Primer	Reverse Primer	Template	Mutation
JMo227_BIK1-K31R-F	JMo228_BIK1-K31R-R	AGTCTCTCAAGTCGGAGATCG TCTTCGACTGTA	TACAGTCGAAGACGATCTCCG ACTTGAGAGACT	pENTR- cBIK1	K31R
JMo501_BIK1-K41R-F	JMo502_BIK1-K41R-R	GGCTCAGAGGACGGAAGGGGAG ATATTGAG	CTCAATATCTCCCCTCCGTCC TCTGAGCC	pENTR- cBIK1	K41R
JMo106_BIK1-K61R-F	JMo107_BIK1-K61R-R	ACCTTTAACGAACTCAGACTC GCCACAAGAAA	TTTCTTGTGGCGAGTCTGAGT TCGTTAAAGGT	pENTR- cBIK1	K61R
JMo503_BIK1-K358R-F	JMo504_BIK1-K358R-R	GACAACCTGGGAAGACCGAGTCA GACCAAT	ATTGGTCTGACTCGGTCTTCCC AAGTTGTC	pENTR- cBIK1	K358R
JMo269_BIK1-K366R_F	JMo270_BIK1-K366R-R	CAGACCAATCCGGTTAGGGAT ACCAAGAACTT	AAGTTTCTTGGTATCCCTAAC CGGATTGGTCTG	pENTR- cBIK1	K366R
JMo271_BIK1-K369R_F	JMo272_BIK1-K369R-R	CCGGTTAAGGATACCAGGAAA CTGGTTTTTAAA	TTTAAAACCAAGTTTCTGGT ATCCTTAACCGG	pENTR- cBIK1	K369R
JMo273_BIK1-K370R_F	JMo274_BIK1-K370R-R	GTAAAGGATACCAAGAGACTT GGTTTTTAAA	AGTTTTAAAACCAAGTCTCTT GGTATCCCTAAC	pENTR- cBIK1	K370R
JMo277_BIK1-K374R_F	JMo278_BIK1-K374R-R	AAGAACTTGGTTTTAGA GGTACTACTAAG	CTTAGTAGTACCAGTTCTAAA ACCAAGTTTCTT	pENTR- cBIK1	K374R
JMo283_BIK1-K388R_F	JMo284_BIK1-K388R-R	AAACGGTTTACACAAAGACCT TTTGGCAGGCAC	GTGCCTGCCAAAAGGTCTTTG TGTAACCGTIT	pENTR- cBIK1	K388R
JMo275_BIK1-K369-370R-F	JMo276_BIK1-K369-370R-R	CCGGTTAAGGATACCAGGAGA CTTGGTTTTTAAA	AGTTTTAAAACCAAGTCTCCT GGTATCCCTAACCGG	pENTR- cBIK1	K369R K370R
JMo117_BIK1-K366R/K369R-F	JMo118_BIK1-K366R/K369R-R	CAGACCAATCCGGTTAGGGAT ACCAGGAACTT	AAGTTTCTTGGTATCCCTAAC CGGATTGGTCTG	K369R	K366R K369R
JMo119_BIK1-K370R/K374R-F	JMo120_BIK1-K370R/K374R-R	GTAAAGGATACCAAGAGACTT GGTTTTTAGA	AGTTCTAAAACCAAGTCTCTT GGTATCCCTAAC	K374R	K370R K374R
JMo121_BIK1-K366R/K369R/K370R-F	JMo122_BIK1-K366R/K369R/K370R-R	CAGACCAATCCGGTTAGGGAT ACCAGGAGACTT	AAGTCTCTGGTATCCCTAAC CGGATTGGTCTG	K369R/ K370R	K366R/ K369R/K370R
JMo123_BIK1-K366R/K370R-F	JMo124_BIK1-K366R/K370R-R	CAGACCAATCCGGTTAGGGAT ACCAAGAGACTT	AAGTCTCTGGTATCCCTAAC CGGATTGGTCTG	K370R	K366R/K370R
JMo133_BIK1-K366.69.70.74R-F	JMo134_BIK1-K366.69.70.74R-R	AGGAGACTTGGTTTTAGA GGTACTACTAAG	CTTAGTAGTACCAGTTCTAAA ACCAAGTCTCCT	K366R/ K369R/ K370R	K366R/ K369R/ K370R/ K374R
JMo135_BIK1-K366.70.74R-F	JMo136_BIK1-K366.70.74R-R	AAGAGACTTGGTTTTAGA GGTACTACTAAG	CTTAGTAGTACCAGTTCTAAA ACCAAGTCTCCT	K366R/ K370R	K366R/ K370R/ K374R
JMo139_BIK1-K366.69.70.88R-F	JMo140_BIK1-K366.69.70.88R-R	CCGGTTAAGGATACCAGGAGA CTTGGTTTTTAAA	AGTTTTAAAACCAAGTCTCCT GGTATCCCTAACCGG	K366R/ K388R	K366R/ K369R/ K370R/ K388R
JMo141_BIK1-K366.70.74.88R-F	JMo142_BIK1-K366.70.74.88R-R	GTTAGGATACCAAGAGACTT GGTTTTTAGA GGTACTACTAAG	CTTAGTAGTACCAGTTCTAAA ACCAAGTCTCTTGGTATCCCT AAC	K366R/ K388R	K366R/ K370R/ K374R/ K388R
JMo155_pGex6p.1G-BIK1-LB	JMo156_pGex6p.1G-BIK1-RB	TCGAGCGGCCCATCGTGACA TGGTCTTGTCTCAGTTC	GCGAGGCAGATCGTCAGTCAC ACAAGTGCTGCCAAAAG	pENTR- cBIK1 mutant of choice	NA Forms BIK1 insert

JMo157_pGex6p.1_Gibson-LB	JMo158_pGex6p.1-Gibson-RB	GTCACGATGCGGCCGCTCGA	TGACTGACGATCTGCCTCGCG	Circular pGex6p.1	NA Forms linear vector backbone
---------------------------	---------------------------	----------------------	-----------------------	----------------------	---

Table S4. Primers used in this thesis for colony PCR and sequencing

Primer Code	Primer Sequence	Use
JMo110_BIK1seq_R1	CAAACCGGTTCCAGGTTTAGTCG	Sequence the middle of BIK1
JMo330_qBIK1_F	TGGGCTCGACCGTACCTCACA	Sequence the middle of BIK1
M13F-20 Invitrogen	GTAAAACGACGGCCAG	Sequence left border and beginning of BIK1
M13R-27 Invitrogen	GGAAACAGCTATGACCATG	Sequence right border and end of BIK1
JM0111_BIK1seq_F1	CATCTATTCAGAAGAGGTGCAT	Colony PCR for BIK1
JMo20_BIK1_GWY_NS_R	CTACACAAGGTGCCTGCCAAAAG	Colony PCR for BIK1
JMo115_PUB25colony_F	GGAATCCAAATACCATATCA	Colony PCR for PUB25
JMo116_PUB25colony_R	TAGCTCCACCGTCGCTAAGG	Colony PCR for PUB25

Table S5. Primers used in this thesis for genotyping and qPCR

Target	Primer name	Primer sequence	Use	
pub22 At3g52540	JMo168_Salk_072621_LB	CATCCTCGAATGAAAGAATGC	Genotyping	
	JMo169_Salk_072632_RB	CTCTCACAAGGCGACAAGATC		
	JMo10_SalkLBb1.3	ATTTTGCCGATTTCGGAAC		
pub23 At2g35930	JMo170_Salk_133841_LB	TCACCCCGAATCACACTCTAC		
	JMo171_Salk_133841_RB	TTTTCATCAGCAGGGATATGC		
	JMo10_SalkLBb1.3	ATTTTGCCGATTTCGGAAC		
pub24 At3g11840	JMo172_Salk_041046_LB	AAACGTTGCAGAAGCTTGAAG		
	JMo173_Salk_041046_RB	TCGATTGAGGATTGATCGATC		
	JMo10_SalkLBb1.3	ATTTTGCCGATTTCGGAAC		
pub25-1 AT3G19380	JMo5_Salk_147032_LP	GATCGCAGCTCATAACGCTAC		
	JMo6_Salk_147032_RP	CATGTCCATAACAAATTTGCC		
	JMo10_SalkLBb1.3	ATTTTGCCGATTTCGGAAC		
pub26-1 AT1G49780	JMo3_Gk308D07_LP	TGCGTGTTCTAAACCAAAAAC		
	JMo4_Gk308D07_RP	ACACTCCGTCTCCGTCATATG		
	JMo8_GKo8706LB	GGGCTACACTGAATTGGTAGCTC		
cpk28-1 At5g66210	JMo17_cpk28-1_genF	GCGGCGGATTCTTTGACTAA		
	JMo18_cpk28-1_genR	AGTACACAACGGCTCATTATGAA		
	JMo8_GKo8706LB	GGGCTACACTGAATTGGTAGCTC		
UBOX	JMo_328_qUBOX_F	TGCGCTGCCAGATAATACACTATT		qPCR
	JMo_329_qUBOX_R	TGCTGCCCAACATCAGGTT		
PUB25 AT3G19380	JMo380_PUB25qPCR_UP_F	GACGTCGTCGGAGTTAGTCTCT		
	JMo468_qPUB25up_R	CTGGACATGTCGTGTTGTTAC		
PUB26 AT1G49780	JMo470_qPUB26_dOWN_F2	GACGGTGCCGCTAATGGTGA		
	JMo469_qPUB26_down_R2	CTCTTAATATCGTCTTCACC		
BIK1 At2g39660	JMo330_qBIK1_F	TGGGCTCGACCGTACCTCACA		
	JMo331_qBIK1_R	CGGGCGCGACTTGGGTTCAA		

Table S6. Constructs used for split-luciferase complementation assays

Gene ID	Gene Name	Clone Name	pCAMBIA300 glycerol stock in <i>A. tumefaciens</i>	Tags	Source	Plasmid Antibiotic Resistance
AT5G66210	CPK28	pCAMBIA1300-35S:CPK28-HA-Nluc	JMg58	Nluc, HA	JM Zhou	Kanamycin
AT3G19380	PUB25	pCAMBIA-1300- Cluc-PUB25-FLAG	JMg56	Cluc, FLAG	JM Zhou	Kanamycin
AT1G49780	PUB26	pCAMBIA-1300- Cluc-PUB26-FLAG	JMg57	Cluc, FLAG	JM Zhou	Kanamycin
AT2G39660	BIK1	pCAMBIA-1300-35S-Cluc-BIK1	JMg76	Cluc	JM Zhou	Kanamycin
AT5G64930	CPR5	pCAMBIA1300-35S:Cluc-CPR5-HA	JMg71	Cluc, HA	JM Zhou	Kanamycin

Table S7. Constructs used for co-immunoprecipitation assays.

Gene ID	Gene Name	Clone Name	pCAMBIA300 glycerol stock in <i>A. tumefaciens</i>	Tags	Source	Plasmid Antibiotic Resistance
AT5G66210	CPK28	pXCSG-35S-CPK28-YFP	JMg23	YFP	S Matschi	Kanamycin, carbenicillin
AT3G19380	PUB25	pCAMBIA1300-35S:PUB25-FLAG	JMg19	FLAG	JM Zhou	Kanamycin
AT1G49780	PUB26	pCAMBIA1300-35S:PUB26-FLAG	JMg9	FLAG	JM Zhou	Kanamycin
AT2G39660	BIK1	pGWB414-35S:BIK1-HA	JMg24	HA	J Monaghan	Spectinomycin
N/A	P19	pBIN:P19	JMg21	N/A	J Monaghan	Kanamycin

Table S8. Constructs used for *in vitro* ubiquitination assays

Gene ID	Gene Name	Clone Name	Glycerol stock in <i>E. coli</i> DH5a	Tags	Source	Plasmid Antibiotic Resistance
Unknown	Wheat E1	pET28a-His-WE1	JMg565	His	JM Zhou	Kanamycin
AT5G41700	UBC8	pET28a-His-AtUBC8	JMg566	His	JM Zhou	Kanamycin
AT3G19380	PUB25	pET28a-PUB25-His	JMg567	His	JM Zhou	Kanamycin
AT1G49780	PUB26 T94D	pET28a-PUB26-His	JMg568	His	JM Zhou	Kanamycin
AT2G39660	BIK1	pGEX6p.1-GST-BIK1	JMg710	GST	D Ciren, L Grubb	Carbenicillin

Table S9. Antibodies and titres used in this thesis

Antibody	Titre Used	Vendor
α - GFP	1:5,000	Roche
α -GST	1:5,000	Sigma
α -Histidine (27E8)	1:5,000	Cell Signaling
α -p42/44MAPK	1:2,000	Cell Signaling
α -Ub (P4D1)	1:2,000	Cell Signaling
α -mouse-HRP (A0168)	1:10,000	Sigma
α -HA-HRP	1:5,000	Roche
α -FLAG-HRP	1:5,000	Sigma

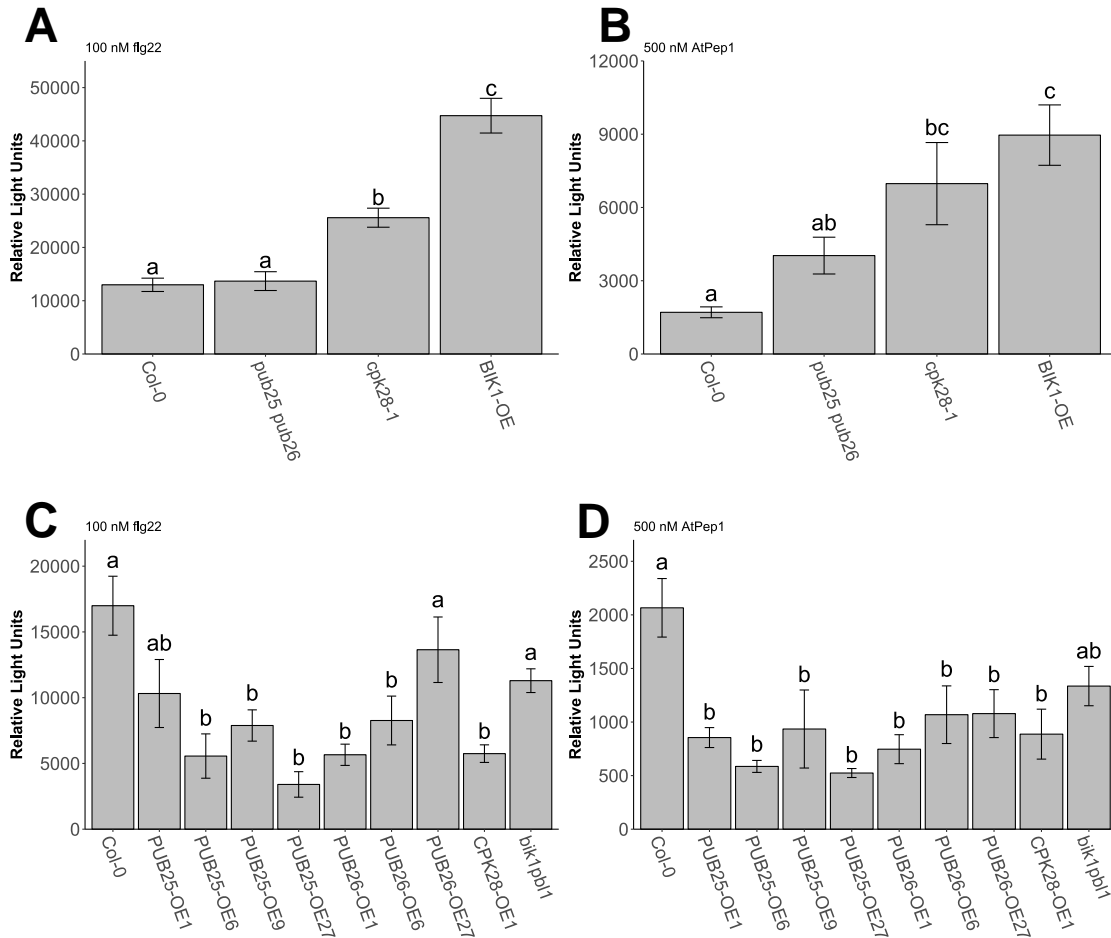


Figure S1. ROS burst analysis of PUB25 and PUB26 knockout and overexpression lines using flg22 and AtPep1 as a peptide elicitor. Oxidative burst of 4-5 week old T3 homozygous *Arabidopsis* upon treatment with 100 nM flg22 (A,C) or 500 nM AtPep1 (B, D) of *pub25-1 pub26-1* and PUB25-OE and PUB26-OE lines in comparison to previously studied genotypes (Monaghan *et al.*, 2014; Veronese *et al.*, 2006; Zhang *et al.*, 2010). 6 leaf discs were tested per genotype. Letters indicate statistically significant groups ($p < 0.05$) based on a one-way ANOVA followed by Tukey HSD. ROS burst assays were performed 3 times with similar results.

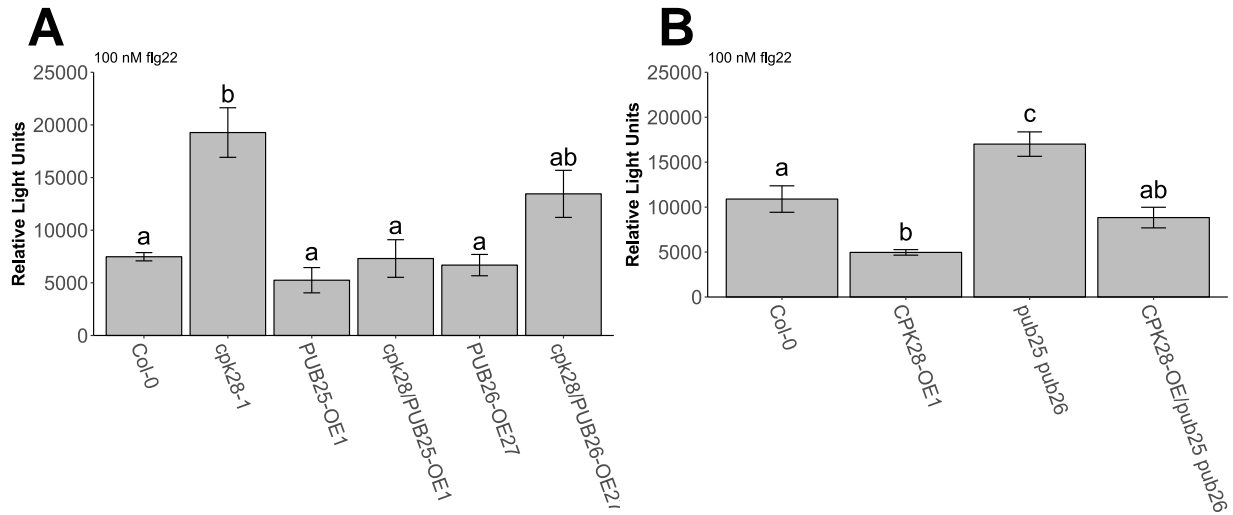


Figure S2. ROS burst assays of epistasis lines using flg22 as a peptide elicitor. A) Oxidative burst assay of T2 generation of 4-5 week old *Arabidopsis* with treatment of 100 nM flg22 on *cpk28-1*/PUB25-OE1 and *cpk28-1*/PUB26-OE for epistasis analysis to determine whether PUB25 or PUB26-OE could suppress the high ROS burst of *cpk28*. B) Epistasis analysis of oxidative burst of CPK28-OE/ *pub25-1 pub26-1* to determine whether *pub25-1 pub26-1* can restore the low ROS of CPK28-OE. Leaf discs were treated with 100 nM flg22. Three repetitions were performed with similar results, and 12 leaf discs were tested per genotype. Letters indicate groups which are statistically significant ($p < 0.05$) based on a one-way ANOVA with Tukey HSD.

Table S10. Plasma membrane ubiquitinated proteins as identified by di-Gly enrichment and LC-MS/MS. Col-0//35S:BIK1-HA lines were treated with water or 1 μ M elf18, microsomal fractionation was performed, followed by di-Gly enrichment. Ubiquitinated proteins were determined by LC-MS/MS, and are organized here based on type of protein. Protein molecular weight, lysine position in peptide, as well as number of sites and spectra seen in total and in each of mock and elf18 treatments is also included. Three repetitions were performed and numbers (#) are representative of how many reps out of the 3 the sites and spectra were observed.

Protein ID	Protein annotation	Molecular weight (Da)	GlyGly (K) site positions	# of GlyGly (K) Sites	# of mock reps seen	# of spectra seen in mock	# of elf18 reps	# of elf18 spectra
<i>Ubiquitin and 26S proteasome-related proteins</i>								
<i>E1 activating enzymes, E2 conjugating enzymes, and E3 ligases</i>								
AT2G30110.1	ATUBA1, MOS5, UBA1 (ubiquitin-activating enzyme 1)	120,253.60	617; 840	2	0	0	1	2
AT1G78870.2	UBC35, UBC13A (ubiquitin-conjugating enzyme 35)	17,192.90	12; 76; 84; 94; 96	5	1	8	1	11
AT1G16890.1	UBC36, UBC13B (ubiquitin-conjugating enzyme 36)	13,631.70	43; 51; 61; 63; 84; 94	6	1	6	2	12
AT1G22500.1	RING/U-box superfamily protein	42,226.70	113; 268; 272; 296	4	1	4	2	10
AT3G05200.1	ATL6/RING/U-box superfamily protein	43,273.60	123; 231; 374; 382	4	1	4	1	5
AT3G06330.1	RING/U-box superfamily protein	46,710.90	142; 162	2	0	0	1	4
AT1G68070.1	Zinc finger, C3HC4 type (RING finger) family protein	38,298.40	338	1	0	0	1	1
AT1G30440.1	Phototropic-responsive NPH3 family protein	73,411.60	426; 429	2	0	0	1	2
<i>Ubiquitin</i>								
AT2G35635.1	UBQ7, RUB2 (ubiquitin 7)	17,150.80	6; 11; 27; 29; 33; 48; 63	7	2	280	2	219
AT2G47110.1	UBQ6 (ubiquitin 6)	17,812.30	6; 11; 27; 29; 33; 48; 63; 113	8	2	183	2	200
AT3G62250.1	UBQ5 (ubiquitin 5)	17,797.40	6; 11; 29; 33; 48; 63; 113; 152	8	2	245	2	232
AT1G53400.1	Ubiquitin domain-containing protein	12,706.50	96	1	1	2	0	0
AT4G24990.1	Ubiquitin family protein	12,836.10	34; 56; 68	3	0	0	1	5
AT4G24690.1	Ubiquitin-associated (UBA)/TS-N domain-containing protein / octicosapeptide/Phox/Bemp1 (PB1) domain-containing protein	76,186.10	200; 212	2	0	0	1	2
<i>Proteosomal proteins</i>								
AT4G38630.1	RPN10, MCB1, ATMCB1, MBP1 (regulatory particle non-ATPase 10)	40,757.90	57; 119; 122; 123; 130	5	2	8	3	19
AT1G53750.1	RPT1A (regulatory particle triple-A 1A)	47,804.30	39; 349	2	1	3	1	3

AT2G32730.1	26S proteasome regulatory complex, non-ATPase subcomplex, Rpn2/Psmd1 subunit	108,980.30	880; 882	2	1	1	1	1
Ubiquitin proteases								
AT1G16860.1	Ubiquitin-specific protease family C19-related protein	50,583.20	323	1	2	5	0	0
AT1G78880.1	Ubiquitin-specific protease family C19-related protein	50,104.80	116	1	0	0	1	1
Protein kinases								
<i>Receptor-like kinases</i>								
AT4G05200.1	CRK25 (cysteine-rich RLK 25)	75,350.70	448; 507	2	3	10	2	13
AT4G23190.1	CRK11, AT-RLK3 (cysteine-rich RLK 11)	74,141.30	183; 349; 366; 368; 378; 400; 451	7	3	20	1	2
AT3G46290.1	HERK1 (hercules receptor kinase 1)	91,469.50	479; 498; 501	3	2	6	0	0
AT1G30570.1	HERK2 (hercules receptor kinase 2)	93,949.70	518	1	1	2	1	2
AT4G08850.1	Leucine-rich repeat receptor-like protein kinase family protein	115,429.70	770; 788; 793; 815	4	2	8	1	6
AT3G08680.1	Leucine-rich repeat protein kinase family protein	69,407.90	407; 410	2	1	2	0	0
AT2G01820.1	Leucine-rich repeat protein kinase family protein	101,961.50	601; 637; 743; 812	4	2	9	2	5
AT1G48480.1	RKL1 (receptor-like kinase 1)	71,133.00	353; 506; 511	3	2	11	2	5
AT1G52310.1	protein kinase family protein / C-type lectin domain-containing protein	61,821.20	292; 296	2	1	3	1	4
AT5G65700.1	BAM1 (Leucine-rich receptor-like protein kinase family protein)	109,208.30	785	1	1	2	1	2
AT3G49670.1	BAM2 (Leucine-rich receptor-like protein kinase family protein)	109,249.60	698; 781; 914; 919	4	0	0	3	16
AT5G49760.1	Leucine-rich repeat protein kinase family protein	104,713.40	600; 605; 625; 685; 785	5	3	3	2	8
AT1G66150.1	TMK1 (transmembrane kinase 1)	102,391.60	640; 746	2	2	5	1	4
AT5G46330.1	FLS2 (Leucine-rich receptor-like protein kinase family protein)	128,833.30	924; 940; 942	3	2	6	1	2
AT5G20480.1	EFR (EF-TU receptor)	113,359.00	1004	1	0	0	1	4
AT1G09970.1	LRR XI-23, RLK7 (Leucine-rich receptor-like protein kinase family protein)	107,385.40	694; 703; 818; 904; 966	5	0	0	1	11
AT4G33430.1	BAK1, RKS10, SERK3, ELG, ATSERK3, ATBAK1 (BR11-associated receptor kinase)	68,163.10	292; 444; 468	3	0	0	1	5
AT5G16590.1	LRR1 (Leucine-rich repeat protein kinase family protein)	67,465.60	15; 19	2	1	2	1	1
AT3G17840.1	RLK902 (receptor-like kinase 902)	70,407.20	305; 315; 336; 347	4	1	6	1	5
AT1G53430.1	Leucine-rich repeat transmembrane protein kinase	113,982.50	652; 655; 751	3	1	1	1	3
AT4G23300.1	CRK22 (cysteine-rich receptor-like protein kinase 22)	73,851.30	352; 358; 369; 371; 381	5	2	15	2	9
AT5G10290.1	leucine-rich repeat transmembrane protein kinase family protein	68,660.10	276; 306; 314; 469	4	2	12	2	18
AT3G28040.1	Leucine-rich receptor-like protein kinase family protein	111,937.90	728; 742; 780	3	3	12	2	6

AT5G63410.1	Leucine-rich repeat protein kinase family protein	76,268.80	378; 397; 427	3	3	10	2	9
AT4G23180.1	CRK10, RLK4 (cysteine-rich receptor-like protein kinase 10)	74,284.90	439; 449; 642	3	1	4	1	7
AT4G11530.1	CRK34 (cysteine-rich receptor-like protein kinase 34)	74,028.70	363	1	2	12	1	4
AT5G54380.1	THE1 (protein kinase family protein)	93,296.60	480; 534; 560; 657	4	3	20	2	18
AT3G51550.1	FER (Malectin/receptor-like protein kinase family protein)	98,152.70	530; 534; 549; 561; 565; 624; 654; 672; 759; 771; 773; 781; 843; 846	14	3	65	3	80
AT2G26730.1	Leucine-rich repeat protein kinase family protein	71,753.00	293; 315; 416	3	3	5	0	0
AT3G14840.2	Leucine-rich repeat transmembrane protein kinase	112,280.80	666; 677; 688; 700; 774; 793; 963	7	3	18	2	19
AT5G48380.1	BIR1 (BAK1-interacting receptor-like kinase 1)	69,144.80	354; 562	2	2	8	2	6
AT5G58300.1	Leucine-rich repeat protein kinase family protein	71,900.30	424	1	1	1	0	0
AT3G28450.1	Leucine-rich repeat protein kinase family protein	66,947.30	281; 290; 294; 514	4	1	1	1	4
AT1G27190.1	Leucine-rich repeat protein kinase family protein	65,426.80	284; 339	2	0	0	2	4
AT3G23750.1	Leucine-rich repeat protein kinase family protein	99,967.00	736	1	0	0	1	1
AT3G21630.1	CERK1, LYSM RLK1 (chitin elicitor receptor kinase 1)	67,316.40	452	1	0	0	1	2
AT3G02880.1	Leucine-rich repeat protein kinase family protein	67,754.50	315; 326	2	0	0	1	2
AT1G56140.1	Leucine-rich repeat transmembrane protein kinase	113,758.70	711	1	0	0	1	1
AT2G26330.1	ER, QRP1 (Leucine-rich receptor-like protein kinase family protein)	107,339.90	668; 671	2	0	0	1	2
AT5G25930.1	Protein kinase family protein with leucine-rich repeat domain	111,970.00	701	1	0	0	1	1
AT2G37050.1	Leucine-rich repeat protein kinase family protein	103,488.20	739	1	0	0	1	1
AT1G51800.1	Leucine-rich repeat protein kinase family protein	99,641.80	721	1	0	0	1	2
AT1G70520.1	CRK2 (cysteine-rich RLK receptor-like protein kinase 2)	72,001.90	379; 461	2	0	0	1	3
AT5G07910.1	Leucine-rich repeat (LRR) family protein	0	unknown	1	2	2	0	0
AT3G14350.2	SRF7 STRUBBELIG-receptor family 7	73,706.70	323; 623	2	1	3	0	0
AT4G22130.2	SRF8 (STRUBBELIG-receptor family 8)	61,184.30	212; 218	2	0	0	1	2
AT1G53730.1	SRF6 (STRUBBELIG-receptor family 6)	78,088.00	657	1	1	1	1	1
<i>Cytoplasmic receptor-like kinases</i>								
AT4G35230.1	BSK1 (BR-signaling kinase 1)	56,819.30	85	1	1	2	1	2
AT2G39660.1	BIK1 (botrytis-induced kinase1)	44,098.90	31; 41; 61; 155; 337; 358; 366; 369; 370; 388	10	1	9	2	18
AT3G24550.1	ATPERK1, PERK1 (proline extensin-like receptor kinase 1)	69,273.10	303	1	2	3	1	1
AT5G13160.1	PBS1 (Protein kinase superfamily protein)	50,385.40	204; 236	2	0	0	1	5
AT5G38990.1	Malectin/receptor-like protein kinase family protein	97,955.40	646	1	0	0	1	1
<i>Calcium-dependent protein kinases</i>								
AT4G04720.1	CPK21 (calcium-dependent protein kinase 21)	59,896.30	84; 215; 526	3	1	1	1	6

AT3G20410.1	CPK9 (calcium-dependent protein kinase 9)	60,364.40	71; 75; 116; 427	4	0	0	1	7
<i>Other protein kinases</i>								
AT3G17410.1	Protein kinase superfamily protein	39,562.20	89; 92; 190; 301	4	2	10	2	10
AT3G59350.1	Protein kinase superfamily protein	45,658.30	116; 133	2	1	3	0	0
AT2G30740.1	Protein kinase superfamily protein	40,500.00	38; 74	2	2	4	2	5
AT2G47060.1	Protein kinase superfamily protein	39,931.40	46	1	1	1	0	0
AT3G54030.1	Protein kinase protein with tetratricopeptide repeat domain	54,790.80	65; 486	2	1	1	1	1
AT3G63260.1	ATMRK1 (Protein kinase superfamily protein)	42,582.80	342	1	2	6	2	14
AT1G06700.1	Protein kinase superfamily protein	39,819.80	71	1	1	2	1	2
AT1G11330.1	S-locus lectin protein kinase family protein	94,152.60	527; 550	2	1	3	0	0
AT1G11050.1	Protein kinase superfamily protein	68,522.90	298; 449	2	1	2	0	0
AT2G17220.1	Protein kinase superfamily protein	45,552.80	100; 103; 243; 348	4	1	2	1	8
AT1G63500.1	Protein kinase protein with tetratricopeptide repeat domain	54,799.80	68; 105; 304	3	1	2	1	6
AT1G66940.1	protein kinase-related	36,658.60	329	1	0	0	1	3
AT5G20050.1	Protein kinase superfamily protein	51,216.00	119; 156	2	0	0	1	3
AT3G59110.1	Protein kinase superfamily protein	57,118.50	206	1	0	0	1	2
AT2G23200.1	Protein kinase superfamily protein	93,382.70	710	1	0	0	1	4
AT5G42440.1	Protein kinase superfamily protein	40,480.10	110	1	0	0	1	2
AT4G28350.1	Concanavalin A-like lectin protein kinase family protein	72,066.70	339; 466	2	0	0	1	5
AT2G19130.1	S-locus lectin protein kinase family protein	92,344.40	498; 591	2	0	0	1	4
AT4G35600.1	CONNEXIN 32 (Protein kinase superfamily protein)	46,340.90	241	1	0	0	1	1
AT1G48210.1	Protein kinase superfamily protein	39,589.60	189; 300	2	0	0	1	4
AT1G11300.1	protein serine/threonine kinases;protein kinases;ATP binding;sugar binding;kinases;carbohydrate binding	184,365.90	514; 527	2	0	0	1	9
AT5G18610.1	Protein kinase superfamily protein	55,932.40	201	1	0	0	1	3
AT3G45780.1	PHOT1, NPH1, JK224, RPT1 (phototropin 1)	111,691.90	526; 527; 899	3	2	6	1	3
AT1G28440.1	HSL1 (HAESA-like 1)	108,935.60	845; 957	2	1	2	1	2
AT1G61380.1	SD1-29 (S-domain-1 29)	89,900.10	493; 506	2	0	0	1	3
<i>Protein phosphatases</i>								
AT1G22280.1	PAPP2C (phytochrome-associated protein phosphatase type 2C)	30,722.10	105; 109	2	3	11	2	7
AT3G51460.1	RHD4 (Phosphoinositide phosphatase family protein)	68,238.80	292	1	1	1	1	2
AT1G01610.1	ATGPAT4, GPAT4 (glycerol-3-phosphate acyltransferase 4)	56,264.80	229	1	1	1	1	1
<i>Proteases</i>								
AT3G02740.1	Eukaryotic aspartyl protease family protein	52,809.00	49	1	1	1	0	0
AT2G32480.1	ARASP (ARABIDOPSIS SERIN PROTEASE)	48,728.50	130	1	1	1	0	0
AT5G53170.1	FTSH11 (FTSH protease 11)	88,719.10	152	1	0	0	1	1
<i>Ribosomal proteins</i>								
AT3G49010.1	ATBBC1, BBC1, RSU2 (breast basic conserved 1)	23,767.50	80; 87	2	2	4	2	4
AT1G67430.2	Ribosomal protein L22p/L17e family protein	14,767.30	43	1	1	1	0	0
AT4G16720.1	Ribosomal protein L23/L15e family protein	24,239.30	56; 83; 93	3	2	12	3	18

AT3G09630.1	Ribosomal protein L4/L1 family	44,703.00	174; 177	2	2	4	0	0
AT4G02230.1	Ribosomal protein L19e family protein	24,202.90	43; 46; 162; 183	4	1	7	0	0
AT1G56070.1	LOS1 (Ribosomal protein S5/Elongation factor G/III/V family protein)	93,891.90	16; 159; 427; 482; 722	5	2	8	2	7
AT1G58380.1	XW6 (Ribosomal protein S5 family protein)	30,741.20	52; 107; 269; 275	4	3	15	3	21
AT1G02780.1	emb2386 (Ribosomal protein L19e family protein)	24,607.50	16; 19; 21; 43; 46; 144; 146; 162; 183	9	3	22	3	30
AT4G31700.1	RPS6, RPS6A (ribosomal protein S6)	28,368.40	14; 15; 64; 215	4	3	14	2	10
AT2G41840.1	Ribosomal protein S5 family protein	30,878.40	108; 270; 276	3	2	11	1	6
AT5G27850.1	Ribosomal protein L18e/L15 superfamily protein	20,967.70	98	1	1	1	0	0
AT1G23290.1	RPL27A, RPL27AB (Ribosomal protein L18e/L15 superfamily protein)	16,292.50	125	1	1	2	0	0
AT3G04840.1	Ribosomal protein S3Ae	29,851.30	45; 55; 62	3	2	11	2	12
AT3G53020.1	STV1, RPL24B, RPL24 (Ribosomal protein L24e family protein)	18,632.80	96; 136; 139	3	1	1	2	2
AT3G58700.1	Ribosomal L5P family protein	20,861.60	51	1	1	1	1	1
AT5G18380.1	Ribosomal protein S5 domain 2-like superfamily protein	16,617.80	26	1	2	5	1	3
AT3G53870.1	Ribosomal protein S3 family protein	27,349.20	62	1	1	9	1	12
AT2G19730.1	Ribosomal L28e protein family	15,895.70	115; 116	2	2	2	2	5
AT3G62870.1	Ribosomal protein L7Ae/L30e/S12e/Gadd45 family protein	29,035.80	116; 249	2	1	3	2	4
AT5G15200.1	Ribosomal protein S4	23,037.40	67	1	1	1	1	1
AT4G29410.1	Ribosomal L28e protein family	15,910.90	115; 116	2	1	2	1	2
AT1G72370.1	P40, AP40, RP40, RPSAA (40s ribosomal protein SA)	32,291.90	93	1	1	1	0	0
AT2G31610.1	Ribosomal protein S3 family protein	27,519.20	62	1	1	5	0	0
AT1G04480.1	Ribosomal protein L14p/L23e family protein	15,027.20	66	1	0	0	1	1
AT3G09200.1	Ribosomal protein L10 family protein	34,133.40	106	1	0	0	1	1
AT2G34480.1	Ribosomal protein L18ae/LX family protein	21,307.90	69; 75	2	0	0	1	2
AT2G47610.1	Ribosomal protein L7Ae/L30e/S12e/Gadd45 family protein	29,130.70	117	1	0	0	1	1
AT4G15000.1	Ribosomal L27e protein family	15,608.50	9	1	0	0	1	2
AT1G43170.1	ARP1, emb2207, RPL3A, RP1 (ribosomal protein 1)	44,559.60	227	1	0	0	1	1
AT3G07110.1	Ribosomal protein L13 family protein	23,466.10	10	1	0	0	1	1
AT2G19750.1	Ribosomal protein S30 family protein	6,887.00	53; 54	2	0	0	1	2
AT1G52300.1	Zinc-binding ribosomal protein family protein	10,840.80	85	1	0	0	1	1
AT5G52650.1	RNA binding Plectin/S10 domain-containing protein	19,552.00	96; 143	2	1	4	1	6
AT5G41520.1	RNA binding Plectin/S10 domain-containing protein	19,734.40	141	1	1	3	1	5
AT5G27350.1	SFP1 (Major facilitator superfamily protein)	51,788.20	245; 252	2	0	0	1	3
ATP/GTP-binding								
AT4G19640.1	ARA7, ARA-7, ATRABF2B, ATRAB5B, RABF2B, ATRAB-F2B, RAB-F2B (Ras-related small GTP-binding family protein)	21,872.90	161	1	1	1	1	1
AT5G47200.1	ATRABD2B, ATRAB1A, RAB1A (RAB GTPase homolog 1A)	22,313.80	58; 182	2	2	2	1	2

AT5G03520.1	ATRAB8C, ATRABE1D, ATRAB-E1D, RAB-E1D, RAB8C (RAB GTPase homolog 8C)	24,038.50	123; 136; 143; 161; 187	5	1	5	1	8
AT2G47000.1	MDR4, PGP4, ABCB4, ATPGP4 (ATP binding cassette subfamily B4)	139,032.80	263; 507; 1039; 1071; 1244; 1262	6	3	17	3	20
AT3G46060.1	ARA3, ARA-3, ATRABE1C, ATRAB8A, RAB8A (RAB GTPase homolog 8A)	23,836.30	136; 143	2	2	2	1	3
AT4G17530.1	RAB1C, ATRAB1C, ATRABD2C (RAB GTPase homolog 1C)	22,318.80	55	1	1	2	1	5
AT5G45130.1	ATRAB5A, ATRABF2A, RABF2A, RAB5A, RHA1, ATRAB-F2A, RAB-F2A (RAB homolog 1)	21,653.80	161	1	1	1	0	0
AT4G17170.1	AT-RAB2, ATRABB1C, ATRAB2A, RAB2A, RABB1C, ATRAB-B1B, RAB-B1B (RAB GTPase homolog B1C)	23,165.10	169; 170	2	2	4	2	5
AT1G75840.1	ARAC5, ATGP3, ROP4, ATROP4 (RAC-like GTP binding protein 5)	21,777.60	167	1	1	2	1	3
AT3G18820.1	ATRABG3F, ATRAB7B, RAB71, RABG3F, RAB7B (RAB GTPase homolog G3F)	23,102.20	32; 149; 174; 178	4	2	5	2	6
AT5G59840.1	Ras-related small GTP-binding family protein	23,835.40	123; 136; 143; 161	4	0	0	1	7
AT2G44610.1	RAB6, ATRABH1B, ATRAB6A, RAB6A (Ras-related small GTP-binding family protein)	23,130.90	9; 11	2	0	0	2	4
AT5G65270.1	AtRABA4a, RABA4a (RAB GTPase homolog A4A)	24,842.60	205	1	0	0	1	1
AT4G39990.1	ATRABA4B, ATRAB11G, ATGB3, RABA4B (RAB GTPase homolog A4B)	24,407.20	203	1	0	0	1	1
ATCG00120.1	ATPA (ATP synthase subunit alpha)	55,329.80	384	1	1	1	0	0
AT3G28860.1	ATMDR1, ATMDR11, PGP19, MDR11, MDR1, ATPGP19, ABCB19, ATABCB19 (ATP binding cassette subfamily B19)	136,792.50	1068	1	3	13	2	11
AT3G42050.1	vacuolar ATP synthase subunit H family protein	50,286.30	30	1	3	6	2	3
AT4G11150.1	TUF, emb2448, TUFF, VHA-E1 (vacuolar ATP synthase subunit E1)	26,060.40	158	1	0	0	1	2
AT2G01470.1	STL2P, ATSEC12 (SEC12P-like 2 protein)	42,794.40	148	1	1	2	2	3
AT5G38480.1	GRF3, RCI1 (general regulatory factor 3)	28,607.40	52	1	1	2	0	0
AT1G20090.1	ARAC4, ROP2, ATROP2, ATRAC4 (RHO-related protein from plants 2)	21,636.50	166	1	1	1	0	0
AT4G09000.1	GRF1, GF14 CHI (general regulatory factor 1)	29,932.90	58	1	0	0	1	4
AT2G04350.1	LACS8 (AMP-dependent synthetase and ligase family protein)	78,344.20	263	1	0	0	1	2
Transporters								
ATPases								
AT3G09840.1	CDC48, ATCDC48, CDC48A (cell division cycle 48)	89,396.00	13; 14; 113; 254; 515; 667; 672; 758	8	3	16	3	37

AT2G18960.1	AHA1, PMA, OST2, HA1 (H(+)-ATPase 1)	104,227.80	27; 139; 175; 312; 338; 343; 351; 355; 386; 405; 441; 442; 911; 926; 934; 936	16	3	76	2	73
AT5G62670.1	AHA11, HA11 (H(+)-ATPase 11)	105,126.80	179; 316; 943	3	2	5	1	3
AT5G44790.1	RAN1, HMA7 (copper-exporting ATPase / responsive-to-antagonist 1 / copper-transporting ATPase)	107,395.60	449; 452	2	2	4	1	4
AT1G76030.1	ATPase, V1 complex, subunit B protein	54,109.70	474	1	1	2	1	2
AT4G30190.1	AHA2, PMA2, HA2 (H(+)-ATPase 2)	104,405.50	27; 139; 175; 312; 338; 343; 351; 355; 386; 405; 441; 442; 449; 888; 897; 911; 926; 934; 936	19	3	92	3	111
AT5G57110.1	ACA8, AT-ACA8 (autoinhibited Ca ²⁺ -ATPase, isoform 8)	116,176.60	21; 315; 655	3	1	1	1	3
AT5G57350.1	AHA3, ATAHA3, HA3 (H(+)-ATPase 3)	104,453.40	28; 140; 313; 339; 387; 450; 927; 935; 937	9	1	12	2	30
AT2G20140.1	AAA-type ATPase family protein	49,348.50	60; 240	2	1	2	1	1
AT2G41560.1	ACA4 (autoinhibited Ca ²⁺)-ATPase, isoform 4)	112,751.40	115; 123; 124; 471	4	1	1	2	6
AT4G39080.1	VHA-A3 (vacuolar proton ATPase A3)	92,836.80	68; 97; 126; 181; 187; 190; 340; 381	8	3	16	2	17
AT4G37640.1	ACA2 (calcium ATPase 2)	110,440.80	740	1	1	2	1	3
AT1G20260.1	ATPase, V1 complex, subunit B protein	54,313.90	475	1	1	3	1	4
AT2G28520.1	VHA-A1 (vacuolar proton ATPase A1)	93,419.20	275	1	2	2	1	2
AT2G21410.1	VHA-A2 (vacuolar proton ATPase A2)	93,108.40	69; 188; 191	3	1	5	1	3
AT2G22950.1	Cation transporter/ E1-E2 ATPase family protein	110,774.50	741	1	1	2	1	2
AT1G07670.1	ATECA4, ECA4 (endomembrane-type CA-ATPase 4)	116,182.40	216	1	1	1	0	0
AT1G13210.1	ACA.1 (autoinhibited Ca ²⁺ /ATPase I)	0	unknown	1	1	1	1	2
AT2G19110.1	HMA4, ATHMA4 (heavy metal atpase 4)	127,207.90	46; 510	2	0	0	1	5
AT3G28710.1	ATPase, V0/A0 complex, subunit C/D	40,793.00	340	1	0	0	1	1
AT3G57330.1	ACA11 (autoinhibited Ca ²⁺ -ATPase 11)	111,946.40	114	1	0	0	1	2
AT5G58290.1	RPT3 (regulatory particle triple-A ATPase 3)	45,752.30	228	1	0	0	1	1
AT4G29900.1	ACA10, CIF1, ATACA10 (autoinhibited Ca ²⁺)-ATPase 10)	116,860.30	320	1	0	0	1	1
AT5G23630.1	PDR2, MIA (phosphate deficiency response 2)	131,118.80	554	1	0	0	1	1
<i>Ion exchanger</i>								
AT1G53210.1	sodium/calcium exchanger family protein / calcium-binding EF hand family protein	63,419.30	401	1	2	2	1	1
AT4G23700.1	ATCHX17, CHX17 (cation/H ⁺ exchanger 17)	89,168.60	600; 739	2	0	0	1	3

AT1G15690.1	AVP1, ATAVP3, AVP-3, AtVHP1;1 (Inorganic H pyrophosphatase family protein)	80,822.50	254; 265; 628; 710; 715	5	3	23	2	26
AT4G27500.1	PPI1 (proton pump interactor 1)	0	unknown	6	1	4	1	7
<i>ABC Transporters</i>								
AT3G62700.1	ATMRP10, MRP10, ABCC14 (multidrug resistance-associated protein 10)	172,142.20	270; 273	2	1	2	1	4
AT1G15210.1	PDR7, ATPDR7 (pleiotropic drug resistance 7)	162,576.40	92; 100; 107; 119	4	2	5	2	8
AT2G36910.1	ATPGP1, PGP1, ABCB1 (ATP binding cassette subfamily B1)	140,576.40	348;605	2	1	2	1	1
AT2G13610.1	ABC-2 type transporter family protein	73,317.10	159; 249	2	2	3	1	4
AT1G59870.1	PEN3, PDR8, ATPDR8, ABCG36, ATABCG36 (ABC-2 and Plant PDR ABC-type transporter family protein)	165,087.40	54; 94; 102; 109; 121; 132; 313; 485; 492; 503; 508; 817; 1110; 1123; 1127	15	3	28	3	49
AT5G06530.1	ABC-2 type transporter family protein	82,935.80	228	1	1	1	1	1
AT1G51500.1	CER5, D3, ABCG12, WBC12, ATWBC12 (ABC-2 type transporter family protein)	76,453.80	293	1	0	0	1	2
AT2G28070.1	ABC-2 type transporter family protein	81,042.40	132; 432	2	0	0	1	5
AT2G26910.1	PDR4, ATPDR4 (pleiotropic drug resistance 4)	161,270.80	443; 1064; 1123; 1129	4	0	0	2	12
<i>Auxin Transporters</i>								
AT1G23080.1	PIN7, ATPIN7 (Auxin efflux carrier family protein)	67,590.50	323; 327; 377; 426	4	2	6	2	8
AT1G70940.1	PIN3, ATPIN3 (Auxin efflux carrier family protein)	69,468.50	325; 329; 332; 347; 354; 394; 447; 459	8	1	8	2	18
AT3G53480.1	PIS1, PDR9, ATPDR9, ABCG37 (pleiotropic drug resistance 9)	164,112.40	1151	1	1	4	1	3
<i>Sugar transporters</i>								
AT1G11260.1	STP1, ATSTP1 (sugar transporter 1)	57,612.10	512; 520	2	1	2	0	0
AT4G36670.1	Major facilitator superfamily protein	52,925.10	210	1	1	2	1	2
AT3G19930.1	STP4, ATSTP4 (sugar transporter 4)	57,097.30	16; 19	2	0	0	1	5
AT1G71880.1	SUC1, ATSUC1 (sucrose-proton symporter 1)	54,860.70	8; 11; 175	3	1	5	1	8
AT1G22710.1	SUC2, SUT1, ATSUC2 (sucrose-proton symporter 2)	54,548.80	8	1	1	4	1	3
<i>Nitrate transporters</i>								
AT1G12110.1	NRT1.1, CHL1-1, NRT1, B-1, ATNRT1, CHL1 (nitrate transporter 1.1)	64,924.50	291	1	1	2	0	0
AT3G16180.1	Major facilitator superfamily protein	65,335.20	281; 286; 589	3	0	0	1	5
<i>Phosphate transporters</i>								
AT2G38940.1	ATPT2, PHT1;4 (phosphate transporter 1;4)	58,601.50	248; 251; 277; 281	4	3	6	2	17
AT5G43360.1	PHT3, ATPT4, PHT1;3 (phosphate transporter 1;3)	57,260.00	248; 252	2	1	6	1	11
AT5G43350.1	ATPT1, PHT1;1 (phosphate transporter 1;1)	57,618.70	248; 251; 524	3	2	8	1	4

AT1G63010.1	Major Facilitator Superfamily with SPX (SYG1/Pho81/XPR1) domain-containing protein	78,226.40	31	1	1	2	1	4
<i>Other transporters</i>								
AT1G32090.1	early-responsive to dehydration stress protein (ERD4)	93,136.70	294	1	1	1	2	2
AT4G04340.1	ERD (early-responsive to dehydration stress) family protein	87,611.30	706; 770	2	1	6	2	9
AT1G30360.1	ERD4 (Early-responsive to dehydration stress protein)	81,939.40	681; 702; 709	3	2	7	2	7
AT5G16880.1	Target of Myb protein 1	45,311.70	17; 26; 37; 39; 173	5	2	11	3	20
AT5G39040.1	ALS1, ATTAP2, TAP2 (transporter associated with antigen processing protein 2)	69,105.10	172	1	1	1	0	0
AT5G39510.1	VTI11, ATVTI1A, ATVTI1, ZIG, SGR4, VTI1A, ZIG1 (Vesicle transport v-SNARE family protein)	24,952.50	21; 22; 37; 42; 73; 85; 89; 113; 181; 184	10	3	17	2	17
AT1G29310.1	SecY protein transport family protein	52,070.70	412	1	1	2	1	2
AT2G02040.1	ATPTR2-B, NTR1, PTR2-B, PTR2, ATPTR2 (peptide transporter 2)	64,423.70	294	1	1	4	0	0
AT4G23640.1	TRH1, ATKT3, KUP4 (Potassium transporter family protein)	86,845.90	671	1	1	1	1	2
AT5G56020.1	Got1/Sft2-like vesicle transport protein family	24,867.80	76	1	0	0	1	1
AT2G46800.1	ZAT, ATMTPI, MTP1, ZAT1, ATCDF1 (zinc transporter of Arabidopsis thaliana)	43,826.60	331	1	0	0	1	1
AT5G46050.1	ATPTR3, PTR3 (peptide transporter 3)	65,273.20	12; 288	2	0	0	1	3
AT2G27810.1	ATNAT12, NAT12 (nucleobase-ascorbate transporter 12)	76,674.60	60; 111	2	0	0	1	2
AT4G02700.1	SULTR3;2 (sulfate transporter 3;2)	71,273.50	588	1	0	0	1	4
AT1G73220.1	AtOCT1, 1-Oct (organic cation/carnitine transporter1)	59,661.50	287	1	0	0	1	4
AT1G32050.1	SCAMP family protein	30,061.80	22; 60	2	1	5	1	3
AT4G31490.1	Coatomer, beta subunit	106,081.10	39; 76; 713	3	1	4	0	0
AT2G01970.1	Endomembrane protein 70 protein family	68,052.50	424	1	1	1	1	2
AT3G05165.1	Major facilitator superfamily protein	51,294.60	216	1	3	27	3	29
AT3G53420.1	PIP2A, PIP2, PIP2;1 (plasma membrane intrinsic protein 2A)	30,475.20	3	1	1	4	1	4
AT2G45960.1	PIP1B, TMP-A, ATHH2, PIP1;2 (plasma membrane intrinsic protein 1B)	30,598.50	14	1	1	2	1	1
AT2G39010.1	PIP2E, PIP2;6 (plasma membrane intrinsic protein 2E)	31,050.20	3	1	0	0	1	1
AT3G23560.1	ALF5 (MATE efflux family protein)	51,854.00	337	1	1	4	0	0
AT5G19620.1	EMB213, OEP80, ATOEP80, TOC75 (outer envelope protein of 80 kDa)	79,937.20	191	1	1	1	0	0
AT1G52190.1	Major facilitator superfamily protein	66,906.80	605	1	0	0	1	3
AT5G53480.1	ARM repeat superfamily protein	96,261.40	234	1	0	0	1	2
AT3G17650.1	YSL5, PDE321 (YELLOW STRIPE like 5)	78,855.40	34	1	0	0	1	2
AT5G14120.1	Major facilitator superfamily protein	63,150.60	576	1	0	0	1	1
AT1G61250.1	SC3 (secretory carrier 3)	32,614.00	71	1	0	0	1	1
<i>Miscellaneous</i>								
<i>Lipid-related</i>								

AT5G40420.1	OLEO2, OLE2 (oleosin 2)	21,279.70	159; 181	2	1	2	0	0
AT3G27660.1	OLEO4, OLE3 (oleosin 4)	20,313.60	168	1	1	2	0	0
AT3G08510.1	ATPLC2, PLC2 (phospholipase C 2)	66,124.00	266; 497; 498	3	3	12	2	11
AT2G20990.1	SYTA, NTMC2TYPE1.1, ATSYTA, NTMC2T1.1, SYT1 (synaptotagmin A)	61,745.30	98; 275; 379; 480; 527	5	1	3	1	6
AT3G01570.1	Oleosin family protein	19,754.70	153	1	1	3	0	0
AT5G64440.1	AtFAAH, FAAH (fatty acid amide hydrolase)	66,081.10	150	1	3	4	1	2
AT1G51570.1	Calcium-dependent lipid-binding (CaLB domain) plant phosphoribosyltransferase family protein	89,156.50	113; 277	2	1	2	1	1
AT1G05500.1	SYTE, ATSYTE, NTMC2TYPE2.1, NTMC2T2.1, SYT5 (Calcium-dependent lipid-binding (CaLB domain) family protein)	62,929.90	282; 414	2	2	3	0	0
AT5G35200.1	ENTH/ANTH/VHS superfamily protein	61,179.40	310; 317	2	1	1	0	0
AT5G61910.4	DCD (Development and Cell Death) domain protein	147,171.30	934; 936; 1002; 1236	4	1	2	2	3
AT1G31812.1	ACBP6, ACBP (acyl-CoA-binding protein 6)	10,386.20	89	1	0	0	1	2
AT4G35790.1	ATPLDDELTA, PLDDELTA (phospholipase D delta)	98,919.20	811	1	0	0	1	1
<i>Oxidation/reduction</i>								
AT5G47910.1	RBOHD, ATRBOHD (respiratory burst oxidase homologue D)	103,913.30	170; 296	2	1	1	2	4
AT4G13770.1	CYP83A1, REF2 (cytochrome P450, family 83, subfamily A, polypeptide 1)	57,450.70	89	1	2	4	2	6
AT3G14690.1	CYP72A15 (cytochrome P450, family 72, subfamily A, polypeptide 15)	58,443.70	90	1	1	1	1	1
AT1G01580.1	FRO2, FRD1, ATFRO2 (ferric reduction oxidase 2)	81,505.60	359	1	1	1	0	0
AT1G62380.1	ACO2, ATACO2 (ACC oxidase 2)	36,183.80	154; 291	2	0	0	1	3
AT5G22140.1	FAD/NAD(P)-binding oxidoreductase family protein	39,709.50	69; 73; 167	3	0	0	1	10
AT5G53560.1	ATB5-A, B5 #2, ATCB5-E, CB5-E (cytochrome B5 isoform E)	15,084.50	15; 20; 74	3	1	2	1	7
AT5G35735.1	Auxin-responsive family protein	43,868.10	386	1	1	1	0	0
AT5G48810.1	ATB5-B, B5 #3, ATCB5-D, CB5-D (cytochrome B5 isoform D)	15,097.40	88; 90	2	1	2	2	5
AT4G33360.1	FLDH (NAD(P)-binding Rossmann-fold superfamily protein)	37,861.50	112; 115; 119	3	3	5	2	6
AT5G02540.1	NAD(P)-binding Rossmann-fold superfamily protein	36,192.60	321; 322	2	1	1	1	2
AT5G17770.1	ATCBR, CBR1, CBR (NADH:cytochrome B5 reductase 1)	31,490.90	143	1	0	0	2	7
AT4G00360.1	CYP86A2, ATT1 (cytochrome P450, family 86, subfamily A, polypeptide 2)	62,531.20	132; 194; 418	3	0	0	1	6
AT4G31500.1	CYP83B1, SUR2, RNT1, RED1, ATR4 (cytochrome P450, family 83, subfamily B, polypeptide 1)	56,849.60	59; 84; 88; 127; 355	5	3	9	2	12
AT1G13110.1	CYP71B7 (cytochrome P450, family 71 subfamily B, polypeptide 7)	57,211.10	90; 157; 158	3	1	1	1	4
AT4G22690.1	CYP706A1 (cytochrome P450, family 706, subfamily A, polypeptide 1)	63,118.50	337	1	1	4	1	4
AT2G30750.1	CYP71A12 (cytochrome P450, family 71, subfamily A, polypeptide 12)	56,857.40	97; 102; 135; 361; 383	5	0	0	1	11
AT1G45201.1	ATLL1, TLL1 (triacylglycerol lipase-like 1)	54,779.70	159; 167;	5	3	13	2	14

			249; 383; 385					
AT4G30210.1	ATR2, AR2 (P450 reductase 2)	79,027.90	198; 418; 538	3	1	1	1	5
AT5G58970.1	ATUCP2, UCP2 (uncoupling protein 2)	33,444.20	56; 149	2	0	0	1	3
AT5G42980.1	ATTRX3, ATH3, ATTRXH3, TRXH3, TRX3 (thioredoxin 3)	13,109.10	54; 55	2	0	0	2	4
<i>SPFH proteins</i>								
AT3G01290.1	ATHIR2 (SPFH/Band 7/PHB domain-containing membrane-associated protein family)	31,321.10	18; 82; 177; 182; 196; 254	6	3	9	2	16
AT5G62740.1	HIR1, ATHIR1 (SPFH/Band 7/PHB domain-containing membrane-associated protein family)	31,430.90	89; 196; 254	3	1	5	1	7
<i>Histone proteins</i>								
AT5G65350.1	HTR11 (histone 3 11)	15,591.90	57; 80	2	1	3	1	2
AT1G07790.1	HTB1 (Histone superfamily protein)	16,403.00	132; 144	2	1	2	1	2
AT4G40030.1	Histone superfamily protein	15,406.80	37; 52; 54; 57; 65; 80; 108	7	2	10	1	6
AT1G52740.1	HTA9 (histone H2A protein 9)	14,272.50	130	1	2	11	2	14
AT5G59910.1	HTB4 (Histone superfamily protein)	16,450.30	142; 146	2	1	3	1	4
AT2G38810.1	HTA8 (histone H2A 8)	14,370.20	132	1	0	0	1	4
<i>Vesicle-associated proteins</i>								
AT2G45140.1	PVA12 (plant VAP homolog 12)	26,442.20	88	1	1	2	1	1
AT3G60600.1	VAP27-1, VAP, (AT)VAP, VAP27 (vesicle associated protein)	28,473.00	136; 184; 205	3	3	5	2	8
AT3G54300.1	ATVAMP727, VAMP727 (vesicle-associated membrane protein 727)	27,459.90	154	1	1	1	1	2
AT4G32150.1	VAMP711, ATVAMP711 (vesicle-associated membrane protein 711)	25,039.40	161	1	1	2	1	2
AT1G04750.1	VAMP7B, VAMP721, ATVAMP721, AT VAMP7B (vesicle-associated membrane protein 721)	24,765.30	97; 108; 113; 115; 135	5	2	14	2	17
AT1G08820.1	VAP27-2 (vamp/synaptobrevin-associated protein 27-2)	43,270.10	320	1	0	0	1	1
AT2G33120.1	SAR1, VAMP722, ATVAMP722 (synaptobrevin-related protein 1)	24,928.70	97; 108; 115; 142; 155; 165	6	1	11	1	19
AT5G58060.1	YKT61, ATYKT61, ATGP1 (SNARE-like superfamily protein)	22,543.90	156	1	0	0	1	1
<i>Cellulose synthase proteins</i>								
AT5G05170.1	CESA3, IXR1, ATCESA3, ATH-B, CEV1 (Cellulose synthase family protein)	119,685.70	165; 193; 202; 205; 427; 434; 456; 459	8	3	24	2	21
AT5G64740.1	CESA6, IXR2, E112, PRC1 (cellulose synthase 6)	122,505.20	227; 231; 444; 708	4	2	7	2	7
AT5G22740.1	ATCSLA02, CSLA02, ATCSLA2, CSLA2 (cellulose synthase-like A02)	61,559.50	156	1	1	4	0	0
AT4G32410.1	CESA1, RSW1, AtCESA1 (cellulose synthase 1)	122,240.70	223; 236; 443; 450; 472; 475	6	3	15	3	15
AT3G03050.1	CSLD3, KJK, ATCSLD3 (cellulose synthase-like D3)	128,592.80	474	1	0	0	1	2
AT4G31590.1	ATCSLC05, CSLC05, ATCSLC5, CSLC5 (Cellulose-synthase-like C5)	79,423.70	286	1	2	3	1	2

<i>Carboxylases</i>								
AT1G53310.1	ATPPC1, PEPC1, ATPEPC1, PPC1 (phosphoenolpyruvate carboxylase 1)	110,289.90	590; 625; 630	3	2	24	2	34
AT2G42600.1	ATPPC2, PPC2 (phosphoenolpyruvate carboxylase 2)	109,757.20	587; 622; 627; 727	4	2	55	1	41
AT3G14940.1	ATPPC3, PPC3 (phosphoenolpyruvate carboxylase 3)	110,164.10	627; 631	2	1	4	1	7
<i>Methyltransferases</i>								
AT1G55450.1	S-adenosyl-L-methionine-dependent methyltransferases superfamily protein	34,476.20	69	1	1	1	0	0
AT1G20330.1	SMT2, CVP1, FRL1 (sterol methyltransferase 2)	40,450.30	269; 270	2	1	2	2	4
<i>Glycosyltransferases</i>								
AT3G07020.1	UDP-Glycosyltransferase superfamily protein	69,322.60	604	1	1	2	1	2
<i>Sugar transferases</i>								
AT5G03760.1	ATCSLA09, CSLA09, ATCSLA9, CSLA9, RAT4 (Nucleotide-diphospho-sugar transferases superfamily protein)	60,920.90	156	1	3	9	0	0
<i>Heat shock proteins</i>								
AT5G56030.2	HSP81-2 (heat shock protein 81-2)	83,130.80	281; 478	2	1	1	1	4
AT3G09440.1	Heat shock protein 70 (Hsp 70) family protein	71,149.90	457; 513	2	1	7	1	5
AT4G28480.1	DNAJ heat shock family protein	38,192.30	7	1	0	0	1	2
AT5G02500.1	HSC70-1, HSP70-1, AT-HSC70-1, HSC70 (heat shock cognate protein 70-1)	71,359.60	252; 457; 506; 513	4	1	12	1	13
AT4G21180.1	ATERDJ2B (DnaJ / Sec63 Brl domains-containing protein)	74,827.20	411	1	0	0	1	2
<i>Hydrolases</i>								
AT5G26667.1	PYR6 (P-loop containing nucleoside triphosphate hydrolases superfamily protein)	23,125.20	54; 111	2	1	3	1	1
AT2G47630.1	alpha/beta-Hydrolases superfamily protein	39,709.50	197	1	1	2	1	3
AT5G58090.1	O-Glycosyl hydrolases family 17 protein	52,213.30	361	1	1	1	1	2
AT4G13940.1	HOG1, EMB1395, SAHH1, MEE58, ATSAHH1 (S-adenosyl-L-homocysteine hydrolase)	53,379.20	211; 435	2	2	3	2	4
AT1G51760.1	IAR3, JR3 (peptidase M20/M25/M40 family protein)	48,263.50	5	1	0	0	1	1
<i>Annexins</i>								
AT1G35720.1	ANNAT1, OXY5, ATOXY5 (annexin 1)	36,204.90	198	1	1	2	1	2
<i>Decarboxylases</i>								
AT1G47290.2	AT3BETAHSD/D1, 3BETAHSD/D1 (3beta-hydroxysteroid-dehydrogenase/decarboxylase isoform 1)	48,125.20	174; 352	2	2	7	2	13
AT3G62830.1	UXS2, ATUXS2, AUD1 (NAD(P)-binding Rossmann-fold superfamily protein)	49,971.70	94	1	1	1	0	0
<i>Dehydrogenases</i>								
AT1G13440.1	GAPC-2, GAPC2 (glyceraldehyde-3-phosphate dehydrogenase C2)	36,913.40	219; 223	2	2	3	2	4
AT1G65930.1	cICDH (cytosolic NADP+-dependent isocitrate dehydrogenase)	45,747.80	9	1	2	2	1	2
AT1G04410.1	Lactate/malate dehydrogenase family protein	35,570.90	111; 119; 237	3	3	7	2	7

AT5G15490.1	UDP-glucose 6-dehydrogenase family protein	53,117.70	91	1	3	8	3	8
AT5G39320.1	UDP-glucose 6-dehydrogenase family protein	53,097.60	91; 99	2	3	5	1	2
<i>Tetraspanin family proteins</i>								
AT2G20230.1	Tetraspanin family protein	29,722.60	246; 257; 269	3	2	8	1	5
AT2G20740.1	Tetraspanin family protein	24,656.20	205; 215	2	1	2	0	0
AT3G45600.1	TET3 (tetraspanin3)	31,889.40	277	1	1	1	0	0
<i>Anhydrases</i>								
AT1G70410.1	ATBCA4, BCA4, CA4 (beta carbonic anhydrase 4)	28,412.90	20; 30; 32; 39; 42; 54; 61; 66; 76; 81; 87; 98; 121	13	3	39	3	39
AT5G14740.1	CA2, CA18, BETA CA2 (carbonic anhydrase 2)	36,615.50	151	1	1	1	1	1
<i>Microtubule-associated proteins</i>								
AT1G19870.1	iqd32 (IQ-domain 32)	86,881.90	116; 117; 350	3	1	3	0	0
AT4G20260.1	ATPCAP1, PCAP1 (plasma-membrane associated cation-binding protein 1)	24,583.20	135	1	1	1	0	0
AT4G14960.2	TUA6 (Tubulin/FtsZ family protein)	49,537.80	163; 164	2	1	1	1	1
<i>hydroxylases</i>								
AT2G30490.1	ATC4H, C4H, CYP73A5, REF3 (cinnamate-4-hydroxylase)	57,794.10	141; 163; 170; 268	4	2	4	1	5
AT5G57800.1	FLP1, YRE, CER3, WAX2 (Fatty acid hydroxylase superfamily)	72,289.80	518	1	0	0	1	1
<i>ADP-ribosylation factors</i>								
AT3G62290.1	ATARFA1E, ARFA1E (ADP-ribosylation factor A1E)	20,608.40	36; 142	2	1	2	1	6
AT1G10630.1	ATARFA1F, ARFA1F (ADP-ribosylation factor A1F)	20,623.50	142	1	2	3	1	1
<i>Glycoproteins</i>								
AT1G17620.1	Late embryogenesis abundant (LEA) hydroxyproline-rich glycoprotein family	0	unknown	1	2	7	2	8
AT3G62150.1	PGP21 (P-glycoprotein 21)	140,338.20	513; 1049; 1254	3	1	6	0	0
AT3G55320.1	PGP20 (P-glycoprotein 20)	155,159.90	1400	1	0	0	1	1
AT5G16620.1	PDE120, TIC40, ATTIC40 (hydroxyproline-rich glycoprotein family protein)	48,903.30	332	1	0	0	1	1
<i>ketoacyl proteins</i>								
AT2G26250.1	FDH, KCS10 (3-ketoacyl-CoA synthase 10)	61,962.50	148; 357; 360; 421; 426	5	1	3	1	6
AT5G04530.1	KCS19 (3-ketoacyl-CoA synthase 19)	52,614.80	56; 62; 321	3	1	2	1	4
AT2G28630.1	KCS12 (3-ketoacyl-CoA synthase 12)	53,976.50	68; 274	2	0	0	1	4
<i>Peroxidases</i>								
AT3G01420.1	ALPHA-DOX1, DOX1, DIOX1, PADOX-1 (Peroxidase superfamily protein)	73,161.00	208	1	1	4	2	10
AT4G35000.1	APX3 (ascorbate peroxidase 3)	31,572.80	125	1	0	0	1	1
AT5G64120.1	Peroxidase superfamily protein	34,889.10	179	2	0	0	1	2

<i>Syntaxins</i>								
AT5G08080.1	SYP132, AT5YP132 (syntaxin of plants 132)	34,225.70	39; 40; 50; 98	4	1	2	1	3
AT5G46860.1	VAM3, ATVAM3, SYP22, AT5YP22, SGR3 (Syntaxin/t-SNARE family protein)	29,481.50	74; 79; 97; 102; 112; 231	6	3	23	3	19
AT3G11820.2	SYP121, AT-SYR1, AT5YP121, SYR1, AT5YR1, PEN1 (syntaxin of plants 121)	34,658.90	59; 90; 114; 144; 145; 169	6	2	9	2	8
AT3G52400.1	SYP122, AT5YP122 (syntaxin of plants 122)	37,837.20	99; 105	2	3	29	3	29
AT3G09740.1	SYP71, AT5YP71 (syntaxin of plants 71)	29,984.20	96; 216; 225	3	3	9	2	11
<i>LMBR-like proteins</i>								
AT5G01460.1	LMBR1-like membrane protein	56,503.80	254	1	2	10	2	18
AT3G08930.1	LMBR1-like membrane protein	56,547.00	254	1	1	3	0	0
<i>Remorins</i>								
AT2G45820.1	Remorin family protein	20,968.10	22; 35; 60; 86	4	1	5	1	9
AT3G61260.1	Remorin family protein	23,144.60	145	1	0	0	1	1
<i>Other</i>								
AT3G56170.1	CAN (Ca-2+ dependent nuclease)	36,134.90	170; 178; 244	3	2	5	0	0
AT2G26300.1	GPA1, GP ALPHA 1, ATGPA1 (G protein alpha subunit 1)	44,547.30	9	1	2	3	1	2
AT3G23820.1	GAE6 (UDP-D-glucuronate 4-epimerase 6)	50,571.20	11; 14	2	2	6	2	5
AT1G27980.1	DPL1, ATDPL1 (dihydrosphingosine phosphate lyase)	59,478.80	244	1	1	1	0	0
AT3G52930.1	Aldolase superfamily protein	38,540.40	38; 131; 132; 306; 354; 357	6	3	5	3	14
AT1G57720.1	Translation elongation factor EF1B, gamma chain	46,401.80	278	1	1	1	1	1
AT3G17970.1	atToc64-III, TOC64-III (translocon at the outer membrane of chloroplasts 64-III)	64,026.90	284	1	3	6	2	5
AT5G17920.1	ATCIMS, ATMETS, ATMS1 (Cobalamin-independent synthase family protein)	84,358.40	142; 279; 400; 406; 688; 739	6	3	14	3	19
AT5G62390.1	ATBAG7, BAG7 (BCL-2-associated athanogene 7)	51,569.80	90; 102; 110; 119; 179; 180; 182; 186; 195; 196; 197; 410	12	2	38	1	20
AT3G50480.1	HR4 (homolog of RPW8 4)	23,389.90	34; 36	2	1	8	1	10
AT3G55440.1	ATCTIMC, TPI, CYTOTPI (triosephosphate isomerase)	27,168.20	195	1	1	1	0	0
AT5G20490.1	XIK, ATXIK, XI-17 (Myosin family protein with Dil domain)	175,056.80	939	1	1	1	0	0
AT1G68720.1	TADA, ATTADA (tRNA arginine adenosine deaminase)	146,563.20	36; 240	2	1	2	1	3
AT5G22760.1	PHD finger family protein	175,671.50	1307	1	1	1	0	0
AT2G36880.1	MAT3 (methionine adenosyltransferase 3)	42,497.80	291	1	1	1	0	0
AT5G52240.1	MSBP1, ATMP1, AtMAPR5 (membrane steroid binding protein 1)	24,405.50	166; 171	2	1	1	1	1
AT2G30620.1	winged-helix DNA-binding transcription factor family protein	28,487.60	49; 156	2	2	3	1	3
AT3G52950.1	CBS / octicosapeptide/Phox/Bemp1 (PB1) domains-containing protein	60,027.00	493	1	1	1	0	0

AT2G30870.1	ATGSTF10, ERD13, ATGSTF4, GSTF10 (glutathione S-transferase PHI 10)	24,230.60	14	1	1	1	1	2
AT5G56360.1	PSL4 (calmodulin-binding protein)	73,214.80	202	1	0	0	1	1
AT1G26630.1	FBR12, ATELF5A-2, ELF5A-2 (Eukaryotic translation initiation factor 5A-1 (eIF-5A 1) protein)	17,140.00	40	1	0	0	1	1
AT1G68820.1	Transmembrane Fragile-X-F-associated protein	53,637.20	379; 380; 418	3	0	0	1	6
AT4G14760.1	kinase interacting (KIP1-like) family protein	196,983.50	901; 908	2	0	0	1	3
AT1G09920.1	TRAF-type zinc finger-related	21,847.90	85; 134	2	0	0	1	3
AT1G64090.1	RTNLB3 (Reticulan like protein B3)	28,698.10	242	1	0	0	1	1
AT5G42090.1	Lung seven transmembrane receptor family protein	50,227.10	345	1	0	0	1	1
AT1G77510.1	ATPDIL1-2, PDI6, ATPDI6, PDIL1-2 (PDI-like 1-2)	56,365.40	497	1	0	0	1	1
AT5G13000.1	ATGSL12, gsl12 (glucan synthase-like 12)	226,191.90	1275	1	0	0	1	1
AT2G27860.1	AXS1 (UDP-D-apiose/UDP-D-xylose synthase 1)	43,639.20	251	1	0	0	1	2
AT5G09810.1	ACT7 (actin 7)	41,736.60	328; 330	2	0	0	2	2
AT3G17390.1	MTO3, SAMS3, MAT4 (S-adenosylmethionine synthetase family protein)	42,795.50	291	1	0	0	2	2
AT4G26690.1	SHV3, MRH5, GPDL2 (PLC-like phosphodiesterase family protein)	82,564.70	515	1	0	0	1	1
AT1G74520.1	ATHVA22A, HVA22A (HVA22 homologue A)	20,679.80	120	1	0	0	1	2
AT3G13920.1	EIF4A1, RH4, TIF4A1 (eukaryotic translation initiation factor 4A1)	46,704.90	61	1	0	0	1	2
AT2G17570.1	Undecaprenyl pyrophosphate synthetase family protein	33,629.40	114	1	0	0	1	1
AT3G48730.1	GSA2 (glutamate-1-semialdehyde 2,1-aminomutase 2)	50,143.40	59	1	0	0	1	1
AT2G21160.1	Translocon-associated protein (TRAP), alpha subunit	28,167.80	224	1	0	0	1	1
AT2G36850.1	ATGSL08, GSL8, GSL08, ATGSL8, CHOR (glucan synthase-like 8)	218,386.40	469	1	0	0	1	1
AT3G19820.1	DWF1, DIM, EVE1, DIM1, CBB1 (cell elongation protein / DWARF1 / DIMINUTO (DIM))	65,395.80	81	1	0	0	1	1
AT1G44575.1	NPQ4, PSBS (Chlorophyll A-B binding family protein)	28,009.70	181	1	0	0	1	1
AT4G29130.1	ATHXK1, GIN2, HXK1 (hexokinase 1)	53,708.00	77; 117	2	1	1	1	1
AT4G21534.1	Diaclyglycerol kinase family protein	53,891.80	59	1	1	2	1	4
AT4G09320.1	NDPK1 (Nucleoside diphosphate kinase family protein)	18,814.30	106	1	0	0	1	2
Uncharacterized proteins								
AT3G27390.1	unknown protein	0	unknown	2	2	5	1	4
AT1G45688.1	unknown protein	0	unknown	1	1	1	1	2
AT2G30930.1	unknown protein	0	unknown	4	1	4	1	8
AT1G65720.1	unknown protein	20,123.40	162; 167; 177	3	3	13	2	19
AT2G22660.2	Protein of unknown function (duplicated DUF1399)	89,487.10	450	1	1	1	0	0
AT1G70770.1	Protein of unknown function DUF2359, transmembrane	66,865.80	81; 398	2	1	1	1	1
AT3G47250.1	Plant protein of unknown function (DUF247)	54,808.80	276; 301	2	1	4	0	0
AT5G08050.1	Protein of unknown function (DUF1118)	16,581.00	33	1	1	1	0	0
AT5G47020.1	unknown protein	152,785.00	1014	1	0	0	1	2

AT3G52920.1	Family of unknown function (DUF662)	20,984.50	118	1	0	0	1	2
AT1G06980.1	unknown protein	0	unknown	1	0	0	1	4
AT4G14230.1	CBS domain-containing protein with a domain of unknown function (DUF21)	53,493.20	328	1	1	1	0	0
AT2G36100.1	Uncharacterised protein family (UPF0497)	21,970.10	18; 25	2	1	1	1	3
AT1G17200.1	Uncharacterised protein family (UPF0497)	21,878.50	9; 22	2	0	0	1	4
AT4G17140.1	pleckstrin homology (PH) domain-containing protein	471,008.30	2522	1	0	0	1	1

Table S11. GO term enrichment for mock treated di-Gly microsomal fractions. Using the list of proteins generated from microsomal preps for mock treated samples, GO term STRING enrichment was performed to determine GO categories of Component, Function and Process. GO term ID, GO term, GO category, FDR and number of enriched genes in the dataset are presented for mock treated samples.

GO Term ID	GO Term	GO Category	FDR p-value	# enriched genes
<i>GO Component</i>				
GO:0016020	membrane	GO Component	##### #	225
GO:0005886	plasma membrane	GO Component	##### #	160
GO:0071944	cell periphery	GO Component	1.82E-95	167
GO:0055044	symplast	GO Component	5.20E-76	99
GO:0009506	plasmodesma	GO Component	5.20E-76	99
GO:0044425	membrane part	GO Component	1.76E-59	156
GO:0016021	integral component of membrane	GO Component	1.94E-54	142
GO:0031224	intrinsic component of membrane	GO Component	5.54E-54	144
GO:0044464	cell part	GO Component	3.31E-51	233
GO:0005623	cell	GO Component	5.22E-51	233
GO:0005575	cellular_component	GO Component	2.51E-49	247
GO:0005773	vacuole	GO Component	2.41E-43	69
GO:0044444	cytoplasmic part	GO Component	1.24E-40	161
GO:0005737	cytoplasm	GO Component	8.54E-37	168
GO:0044422	organelle part	GO Component	5.16E-35	126

		nt		
GO:004446	intracellular organelle part	GO Component	1.65E-34	125
GO:0098588	bounding membrane of organelle	GO Component	9.24E-34	75
GO:0012505	endomembrane system	GO Component	5.24E-33	78
GO:0005774	vacuolar membrane	GO Component	2.92E-32	48
GO:0098805	whole membrane	GO Component	1.16E-29	56
GO:0031090	organelle membrane	GO Component	1.36E-27	78
GO:0044445	cytosolic part	GO Component	1.76E-26	36
GO:0022626	cytosolic ribosome	GO Component	5.83E-25	34
GO:0043229	intracellular organelle	GO Component	8.78E-25	169
GO:0005794	Golgi apparatus	GO Component	4.76E-24	49
GO:0044391	ribosomal subunit	GO Component	1.29E-23	31
GO:0005622	intracellular	GO Component	4.04E-23	177
GO:0044424	intracellular part	GO Component	2.83E-22	174
GO:0005829	cytosol	GO Component	3.45E-22	63
GO:0043231	intracellular membrane-bounded organelle	GO Component	2.88E-21	159
GO:0043232	intracellular non-membrane-bounded organelle	GO Component	1.83E-18	51
GO:0032991	macromolecular complex	GO Component	4.10E-18	64
GO:0022627	cytosolic small ribosomal subunit	GO Component	3.29E-13	15

GO:002 2625	cytosolic large ribosomal subunit	GO Compone nt	7.82E- 13	16
GO:000 5783	endoplasmic reticulum	GO Compone nt	1.79E- 11	31
GO:000 5730	nucleolus	GO Compone nt	8.06E- 10	20
GO:000 5618	cell wall	GO Compone nt	3.14E- 09	26
GO:000 0325	plant-type vacuole	GO Compone nt	6.90E- 09	13
GO:000 5768	endosome	GO Compone nt	1.90E- 08	19
GO:003 1981	nuclear lumen	GO Compone nt	5.72E- 08	24
GO:000 9536	plastid	GO Compone nt	5.81E- 07	47
GO:000 5789	endoplasmic reticulum membrane	GO Compone nt	7.23E- 07	18
GO:000 9507	chloroplast	GO Compone nt	7.74E- 07	46
GO:004 2175	nuclear outer membrane-endoplasmic reticulum membrane network	GO Compone nt	7.74E- 07	18
GO:003 3176	proton-transporting V-type ATPase complex	GO Compone nt	9.92E- 07	6
GO:003 1201	SNARE complex	GO Compone nt	3.46E- 06	7
GO:004 4431	Golgi apparatus part	GO Compone nt	4.38E- 06	19
GO:003 1988	membrane-bounded vesicle	GO Compone nt	7.29E- 06	11
GO:001 6469	proton-transporting two-sector ATPase complex	GO Compone nt	9.51E- 06	7
GO:001 6471	vacuolar proton-transporting V-type ATPase complex	GO Compone nt	1.83E- 05	4
GO:001 2511	monolayer-surrounded lipid storage body	GO Compone nt	1.83E- 05	4
GO:000	plant-type vacuole membrane	GO	2.82E-	8

9705		Component	05	
GO:0016023	cytoplasmic membrane-bounded vesicle	GO Component	4.47E-05	10
GO:0000220	vacuolar proton-transporting V-type ATPase, V0 domain	GO Component	5.30E-05	3
GO:0043234	protein complex	GO Component	6.25E-05	30
GO:0098796	membrane protein complex	GO Component	6.40E-05	16
GO:0000786	nucleosome	GO Component	6.81E-05	6
GO:0000139	Golgi membrane	GO Component	9.97E-05	15
GO:0033180	proton-transporting V-type ATPase, V1 domain	GO Component	4.12E-04	3
GO:0044459	plasma membrane part	GO Component	5.54E-04	12
GO:0033178	proton-transporting two-sector ATPase complex, catalytic domain	GO Component	7.89E-04	4
GO:0005802	trans-Golgi network	GO Component	8.81E-04	9
GO:0010008	endosome membrane	GO Component	0.00112	8
GO:0000785	chromatin	GO Component	0.0018	6
GO:0030139	endocytic vesicle	GO Component	0.00224	3
GO:0012506	vesicle membrane	GO Component	0.00264	6
GO:0048046	apoplast	GO Component	0.00376	13
GO:0030133	transport vesicle	GO Component	0.0045	4
GO:0008540	proteasome regulatory particle, base subcomplex	GO Component	0.00568	2
GO:0000788	nuclear nucleosome	GO Component	0.0093	2

		nt		
GO:0035618	root hair	GO Component	0.0136	2
GO:0035619	root hair tip	GO Component	0.0136	2
GO:0030659	cytoplasmic vesicle membrane	GO Component	0.0166	5
GO:0030658	transport vesicle membrane	GO Component	0.0168	3
GO:0044426	cell wall part	GO Component	0.0179	2
GO:0005838	proteasome regulatory particle	GO Component	0.0179	2
GO:0022624	proteasome accessory complex	GO Component	0.0179	2
GO:0031226	intrinsic component of plasma membrane	GO Component	0.0194	8
GO:0031595	nuclear proteasome complex	GO Component	0.0224	2
GO:0031597	cytosolic proteasome complex	GO Component	0.0224	2
GO:0009986	cell surface	GO Component	0.0352	2
GO:0009505	plant-type cell wall	GO Component	0.0394	6
GO:0005887	integral component of plasma membrane	GO Component	0.0443	6
GO:0009898	cytoplasmic side of plasma membrane	GO Component	0.049	2
GO Function				
GO:0032553	ribonucleotide binding	GO Function	2.97E-35	96
GO:0032550	purine ribonucleoside binding	GO Function	2.97E-35	95
GO:0035639	purine ribonucleoside triphosphate binding	GO Function	2.97E-35	95
GO:0032555	purine ribonucleotide binding	GO Function	4.22E-35	95
GO:0043168	anion binding	GO Function	5.58E-34	102

GO:000 0166	nucleotide binding	GO Function	5.85E- 33	100
GO:000 3674	molecular_function	GO Function	7.52E- 32	199
GO:004 3167	ion binding	GO Function	7.28E- 29	133
GO:000 5488	binding	GO Function	9.63E- 29	164
GO:000 5524	ATP binding	GO Function	2.56E- 27	80
GO:000 5515	protein binding	GO Function	7.69E- 26	59
GO:190 1363	heterocyclic compound binding	GO Function	7.69E- 25	127
GO:009 7159	organic cyclic compound binding	GO Function	7.82E- 25	127
GO:001 9899	enzyme binding	GO Function	1.31E- 22	35
GO:000 3824	catalytic activity	GO Function	1.60E- 22	140
GO:001 6817	hydrolase activity, acting on acid anhydrides	GO Function	2.27E- 22	45
GO:001 7111	nucleoside-triphosphatase activity	GO Function	2.99E- 21	42
GO:001 6462	pyrophosphatase activity	GO Function	3.90E- 21	43
GO:001 6820	hydrolase activity, acting on acid anhydrides, catalyzing transmembrane movement of substances	GO Function	7.89E- 20	23
GO:004 3492	ATPase activity, coupled to movement of substances	GO Function	4.03E- 18	22
GO:004 2626	ATPase activity, coupled to transmembrane movement of substances	GO Function	9.54E- 18	21
GO:001 6887	ATPase activity	GO Function	1.77E- 17	30
GO:001 5405	P-P-bond-hydrolysis-driven transmembrane transporter activity	GO Function	1.93E- 17	22
GO:002 2804	active transmembrane transporter activity	GO Function	1.02E- 16	31
GO:000 5215	transporter activity	GO Function	4.30E- 16	46
GO:000 3735	structural constituent of ribosome	GO Function	4.66E- 16	27
GO:002 2857	transmembrane transporter activity	GO Function	1.98E- 15	41
GO:004 2623	ATPase activity, coupled	GO Function	3.16E- 15	24
GO:000 5198	structural molecule activity	GO Function	3.24E- 15	29
GO:000 4672	protein kinase activity	GO Function	3.52E- 15	39
GO:000 1653	peptide receptor activity	GO Function	5.41E- 15	23
GO:001 9829	cation-transporting ATPase activity	GO Function	6.14E- 15	15

GO:001 9199	transmembrane receptor protein kinase activity	GO Function	7.12E- 15	23
GO:003 1625	ubiquitin protein ligase binding	GO Function	1.05E- 14	24
GO:001 6773	phosphotransferase activity, alcohol group as acceptor	GO Function	1.71E- 14	41
GO:003 8023	signaling receptor activity	GO Function	2.30E- 14	24
GO:000 4675	transmembrane receptor protein serine/threonine kinase activity	GO Function	4.00E- 14	22
GO:001 6301	kinase activity	GO Function	4.20E- 14	42
GO:000 4871	signal transducer activity	GO Function	1.83E- 12	26
GO:002 2892	substrate-specific transporter activity	GO Function	2.16E- 12	35
GO:002 2891	substrate-specific transmembrane transporter activity	GO Function	1.58E- 11	32
GO:000 4674	protein serine/threonine kinase activity	GO Function	2.49E- 11	32
GO:003 6442	hydrogen-exporting ATPase activity	GO Function	6.32E- 10	9
GO:001 5662	ATPase activity, coupled to transmembrane movement of ions, phosphorylative mechanism	GO Function	8.79E- 10	9
GO:001 6787	hydrolase activity	GO Function	1.68E- 09	56
GO:000 8324	cation transmembrane transporter activity	GO Function	1.77E- 09	22
GO:001 6740	transferase activity	GO Function	3.99E- 09	59
GO:001 5075	ion transmembrane transporter activity	GO Function	1.17E- 08	24
GO:000 5525	GTP binding	GO Function	1.76E- 07	15
GO:002 2890	inorganic cation transmembrane transporter activity	GO Function	3.08E- 06	16
GO:000 0149	SNARE binding	GO Function	3.08E- 06	7
GO:000 3924	GTPase activity	GO Function	6.58E- 06	11
GO:000 5388	calcium-transporting ATPase activity	GO Function	9.31E- 06	5
GO:000 5507	copper ion binding	GO Function	1.80E- 05	11
GO:004 6961	proton-transporting ATPase activity, rotational mechanism	GO Function	3.74E- 05	5
GO:001 6004	phospholipase activator activity	GO Function	4.16E- 05	3
GO:000 8553	hydrogen-exporting ATPase activity, phosphorylative mechanism	GO Function	1.37E- 04	4
GO:000 8964	phosphoenolpyruvate carboxylase activity	GO Function	1.61E- 04	3
GO:001 0329	auxin efflux transmembrane transporter activity	GO Function	2.04E- 04	5

GO:001 5078	hydrogen ion transmembrane transporter activity	GO Function	2.24E- 04	9
GO:000 9678	hydrogen-translocating pyrophosphatase activity	GO Function	3.66E- 04	3
GO:000 4715	non-membrane spanning protein tyrosine kinase activity	GO Function	3.66E- 04	3
GO:000 5484	SNAP receptor activity	GO Function	4.76E- 04	5
GO:001 9901	protein kinase binding	GO Function	6.53E- 04	5
GO:001 5293	symporter activity	GO Function	7.16E- 04	8
GO:004 6872	metal ion binding	GO Function	7.16E- 04	51
GO:001 5077	monovalent inorganic cation transmembrane transporter activity	GO Function	9.53E- 04	10
GO:000 4713	protein tyrosine kinase activity	GO Function	0.00124	4
GO:004 6914	transition metal ion binding	GO Function	0.00236	26
GO:005 1117	ATPase binding	GO Function	0.00264	3
GO:004 7259	glucomannan 4-beta-mannosyltransferase activity	GO Function	0.00303	2
GO:000 8506	sucrose:proton symporter activity	GO Function	0.00884	2
GO:007 2509	divalent inorganic cation transmembrane transporter activity	GO Function	0.00994	6
GO:001 6831	carboxy-lyase activity	GO Function	0.0103	5
GO:000 5351	sugar:proton symporter activity	GO Function	0.0132	4
GO:000 5315	inorganic phosphate transmembrane transporter activity	GO Function	0.0153	3
GO:000 3979	UDP-glucose 6-dehydrogenase activity	GO Function	0.0164	2
GO:001 5144	carbohydrate transmembrane transporter activity	GO Function	0.0174	6
GO:001 5291	secondary active transmembrane transporter activity	GO Function	0.0243	9
GO:001 0328	auxin influx transmembrane transporter activity	GO Function	0.0262	2
GO:005 1753	mannan synthase activity	GO Function	0.0377	2
GO:002 0037	heme binding	GO Function	0.0377	9
GO:000 5543	phospholipid binding	GO Function	0.0484	5
GO:004 6873	metal ion transmembrane transporter activity	GO Function	0.0496	7
GO Process				
GO:005 1179	localization	GO Process	5.71E- 30	89
GO:000	cellular process	GO	6.27E-	193

9987		Process	29	
GO:005 1234	establishment of localization	GO Process	7.06E- 29	86
GO:000 6810	transport	GO Process	1.60E- 28	85
GO:005 0896	response to stimulus	GO Process	7.02E- 27	125
GO:190 2578	single-organism localization	GO Process	1.36E- 25	70
GO:000 8150	biological_process	GO Process	1.43E- 24	205
GO:004 4765	single-organism transport	GO Process	1.56E- 24	68
GO:004 4699	single-organism process	GO Process	1.75E- 21	154
GO:004 4763	single-organism cellular process	GO Process	2.99E- 20	134
GO:000 8152	metabolic process	GO Process	4.78E- 19	168
GO:004 2221	response to chemical	GO Process	4.78E- 19	78
GO:000 6796	phosphate-containing compound metabolic process	GO Process	2.02E- 17	61
GO:005 1716	cellular response to stimulus	GO Process	5.45E- 17	69
GO:004 4267	cellular protein metabolic process	GO Process	2.33E- 16	77
GO:001 0033	response to organic substance	GO Process	2.48E- 16	62
GO:005 5085	transmembrane transport	GO Process	1.51E- 15	45
GO:000 7165	signal transduction	GO Process	2.49E- 15	54
GO:000 7154	cell communication	GO Process	3.35E- 15	58
GO:004 4700	single organism signaling	GO Process	7.93E- 15	54
GO:001 9538	protein metabolic process	GO Process	7.93E- 15	78
GO:000 6468	protein phosphorylation	GO Process	1.77E- 14	39
GO:190 1564	organonitrogen compound metabolic process	GO Process	2.87E- 14	51
GO:000 9725	response to hormone	GO Process	7.77E- 14	53
GO:001 6192	vesicle-mediated transport	GO Process	7.91E- 14	25
GO:001 6310	phosphorylation	GO Process	8.40E- 14	44
GO:007 1840	cellular component organization or biogenesis	GO Process	1.06E- 13	61
GO:000 7178	transmembrane receptor protein serine/threonine kinase signaling pathway	GO Process	1.27E- 13	22
GO:000	response to endogenous stimulus	GO	1.75E-	54

9719		Process	13	
GO:0006412	translation	GO Process	6.99E-13	28
GO:0006811	ion transport	GO Process	9.31E-13	36
GO:0051641	cellular localization	GO Process	1.27E-12	29
GO:0016043	cellular component organization	GO Process	1.72E-12	57
GO:0046777	protein autophosphorylation	GO Process	1.92E-12	24
GO:1901566	organonitrogen compound biosynthetic process	GO Process	3.54E-12	40
GO:0033036	macromolecule localization	GO Process	4.96E-12	34
GO:0071310	cellular response to organic substance	GO Process	1.31E-11	41
GO:0098655	cation transmembrane transport	GO Process	1.42E-11	25
GO:0006812	cation transport	GO Process	1.62E-11	26
GO:0034220	ion transmembrane transport	GO Process	1.79E-11	30
GO:0071704	organic substance metabolic process	GO Process	5.92E-11	132
GO:0044237	cellular metabolic process	GO Process	7.41E-11	128
GO:0009605	response to external stimulus	GO Process	9.80E-11	44
GO:0044238	primary metabolic process	GO Process	1.17E-10	127
GO:0015031	protein transport	GO Process	2.00E-10	28
GO:0071702	organic substance transport	GO Process	2.33E-10	38
GO:0015991	ATP hydrolysis coupled proton transport	GO Process	3.16E-10	10
GO:0007264	small GTPase mediated signal transduction	GO Process	3.47E-10	13
GO:0006950	response to stress	GO Process	4.67E-10	64
GO:0032870	cellular response to hormone stimulus	GO Process	7.12E-10	36
GO:0051704	multi-organism process	GO Process	8.57E-10	42
GO:0009628	response to abiotic stimulus	GO Process	1.24E-09	45
GO:0070727	cellular macromolecule localization	GO Process	1.87E-09	21
GO:0015992	proton transport	GO Process	3.93E-09	16
GO:0051649	establishment of localization in cell	GO Process	4.21E-09	23
GO:009	inorganic cation transmembrane transport	GO	5.13E-	19

8662		Process	09	
GO:009 8660	inorganic ion transmembrane transport	GO Process	1.05E- 08	20
GO:000 9755	hormone-mediated signaling pathway	GO Process	1.29E- 08	33
GO:004 6907	intracellular transport	GO Process	1.40E- 08	21
GO:001 5672	monovalent inorganic cation transport	GO Process	1.51E- 08	18
GO:005 1707	response to other organism	GO Process	3.72E- 08	34
GO:000 9617	response to bacterium	GO Process	3.78E- 08	19
GO:004 6034	ATP metabolic process	GO Process	3.78E- 08	13
GO:004 6128	purine ribonucleoside metabolic process	GO Process	3.94E- 08	15
GO:190 1657	glycosyl compound metabolic process	GO Process	3.94E- 08	18
GO:000 6886	intracellular protein transport	GO Process	5.15E- 08	18
GO:005 5086	nucleobase-containing small molecule metabolic process	GO Process	5.21E- 08	20
GO:000 6906	vesicle fusion	GO Process	6.30E- 08	9
GO:003 4613	cellular protein localization	GO Process	1.54E- 07	18
GO:006 1025	membrane fusion	GO Process	1.66E- 07	10
GO:004 4085	cellular component biogenesis	GO Process	1.69E- 07	24
GO:001 6050	vesicle organization	GO Process	2.17E- 07	10
GO:000 9117	nucleotide metabolic process	GO Process	2.44E- 07	18
GO:000 6754	ATP biosynthetic process	GO Process	4.61E- 07	8
GO:006 1024	membrane organization	GO Process	6.77E- 07	13
GO:004 4281	small molecule metabolic process	GO Process	8.54E- 07	39
GO:006 5007	biological regulation	GO Process	1.37E- 06	83
GO:000 6464	cellular protein modification process	GO Process	2.60E- 06	45
GO:190 1135	carbohydrate derivative metabolic process	GO Process	2.73E- 06	21
GO:003 2482	Rab protein signal transduction	GO Process	2.96E- 06	8
GO:004 2742	defense response to bacterium	GO Process	2.96E- 06	15
GO:004 4802	single-organism membrane organization	GO Process	3.24E- 06	11
GO:190	hydrogen ion transmembrane transport	GO	3.50E-	11

2600		Process	06	
GO:0071822	protein complex subunit organization	GO Process	3.89E-06	15
GO:1901659	glycosyl compound biosynthetic process	GO Process	4.43E-06	11
GO:0043412	macromolecule modification	GO Process	4.60E-06	46
GO:0046129	purine ribonucleoside biosynthetic process	GO Process	7.23E-06	9
GO:0016049	cell growth	GO Process	7.44E-06	14
GO:0040007	growth	GO Process	8.69E-06	15
GO:0010035	response to inorganic substance	GO Process	9.18E-06	24
GO:0050789	regulation of biological process	GO Process	1.14E-05	73
GO:1901700	response to oxygen-containing compound	GO Process	1.18E-05	32
GO:0009165	nucleotide biosynthetic process	GO Process	1.18E-05	12
GO:0050794	regulation of cellular process	GO Process	1.24E-05	68
GO:0048878	chemical homeostasis	GO Process	1.70E-05	13
GO:0022607	cellular component assembly	GO Process	1.78E-05	17
GO:0097305	response to alcohol	GO Process	1.90E-05	19
GO:0010119	regulation of stomatal movement	GO Process	2.04E-05	7
GO:0060560	developmental growth involved in morphogenesis	GO Process	2.04E-05	12
GO:0006887	exocytosis	GO Process	2.68E-05	7
GO:0046686	response to cadmium ion	GO Process	3.18E-05	14
GO:1902582	single-organism intracellular transport	GO Process	3.85E-05	13
GO:0070072	vacuolar proton-transporting V-type ATPase complex assembly	GO Process	3.95E-05	3
GO:0010038	response to metal ion	GO Process	5.02E-05	16
GO:0001101	response to acid chemical	GO Process	5.70E-05	26
GO:0009629	response to gravity	GO Process	5.76E-05	7
GO:0098542	defense response to other organism	GO Process	6.28E-05	24
GO:0009737	response to abscisic acid	GO Process	6.62E-05	17
GO:0019637	organophosphate metabolic process	GO Process	7.09E-05	19
GO:004	developmental cell growth	GO	8.25E-	9

8588		Process	05	
GO:004 3170	macromolecule metabolic process	GO Process	9.93E- 05	87
GO:000 9926	auxin polar transport	GO Process	9.95E- 05	7
GO:003 5556	intracellular signal transduction	GO Process	1.02E- 04	19
GO:004 4260	cellular macromolecule metabolic process	GO Process	1.06E- 04	82
GO:000 6461	protein complex assembly	GO Process	1.07E- 04	11
GO:006 5003	macromolecular complex assembly	GO Process	1.14E- 04	12
GO:000 6970	response to osmotic stress	GO Process	1.32E- 04	17
GO:000 9606	tropism	GO Process	1.32E- 04	7
GO:007 0271	protein complex biogenesis	GO Process	1.32E- 04	11
GO:000 7035	vacuolar acidification	GO Process	1.36E- 04	3
GO:003 3993	response to lipid	GO Process	1.48E- 04	19
GO:000 6855	drug transmembrane transport	GO Process	1.55E- 04	6
GO:000 6952	defense response	GO Process	1.68E- 04	29
GO:190 1137	carbohydrate derivative biosynthetic process	GO Process	1.95E- 04	14
GO:004 2493	response to drug	GO Process	1.98E- 04	6
GO:004 4710	single-organism metabolic process	GO Process	2.00E- 04	62
GO:000 6996	organelle organization	GO Process	2.00E- 04	25
GO:001 0315	auxin efflux	GO Process	2.42E- 04	5
GO:000 6888	ER to Golgi vesicle-mediated transport	GO Process	2.42E- 04	5
GO:001 0148	transpiration	GO Process	3.10E- 04	3
GO:003 4622	cellular macromolecular complex assembly	GO Process	3.94E- 04	10
GO:007 0588	calcium ion transmembrane transport	GO Process	4.02E- 04	6
GO:000 9630	gravitropism	GO Process	4.46E- 04	6
GO:001 0043	response to zinc ion	GO Process	4.70E- 04	5
GO:005 1235	maintenance of location	GO Process	5.33E- 04	4
GO:000 9833	plant-type primary cell wall biogenesis	GO Process	5.88E- 04	3
GO:004	vesicle docking	GO	6.36E-	5

8278		Process	04	
GO:190 2580	single-organism cellular localization	GO Process	7.63E- 04	9
GO:009 0407	organophosphate biosynthetic process	GO Process	7.79E- 04	13
GO:199 0267	response to transition metal nanoparticle	GO Process	7.87E- 04	7
GO:004 8856	anatomical structure development	GO Process	8.87E- 04	35
GO:004 3933	macromolecular complex subunit organization	GO Process	9.27E- 04	17
GO:000 6612	protein targeting to membrane	GO Process	0.00105	4
GO:006 5008	regulation of biological quality	GO Process	0.00105	25
GO:001 8108	peptidyl-tyrosine phosphorylation	GO Process	0.00105	4
GO:000 9826	unidimensional cell growth	GO Process	0.00116	9
GO:006 0548	negative regulation of cell death	GO Process	0.00128	4
GO:004 8767	root hair elongation	GO Process	0.00135	5
GO:007 0838	divalent metal ion transport	GO Process	0.00135	7
GO:000 6833	water transport	GO Process	0.00135	5
GO:004 8523	negative regulation of cellular process	GO Process	0.00143	14
GO:003 0308	negative regulation of cell growth	GO Process	0.00145	3
GO:005 1651	maintenance of location in cell	GO Process	0.00145	3
GO:000 9932	cell tip growth	GO Process	0.00159	7
GO:190 2589	single-organism organelle organization	GO Process	0.00159	16
GO:000 9651	response to salt stress	GO Process	0.00183	14
GO:003 2535	regulation of cellular component size	GO Process	0.00191	7
GO:000 0902	cell morphogenesis	GO Process	0.00229	10
GO:004 4711	single-organism biosynthetic process	GO Process	0.00238	30
GO:004 3181	vacuolar sequestering	GO Process	0.00238	2
GO:003 2119	sequestering of zinc ion	GO Process	0.00238	2
GO:007 1366	cellular response to indolebutyric acid stimulus	GO Process	0.00238	2
GO:007 2661	protein targeting to plasma membrane	GO Process	0.00238	2
GO:004	negative regulation of biological process	GO	0.00282	18

8519		Process		
GO:005 5082	cellular chemical homeostasis	GO Process	0.00321	7
GO:007 1365	cellular response to auxin stimulus	GO Process	0.00338	9
GO:000 6099	tricarboxylic acid cycle	GO Process	0.00371	5
GO:004 4767	single-organism developmental process	GO Process	0.00374	37
GO:001 5986	ATP synthesis coupled proton transport	GO Process	0.00382	4
GO:000 9966	regulation of signal transduction	GO Process	0.00404	9
GO:004 8468	cell development	GO Process	0.00447	10
GO:008 0147	root hair cell development	GO Process	0.00478	5
GO:001 0053	root epidermal cell differentiation	GO Process	0.00486	6
GO:000 8361	regulation of cell size	GO Process	0.00507	5
GO:000 9415	response to water	GO Process	0.00507	10
GO:003 2501	multicellular organismal process	GO Process	0.00507	36
GO:003 3554	cellular response to stress	GO Process	0.00512	17
GO:004 8583	regulation of response to stimulus	GO Process	0.00527	13
GO:004 3481	anthocyanin accumulation in tissues in response to UV light	GO Process	0.00624	2
GO:001 0118	stomatal movement	GO Process	0.00682	4
GO:000 9060	aerobic respiration	GO Process	0.00732	5
GO:000 6897	endocytosis	GO Process	0.00732	5
GO:000 6807	nitrogen compound metabolic process	GO Process	0.00758	60
GO:000 6605	protein targeting	GO Process	0.00764	7
GO:001 0817	regulation of hormone levels	GO Process	0.00794	8
GO:000 9653	anatomical structure morphogenesis	GO Process	0.00818	16
GO:000 9743	response to carbohydrate	GO Process	0.00818	6
GO:004 8364	root development	GO Process	0.00827	11
GO:002 2622	root system development	GO Process	0.00847	11
GO:005 2544	defense response by callose deposition in cell wall	GO Process	0.00882	3
GO:005	response to freezing	GO	0.00882	3

0826		Process		
GO:0071470	cellular response to osmotic stress	GO Process	0.00917	4
GO:1901576	organic substance biosynthetic process	GO Process	0.00948	59
GO:0043436	oxoacid metabolic process	GO Process	0.0095	22
GO:1901879	regulation of protein depolymerization	GO Process	0.0106	3
GO:0010255	glucose mediated signaling pathway	GO Process	0.0112	2
GO:0010344	seed oilbody biogenesis	GO Process	0.0112	2
GO:0006065	UDP-glucuronate biosynthetic process	GO Process	0.0112	2
GO:0034641	cellular nitrogen compound metabolic process	GO Process	0.0121	55
GO:0009266	response to temperature stimulus	GO Process	0.0123	13
GO:0009058	biosynthetic process	GO Process	0.0128	61
GO:0048765	root hair cell differentiation	GO Process	0.0128	5
GO:0034284	response to monosaccharide	GO Process	0.0131	4
GO:0044707	single-multicellular organism process	GO Process	0.0134	33
GO:0000904	cell morphogenesis involved in differentiation	GO Process	0.0135	7
GO:0034219	carbohydrate transmembrane transport	GO Process	0.0143	6
GO:0030001	metal ion transport	GO Process	0.0149	9
GO:0009414	response to water deprivation	GO Process	0.0149	9
GO:0044702	single organism reproductive process	GO Process	0.015	19
GO:0010054	trichoblast differentiation	GO Process	0.0152	5
GO:0048731	system development	GO Process	0.0154	25
GO:0010541	acropetal auxin transport	GO Process	0.0164	3
GO:0009733	response to auxin	GO Process	0.0165	10
GO:0051049	regulation of transport	GO Process	0.0169	6
GO:0010155	regulation of proton transport	GO Process	0.0172	2
GO:0043623	cellular protein complex assembly	GO Process	0.0183	6
GO:0033500	carbohydrate homeostasis	GO Process	0.0186	3
GO:002	reproductive process	GO	0.0191	21

2414		Process		
GO:004 3254	regulation of protein complex assembly	GO Process	0.0227	4
GO:000 9856	pollination	GO Process	0.0245	7
GO:000 6094	gluconeogenesis	GO Process	0.0246	2
GO:000 6882	cellular zinc ion homeostasis	GO Process	0.0246	2
GO:000 7010	cytoskeleton organization	GO Process	0.0246	6
GO:006 0919	auxin influx	GO Process	0.0246	2
GO:001 5976	carbon utilization	GO Process	0.0246	2
GO:001 0015	root morphogenesis	GO Process	0.0249	7
GO:000 0281	mitotic cytokinesis	GO Process	0.0259	4
GO:000 8643	carbohydrate transport	GO Process	0.0266	7
GO:000 6334	nucleosome assembly	GO Process	0.0269	3
GO:001 0252	auxin homeostasis	GO Process	0.0269	3
GO:007 1554	cell wall organization or biogenesis	GO Process	0.0281	13
GO:004 4703	multi-organism reproductive process	GO Process	0.0284	8
GO:000 9958	positive gravitropism	GO Process	0.0298	3
GO:001 5977	carbon fixation	GO Process	0.0298	3
GO:004 4271	cellular nitrogen compound biosynthetic process	GO Process	0.03	42
GO:007 1214	cellular response to abiotic stimulus	GO Process	0.0305	7
GO:001 7157	regulation of exocytosis	GO Process	0.0324	2
GO:009 0332	stomatal closure	GO Process	0.0324	2
GO:003 1497	chromatin assembly	GO Process	0.0329	3
GO:007 1555	cell wall organization	GO Process	0.033	12
GO:004 8869	cellular developmental process	GO Process	0.0334	15
GO:000 7275	multicellular organismal development	GO Process	0.0334	31
GO:000 9734	auxin-activated signaling pathway	GO Process	0.0339	7
GO:001 6482	cytoplasmic transport	GO Process	0.0339	7
GO:004	cellular biosynthetic process	GO	0.036	55

4249		Process		
GO:0009637	response to blue light	GO Process	0.0397	4
GO:0042274	ribosomal small subunit biogenesis	GO Process	0.0398	2
GO:1901800	positive regulation of proteasomal protein catabolic process	GO Process	0.0398	2
GO:0019752	carboxylic acid metabolic process	GO Process	0.0398	19
GO:0014070	response to organic cyclic compound	GO Process	0.0398	8
GO:0010359	regulation of anion channel activity	GO Process	0.0398	2
GO:0045899	positive regulation of RNA polymerase II transcriptional preinitiation complex assembly	GO Process	0.0398	2
GO:0051129	negative regulation of cellular component organization	GO Process	0.0398	3
GO:0009620	response to fungus	GO Process	0.0421	13
GO:0010540	basipetal auxin transport	GO Process	0.0425	3
GO:0009741	response to brassinosteroid	GO Process	0.0427	4
GO:1901701	cellular response to oxygen-containing compound	GO Process	0.0443	12
GO:0000226	microtubule cytoskeleton organization	GO Process	0.0451	4
GO:0051128	regulation of cellular component organization	GO Process	0.0488	7
GO:0006733	oxidoreduction coenzyme metabolic process	GO Process	0.049	5
GO:0046500	S-adenosylmethionine metabolic process	GO Process	0.0494	2

Table S12. GO term enrichment for elf18 treated di-Gly microsomal fractions. Using the list of proteins generated from microsomal preps for elf18 treated samples, GO term STRING enrichment was performed to determine GO categories of Component, Function and Process. GO term ID, GO term, GO category, FDR and number of enriched genes in the dataset are presented for elf18 treated samples.

GO Term ID	GO Term	GO Category	FDR P Value	# enriched genes
GO:0005886	plasma membrane	GO Component	1.58E-121	196
GO:0071944	cell periphery	GO Component	2.50E-116	205
GO:0016020	membrane	GO Component	1.92E-106	257
GO:0055044	symplast	GO Component	2.20E-76	108
GO:0009506	plasmodesma	GO Component	2.20E-76	108
GO:0044425	membrane part	GO Component	1.17E-65	184
GO:0016021	integral component of membrane	GO Component	2.11E-62	170
GO:0031224	intrinsic component of membrane	GO Component	1.82E-61	172
GO:0044464	cell part	GO Component	5.70E-57	281
GO:0005623	cell	GO Component	9.90E-57	281
GO:0005575	cellular_component	GO Component	4.90E-51	294
GO:0044444	cytoplasmic part	GO Component	2.63E-42	188
GO:0005773	vacuole	GO Component	8.42E-41	73
GO:0005737	cytoplasm	GO Component	3.04E-38	197
GO:0012505	endomembrane system	GO Component	8.35E-38	93

GO:004 4422	organelle part	GO Compone nt	3.74E- 35	144
GO:000 5774	vacuolar membrane	GO Compone nt	3.74E- 35	55
GO:009 8588	bounding membrane of organelle	GO Compone nt	4.01E- 35	85
GO:004 4446	intracellular organelle part	GO Compone nt	9.05E- 35	143
GO:009 8805	whole membrane	GO Compone nt	9.40E- 32	64
GO:003 1090	organelle membrane	GO Compone nt	3.04E- 29	90
GO:004 4445	cytosolic part	GO Compone nt	9.28E- 29	41
GO:002 2626	cytosolic ribosome	GO Compone nt	2.79E- 26	38
GO:000 5794	Golgi apparatus	GO Compone nt	9.62E- 25	55
GO:004 3229	intracellular organelle	GO Compone nt	3.48E- 23	195
GO:004 4391	ribosomal subunit	GO Compone nt	5.07E- 23	33
GO:000 5622	intracellular	GO Compone nt	8.12E- 23	208
GO:000 5829	cytosol	GO Compone nt	2.35E- 22	71
GO:000 5840	ribosome	GO Compone nt	2.49E- 22	39
GO:004 4424	intracellular part	GO Compone nt	8.85E- 22	204
GO:004 3231	intracellular membrane-bounded organelle	GO Compone nt	2.40E- 21	187
GO:000 5783	endoplasmic reticulum	GO Compone nt	1.30E- 17	43
GO:003 2991	macromolecular complex	GO Compone nt	1.33E- 16	70
GO:004	intracellular non-membrane-bounded organelle	GO	4.73E-	52

3232		Component	15	
GO:0005730	nucleolus	GO Component	3.42E-13	26
GO:0015934	large ribosomal subunit	GO Component	8.94E-13	18
GO:0022625	cytosolic large ribosomal subunit	GO Component	1.45E-12	17
GO:0022627	cytosolic small ribosomal subunit	GO Component	7.03E-12	15
GO:0005618	cell wall	GO Component	3.22E-11	32
GO:0005768	endosome	GO Component	8.72E-11	24
GO:0031981	nuclear lumen	GO Component	1.15E-10	31
GO:0070013	intracellular organelle lumen	GO Component	1.27E-09	33
GO:0044432	endoplasmic reticulum part	GO Component	2.44E-09	25
GO:0005789	endoplasmic reticulum membrane	GO Component	5.44E-09	23
GO:0042175	nuclear outer membrane-endoplasmic reticulum membrane network	GO Component	5.98E-09	23
GO:0000325	plant-type vacuole	GO Component	7.86E-09	14
GO:0033176	proton-transporting V-type ATPase complex	GO Component	9.68E-08	7
GO:0009536	plastid	GO Component	3.10E-07	55
GO:0009507	chloroplast	GO Component	3.70E-07	54
GO:0016469	proton-transporting two-sector ATPase complex	GO Component	2.90E-06	8
GO:0044459	plasma membrane part	GO Component	3.45E-06	17
GO:0098796	membrane protein complex	GO Component	4.71E-06	20

		nt		
GO:003 1201	SNARE complex	GO Compone nt	1.35E- 05	7
GO:000 9705	plant-type vacuole membrane	GO Compone nt	1.52E- 05	9
GO:000 0786	nucleosome	GO Compone nt	1.83E- 05	7
GO:000 5802	trans-Golgi network	GO Compone nt	3.52E- 05	12
GO:001 6471	vacuolar proton-transporting V-type ATPase complex	GO Compone nt	4.21E- 05	4
GO:004 4431	Golgi apparatus part	GO Compone nt	9.06E- 05	19
GO:000 0220	vacuolar proton-transporting V-type ATPase, V0 domain	GO Compone nt	1.00E- 04	3
GO:003 3179	proton-transporting V-type ATPase, V0 domain	GO Compone nt	1.02E- 04	4
GO:001 0008	endosome membrane	GO Compone nt	1.67E- 04	10
GO:004 3234	protein complex	GO Compone nt	2.62E- 04	33
GO:003 3180	proton-transporting V-type ATPase, V1 domain	GO Compone nt	7.86E- 04	3
GO:000 0785	chromatin	GO Compone nt	8.40E- 04	7
GO:003 1595	nuclear proteasome complex	GO Compone nt	0.0012	3
GO:003 1597	cytosolic proteasome complex	GO Compone nt	0.0012	3
GO:003 1226	intrinsic component of plasma membrane	GO Compone nt	0.00172	11
GO:003 3178	proton-transporting two-sector ATPase complex, catalytic domain	GO Compone nt	0.00177	4
GO:003 0658	transport vesicle membrane	GO Compone nt	0.00249	4
GO:004 8046	apoplast	GO Compone nt	0.00319	15

GO:0000139	Golgi membrane	GO Component	0.0035	14
GO:0031984	organelle subcompartment	GO Component	0.004	19
GO:0030176	integral component of endoplasmic reticulum membrane	GO Component	0.00525	3
GO:0031988	membrane-bounded vesicle	GO Component	0.00698	8
GO:0009505	plant-type cell wall	GO Component	0.00746	8
GO:0012506	vesicle membrane	GO Component	0.00772	6
GO:0008540	proteasome regulatory particle, base subcomplex	GO Component	0.00847	2
GO:0005887	integral component of plasma membrane	GO Component	0.00859	8
GO:0030133	transport vesicle	GO Component	0.00948	4
GO:0098562	cytoplasmic side of membrane	GO Component	0.0131	3
GO:0000788	nuclear nucleosome	GO Component	0.0134	2
GO:0000502	proteasome complex	GO Component	0.0138	4
GO:0035618	root hair	GO Component	0.0194	2
GO:0035619	root hair tip	GO Component	0.0194	2
GO:0032588	trans-Golgi network membrane	GO Component	0.0224	3
GO:0016023	cytoplasmic membrane-bounded vesicle	GO Component	0.0248	7
GO:0044426	cell wall part	GO Component	0.0252	2
GO:0005838	proteasome regulatory particle	GO Component	0.0252	2
GO:002	proteasome accessory complex	GO	0.0252	2

2624		Component		
GO:003 1301	integral component of organelle membrane	GO Component	0.0292	4
GO:003 1901	early endosome membrane	GO Component	0.0324	2
GO:003 0659	cytoplasmic vesicle membrane	GO Component	0.0352	5
GO:000 9986	cell surface	GO Component	0.049	2
GO:003 2550	purine ribonucleoside binding	GO Function	4.07E- 44	118
GO:003 5639	purine ribonucleoside triphosphate binding	GO Function	4.07E- 44	118
GO:003 2553	ribonucleotide binding	GO Function	4.83E- 44	119
GO:003 2555	purine ribonucleotide binding	GO Function	5.67E- 44	118
GO:000 0166	nucleotide binding	GO Function	8.18E- 42	125
GO:003 6094	small molecule binding	GO Function	1.17E- 41	127
GO:004 3168	anion binding	GO Function	2.39E- 41	125
GO:000 5524	ATP binding	GO Function	6.47E- 37	103
GO:000 3674	molecular_function	GO Function	4.29E- 36	241
GO:004 3167	ion binding	GO Function	6.23E- 33	160
GO:190 1363	heterocyclic compound binding	GO Function	1.51E- 30	157
GO:009 7159	organic cyclic compound binding	GO Function	1.55E- 30	157
GO:000 5488	binding	GO Function	2.57E- 29	192
GO:000 5515	protein binding	GO Function	9.62E- 29	69
GO:000 3824	catalytic activity	GO Function	3.66E- 28	174
GO:001 6817	hydrolase activity, acting on acid anhydrides	GO Function	2.90E- 26	54
GO:001 9899	enzyme binding	GO Function	1.01E- 25	41
GO:001 7111	nucleoside-triphosphatase activity	GO Function	1.53E- 25	51
GO:001 6462	pyrophosphatase activity	GO Function	3.45E- 25	52
GO:001	ATPase activity	GO	1.27E-	37

6887		Function	21	
GO:0004672	protein kinase activity	GO Function	6.48E- 21	51
GO:0019199	transmembrane receptor protein kinase activity	GO Function	4.11E- 20	30
GO:0005215	transporter activity	GO Function	5.60E- 20	57
GO:0016301	kinase activity	GO Function	1.60E- 19	55
GO:0016773	phosphotransferase activity, alcohol group as acceptor	GO Function	1.60E- 19	53
GO:0001653	peptide receptor activity	GO Function	3.08E- 19	29
GO:0038023	signaling receptor activity	GO Function	4.01E- 19	31
GO:0016820	hydrolase activity, acting on acid anhydrides, catalyzing transmembrane movement of substances	GO Function	4.46E- 19	24
GO:0004674	protein serine/threonine kinase activity	GO Function	7.89E- 19	46
GO:0022892	substrate-specific transporter activity	GO Function	8.22E- 19	48
GO:0022857	transmembrane transporter activity	GO Function	1.27E- 18	50
GO:0031625	ubiquitin protein ligase binding	GO Function	1.33E- 18	30
GO:0004675	transmembrane receptor protein serine/threonine kinase activity	GO Function	2.16E- 18	28
GO:0043492	ATPase activity, coupled to movement of substances	GO Function	1.69E- 17	23
GO:0042626	ATPase activity, coupled to transmembrane movement of substances	GO Function	3.10E- 17	22
GO:0022804	active transmembrane transporter activity	GO Function	7.56E- 17	34
GO:0022891	substrate-specific transmembrane transporter activity	GO Function	7.85E- 17	43
GO:0015405	P-P-bond-hydrolysis-driven transmembrane transporter activity	GO Function	8.53E- 17	23
GO:0019829	cation-transporting ATPase activity	GO Function	1.61E- 16	17
GO:0042623	ATPase activity, coupled	GO Function	2.81E- 16	27
GO:0004871	signal transducer activity	GO Function	3.00E- 16	33
GO:0003735	structural constituent of ribosome	GO Function	8.93E- 16	29
GO:0005198	structural molecule activity	GO Function	1.26E- 14	31
GO:0008324	cation transmembrane transporter activity	GO Function	4.00E- 14	30
GO:0015075	ion transmembrane transporter activity	GO Function	4.81E- 14	34
GO:0016740	transferase activity	GO Function	1.21E- 12	76
GO:001	ATPase activity, coupled to transmembrane movement of ions,	GO	3.92E-	11

5662	phosphorylative mechanism	Function	12	
GO:001 6787	hydrolase activity	GO Function	1.02E- 09	65
GO:002 2890	inorganic cation transmembrane transporter activity	GO Function	1.71E- 09	22
GO:003 6442	hydrogen-exporting ATPase activity	GO Function	3.96E- 09	9
GO:000 5388	calcium-transporting ATPase activity	GO Function	5.87E- 07	6
GO:000 3924	GTPase activity	GO Function	9.03E- 07	13
GO:000 5525	GTP binding	GO Function	2.98E- 06	15
GO:000 0149	SNARE binding	GO Function	1.28E- 05	7
GO:001 5078	hydrogen ion transmembrane transporter activity	GO Function	2.65E- 05	11
GO:001 5077	monovalent inorganic cation transmembrane transporter activity	GO Function	4.76E- 05	13
GO:001 5293	symporter activity	GO Function	7.57E- 05	10
GO:000 8506	sucrose:proton symporter activity	GO Function	8.00E- 05	3
GO:007 2509	divalent inorganic cation transmembrane transporter activity	GO Function	9.62E- 05	9
GO:004 6961	proton-transporting ATPase activity, rotational mechanism	GO Function	1.03E- 04	5
GO:004 3169	cation binding	GO Function	2.76E- 04	62
GO:000 8964	phosphoenolpyruvate carboxylase activity	GO Function	3.01E- 04	3
GO:000 8553	hydrogen-exporting ATPase activity, phosphorylative mechanism	GO Function	3.07E- 04	4
GO:001 0329	auxin efflux transmembrane transporter activity	GO Function	5.61E- 04	5
GO:004 6906	tetrapyrrole binding	GO Function	6.58E- 04	14
GO:001 5294	solute:cation symporter activity	GO Function	6.76E- 04	6
GO:000 9678	hydrogen-translocating pyrophosphatase activity	GO Function	6.85E- 04	3
GO:000 5507	copper ion binding	GO Function	7.67E- 04	10
GO:004 6872	metal ion binding	GO Function	8.09E- 04	60
GO:002 0037	heme binding	GO Function	0.00106	13
GO:000 5484	SNAP receptor activity	GO Function	0.00125	5
GO:001 5144	carbohydrate transmembrane transporter activity	GO Function	0.00156	8
GO:000 5516	calmodulin binding	GO Function	0.00189	8
GO:004	metal ion transmembrane transporter activity	GO	0.0023	10

6873		Function		
GO:0005351	sugar:proton symporter activity	GO Function	0.00252	5
GO:0004713	protein tyrosine kinase activity	GO Function	0.00265	4
GO:0036402	proteasome-activating ATPase activity	GO Function	0.00317	3
GO:0070405	ammonium ion binding	GO Function	0.00437	2
GO:0017025	TBP-class protein binding	GO Function	0.00453	3
GO:0051117	ATPase binding	GO Function	0.00453	3
GO:0019900	kinase binding	GO Function	0.00638	5
GO:0015291	secondary active transmembrane transporter activity	GO Function	0.00801	11
GO:0016760	cellulose synthase (UDP-forming) activity	GO Function	0.00872	4
GO:0046914	transition metal ion binding	GO Function	0.0118	28
GO:0019901	protein kinase binding	GO Function	0.0193	4
GO:0080054	low-affinity nitrate transmembrane transporter activity	GO Function	0.0235	2
GO:0003979	UDP-glucose 6-dehydrogenase activity	GO Function	0.0235	2
GO:0005315	inorganic phosphate transmembrane transporter activity	GO Function	0.0258	3
GO:0035251	UDP-glucosyltransferase activity	GO Function	0.0313	7
GO:0051287	NAD binding	GO Function	0.0313	5
GO:0004715	non-membrane spanning protein tyrosine kinase activity	GO Function	0.0359	2
GO:0010328	auxin influx transmembrane transporter activity	GO Function	0.0359	2
GO:1901618	organic hydroxy compound transmembrane transporter activity	GO Function	0.0408	4
GO:0051179	localization	GO Process	6.77E-34	105
GO:0051234	establishment of localization	GO Process	6.77E-34	104
GO:0006810	transport	GO Process	8.16E-34	103
GO:0009987	cellular process	GO Process	2.68E-33	234
GO:1902578	single-organism localization	GO Process	5.35E-33	88
GO:0050896	response to stimulus	GO Process	1.84E-32	153
GO:0044765	single-organism transport	GO Process	4.78E-32	86

GO:0008150	biological_process	GO Process	2.41E-28	250
GO:0044763	single-organism cellular process	GO Process	7.08E-28	171
GO:0044699	single-organism process	GO Process	2.48E-25	188
GO:0042221	response to chemical	GO Process	9.01E-23	95
GO:0044267	cellular protein metabolic process	GO Process	7.36E-22	98
GO:0008152	metabolic process	GO Process	2.47E-20	201
GO:0055085	transmembrane transport	GO Process	2.48E-20	57
GO:0006468	protein phosphorylation	GO Process	4.41E-20	51
GO:0010033	response to organic substance	GO Process	3.07E-19	75
GO:0006796	phosphate-containing compound metabolic process	GO Process	6.85E-19	71
GO:0019538	protein metabolic process	GO Process	1.28E-18	97
GO:0016310	phosphorylation	GO Process	3.45E-18	56
GO:0007178	transmembrane receptor protein serine/threonine kinase signaling pathway	GO Process	8.32E-18	28
GO:0009725	response to hormone	GO Process	1.83E-17	66
GO:0051716	cellular response to stimulus	GO Process	6.19E-17	78
GO:0006811	ion transport	GO Process	6.55E-17	46
GO:0009719	response to endogenous stimulus	GO Process	8.24E-17	67
GO:0046777	protein autophosphorylation	GO Process	1.09E-16	31
GO:0034220	ion transmembrane transport	GO Process	1.95E-16	40
GO:0006812	cation transport	GO Process	8.12E-16	34
GO:0051704	multi-organism process	GO Process	1.46E-15	58
GO:0098655	cation transmembrane transport	GO Process	2.77E-15	32
GO:0006950	response to stress	GO Process	1.46E-14	84
GO:0051641	cellular localization	GO Process	3.61E-14	34
GO:0009605	response to external stimulus	GO Process	3.85E-14	56
GO:0007154	cell communication	GO Process	7.16E-14	63
GO:0007165	signal transduction	GO Process	8.19E-14	58

GO:004 4237	cellular metabolic process	GO Process	1.75E- 13	159
GO:007 1702	organic substance transport	GO Process	2.19E- 13	48
GO:004 4700	single organism signaling	GO Process	2.90E- 13	58
GO:000 6412	translation	GO Process	4.47E- 13	31
GO:003 3036	macromolecule localization	GO Process	8.89E- 13	39
GO:007 0727	cellular macromolecule localization	GO Process	1.55E- 12	27
GO:190 1564	organonitrogen compound metabolic process	GO Process	2.22E- 12	54
GO:005 1707	response to other organism	GO Process	2.35E- 12	46
GO:001 6192	vesicle-mediated transport	GO Process	6.20E- 12	25
GO:009 8660	inorganic ion transmembrane transport	GO Process	8.05E- 12	26
GO:001 5031	protein transport	GO Process	9.15E- 12	33
GO:190 1566	organonitrogen compound biosynthetic process	GO Process	1.08E- 11	44
GO:005 1649	establishment of localization in cell	GO Process	1.08E- 11	29
GO:009 8662	inorganic cation transmembrane transport	GO Process	1.25E- 11	24
GO:007 1840	cellular component organization or biogenesis	GO Process	1.27E- 11	65
GO:007 1310	cellular response to organic substance	GO Process	1.36E- 11	46
GO:004 6907	intracellular transport	GO Process	1.80E- 11	27
GO:000 6886	intracellular protein transport	GO Process	2.06E- 11	24
GO:004 2742	defense response to bacterium	GO Process	2.15E- 11	23
GO:000 9617	response to bacterium	GO Process	2.22E- 11	25
GO:007 0887	cellular response to chemical stimulus	GO Process	2.99E- 11	48
GO:001 5991	ATP hydrolysis coupled proton transport	GO Process	7.05E- 11	11
GO:003 4613	cellular protein localization	GO Process	9.62E- 11	24
GO:001 6043	cellular component organization	GO Process	1.10E- 10	61
GO:007 1704	organic substance metabolic process	GO Process	1.12E- 10	155
GO:003 2870	cellular response to hormone stimulus	GO Process	3.73E- 10	41
GO:004 4238	primary metabolic process	GO Process	4.86E- 10	148

GO:001 5992	proton transport	GO Process	1.06E- 09	18
GO:001 5672	monovalent inorganic cation transport	GO Process	1.40E- 09	21
GO:000 9628	response to abiotic stimulus	GO Process	1.54E- 09	51
GO:000 6952	defense response	GO Process	3.34E- 09	44
GO:000 6464	cellular protein modification process	GO Process	3.88E- 09	59
GO:000 9755	hormone-mediated signaling pathway	GO Process	4.53E- 09	38
GO:009 8542	defense response to other organism	GO Process	8.24E- 09	35
GO:004 3412	macromolecule modification	GO Process	1.24E- 08	60
GO:190 2582	single-organism intracellular transport	GO Process	1.49E- 08	19
GO:004 8878	chemical homeostasis	GO Process	2.95E- 08	18
GO:000 7264	small GTPase mediated signal transduction	GO Process	4.99E- 08	12
GO:003 2482	Rab protein signal transduction	GO Process	7.26E- 08	10
GO:006 5007	biological regulation	GO Process	8.99E- 08	102
GO:000 6906	vesicle fusion	GO Process	3.95E- 07	9
GO:004 4260	cellular macromolecule metabolic process	GO Process	4.29E- 07	107
GO:004 4802	single-organism membrane organization	GO Process	4.70E- 07	13
GO:004 6686	response to cadmium ion	GO Process	8.06E- 07	18
GO:006 1024	membrane organization	GO Process	1.19E- 06	14
GO:006 1025	membrane fusion	GO Process	1.23E- 06	10
GO:001 0035	response to inorganic substance	GO Process	1.27E- 06	29
GO:004 4281	small molecule metabolic process	GO Process	2.09E- 06	44
GO:004 4085	cellular component biogenesis	GO Process	2.48E- 06	25
GO:004 2592	homeostatic process	GO Process	2.82E- 06	20
GO:005 0789	regulation of biological process	GO Process	4.14E- 06	88
GO:004 6128	purine ribonucleoside metabolic process	GO Process	4.16E- 06	14
GO:190 2600	hydrogen ion transmembrane transport	GO Process	4.24E- 06	12
GO:190 2580	single-organism cellular localization	GO Process	4.37E- 06	13

GO:190 1657	glycosyl compound metabolic process	GO Process	4.88E- 06	17
GO:000 9205	purine ribonucleoside triphosphate metabolic process	GO Process	5.36E- 06	12
GO:004 3170	macromolecule metabolic process	GO Process	5.76E- 06	109
GO:000 9206	purine ribonucleoside triphosphate biosynthetic process	GO Process	5.91E- 06	8
GO:001 0148	transpiration	GO Process	6.66E- 06	4
GO:006 5008	regulation of biological quality	GO Process	1.12E- 05	34
GO:001 0038	response to metal ion	GO Process	1.36E- 05	19
GO:005 0794	regulation of cellular process	GO Process	1.53E- 05	80
GO:007 0838	divalent metal ion transport	GO Process	1.63E- 05	10
GO:000 9737	response to abscisic acid	GO Process	2.45E- 05	20
GO:004 6034	ATP metabolic process	GO Process	2.45E- 05	11
GO:190 1700	response to oxygen-containing compound	GO Process	2.64E- 05	36
GO:005 5086	nucleobase-containing small molecule metabolic process	GO Process	2.87E- 05	18
GO:000 6833	water transport	GO Process	2.87E- 05	7
GO:000 6754	ATP biosynthetic process	GO Process	3.42E- 05	7
GO:009 7305	response to alcohol	GO Process	3.44E- 05	21
GO:190 1659	glycosyl compound biosynthetic process	GO Process	3.45E- 05	11
GO:000 6605	protein targeting	GO Process	3.71E- 05	11
GO:004 6129	purine ribonucleoside biosynthetic process	GO Process	4.05E- 05	9
GO:000 6888	ER to Golgi vesicle-mediated transport	GO Process	4.53E- 05	6
GO:005 5082	cellular chemical homeostasis	GO Process	5.92E- 05	10
GO:190 1135	carbohydrate derivative metabolic process	GO Process	7.70E- 05	21
GO:007 0072	vacuolar proton-transporting V-type ATPase complex assembly	GO Process	7.90E- 05	3
GO:000 2764	immune response-regulating signaling pathway	GO Process	7.90E- 05	3
GO:001 0119	regulation of stomatal movement	GO Process	8.36E- 05	7
GO:001 6049	cell growth	GO Process	8.50E- 05	14
GO:000 9117	nucleotide metabolic process	GO Process	9.99E- 05	16

GO:0009165	nucleotide biosynthetic process	GO Process	9.99E-05	12
GO:0010043	response to zinc ion	GO Process	9.99E-05	6
GO:0033993	response to lipid	GO Process	1.01E-04	22
GO:0006887	exocytosis	GO Process	1.06E-04	7
GO:0040007	growth	GO Process	1.07E-04	15
GO:0001101	response to acid chemical	GO Process	1.25E-04	29
GO:0006612	protein targeting to membrane	GO Process	1.26E-04	5
GO:0009150	purine ribonucleotide metabolic process	GO Process	1.26E-04	12
GO:0070588	calcium ion transmembrane transport	GO Process	1.34E-04	7
GO:0009266	response to temperature stimulus	GO Process	1.55E-04	19
GO:0060548	negative regulation of cell death	GO Process	1.60E-04	5
GO:0060560	developmental growth involved in morphogenesis	GO Process	1.63E-04	12
GO:0006970	response to osmotic stress	GO Process	1.72E-04	19
GO:0048193	Golgi vesicle transport	GO Process	1.90E-04	7
GO:0009629	response to gravity	GO Process	2.13E-04	7
GO:0071822	protein complex subunit organization	GO Process	2.13E-04	14
GO:0009735	response to cytokinin	GO Process	2.34E-04	12
GO:0044710	single-organism metabolic process	GO Process	2.54E-04	73
GO:0098581	detection of external biotic stimulus	GO Process	2.54E-04	3
GO:0007035	vacuolar acidification	GO Process	2.54E-04	3
GO:0055069	zinc ion homeostasis	GO Process	2.58E-04	4
GO:0009926	auxin polar transport	GO Process	3.63E-04	7
GO:0030001	metal ion transport	GO Process	4.10E-04	13
GO:1990267	response to transition metal nanoparticle	GO Process	4.16E-04	8
GO:0009606	tropism	GO Process	4.90E-04	7
GO:0016482	cytoplasmic transport	GO Process	4.90E-04	11
GO:0006855	drug transmembrane transport	GO Process	4.93E-04	6

GO:190 1137	carbohydrate derivative biosynthetic process	GO Process	5.05E- 04	15
GO:000 9651	response to salt stress	GO Process	5.07E- 04	17
GO:000 9152	purine ribonucleotide biosynthetic process	GO Process	5.56E- 04	8
GO:007 1554	cell wall organization or biogenesis	GO Process	5.76E- 04	19
GO:004 2493	response to drug	GO Process	6.17E- 04	6
GO:001 0315	auxin efflux	GO Process	6.32E- 04	5
GO:000 6461	protein complex assembly	GO Process	6.62E- 04	11
GO:007 1669	plant-type cell wall organization or biogenesis	GO Process	6.93E- 04	10
GO:007 0271	protein complex biogenesis	GO Process	8.03E- 04	11
GO:002 2607	cellular component assembly	GO Process	8.39E- 04	16
GO:005 0801	ion homeostasis	GO Process	8.84E- 04	9
GO:005 1128	regulation of cellular component organization	GO Process	9.12E- 04	11
GO:000 6882	cellular zinc ion homeostasis	GO Process	0.00104	3
GO:000 9833	plant-type primary cell wall biogenesis	GO Process	0.00104	3
GO:003 2535	regulation of cellular component size	GO Process	0.00111	8
GO:001 9725	cellular homeostasis	GO Process	0.00124	12
GO:003 3554	cellular response to stress	GO Process	0.0013	21
GO:000 9630	gravitropism	GO Process	0.00133	6
GO:004 8583	regulation of response to stimulus	GO Process	0.0014	16
GO:005 1274	beta-glucan biosynthetic process	GO Process	0.00146	6
GO:003 5556	intracellular signal transduction	GO Process	0.00152	19
GO:004 8278	vesicle docking	GO Process	0.00157	5
GO:000 8361	regulation of cell size	GO Process	0.0016	6
GO:003 4219	carbohydrate transmembrane transport	GO Process	0.00162	8
GO:005 1273	beta-glucan metabolic process	GO Process	0.00196	7
GO:001 8108	peptidyl-tyrosine phosphorylation	GO Process	0.00218	4
GO:004 8588	developmental cell growth	GO Process	0.00222	8

GO:0010053	root epidermal cell differentiation	GO Process	0.00225	7
GO:0044711	single-organism biosynthetic process	GO Process	0.00234	35
GO:1901800	positive regulation of proteasomal protein catabolic process	GO Process	0.00243	3
GO:0010359	regulation of anion channel activity	GO Process	0.00243	3
GO:0045899	positive regulation of RNA polymerase II transcriptional preinitiation complex assembly	GO Process	0.00243	3
GO:0044703	multi-organism reproductive process	GO Process	0.00243	11
GO:0051651	maintenance of location in cell	GO Process	0.00243	3
GO:0048856	anatomical structure development	GO Process	0.00288	39
GO:0045087	innate immune response	GO Process	0.00295	11
GO:0006885	regulation of pH	GO Process	0.00297	4
GO:0009620	response to fungus	GO Process	0.00305	18
GO:0048767	root hair elongation	GO Process	0.00311	5
GO:0043181	vacuolar sequestering	GO Process	0.00321	2
GO:0032119	sequestering of zinc ion	GO Process	0.00321	2
GO:0002221	pattern recognition receptor signaling pathway	GO Process	0.00321	2
GO:0071366	cellular response to indolebutyric acid stimulus	GO Process	0.00321	2
GO:0072661	protein targeting to plasma membrane	GO Process	0.00321	2
GO:0048523	negative regulation of cellular process	GO Process	0.00332	15
GO:0009624	response to nematode	GO Process	0.00359	6
GO:0071555	cell wall organization	GO Process	0.00405	16
GO:0048765	root hair cell differentiation	GO Process	0.00491	6
GO:0090407	organophosphate biosynthetic process	GO Process	0.00492	13
GO:0009856	pollination	GO Process	0.00494	9
GO:0008643	carbohydrate transport	GO Process	0.00564	9
GO:0032501	multicellular organismal process	GO Process	0.0058	42
GO:0010054	trichoblast differentiation	GO Process	0.00606	6
GO:0055080	cation homeostasis	GO Process	0.0061	7

GO:004 3254	regulation of protein complex assembly	GO Process	0.00618	5
GO:001 0817	regulation of hormone levels	GO Process	0.00687	9
GO:000 8219	cell death	GO Process	0.00718	7
GO:001 9637	organophosphate metabolic process	GO Process	0.0073	17
GO:000 9409	response to cold	GO Process	0.00777	12
GO:000 6099	tricarboxylic acid cycle	GO Process	0.00802	5
GO:003 0003	cellular cation homeostasis	GO Process	0.00802	5
GO:009 8771	inorganic ion homeostasis	GO Process	0.00827	7
GO:001 6045	detection of bacterium	GO Process	0.00827	2
GO:004 3481	anthocyanin accumulation in tissues in response to UV light	GO Process	0.00827	2
GO:005 1049	regulation of transport	GO Process	0.00956	7
GO:004 3069	negative regulation of programmed cell death	GO Process	0.00957	3
GO:008 0147	root hair cell development	GO Process	0.0101	5
GO:004 8519	negative regulation of biological process	GO Process	0.0108	19
GO:000 9816	defense response to bacterium, incompatible interaction	GO Process	0.0115	4
GO:000 9832	plant-type cell wall biogenesis	GO Process	0.0118	6
GO:004 8364	root development	GO Process	0.0126	12
GO:001 0118	stomatal movement	GO Process	0.0127	4
GO:002 2622	root system development	GO Process	0.0129	12
GO:004 3436	oxoacid metabolic process	GO Process	0.0134	25
GO:004 4767	single-organism developmental process	GO Process	0.0139	41
GO:005 2544	defense response by callose deposition in cell wall	GO Process	0.0142	3
GO:000 9966	regulation of signal transduction	GO Process	0.0143	9
GO:001 5698	inorganic anion transport	GO Process	0.0147	6
GO:001 0255	glucose mediated signaling pathway	GO Process	0.015	2
GO:008 0055	low-affinity nitrate transport	GO Process	0.015	2
GO:000 6065	UDP-glucuronate biosynthetic process	GO Process	0.015	2

GO:001 0256	endomembrane system organization	GO Process	0.0152	4
GO:001 2501	programmed cell death	GO Process	0.0152	6
GO:005 0832	defense response to fungus	GO Process	0.0152	15
GO:000 9060	aerobic respiration	GO Process	0.0152	5
GO:000 9814	defense response, incompatible interaction	GO Process	0.0154	7
GO:004 8468	cell development	GO Process	0.0168	10
GO:000 9826	unidimensional cell growth	GO Process	0.0169	8
GO:001 0015	root morphogenesis	GO Process	0.0189	8
GO:000 6996	organelle organization	GO Process	0.0191	23
GO:004 8869	cellular developmental process	GO Process	0.0192	18
GO:002 1700	developmental maturation	GO Process	0.0198	7
GO:004 4707	single-multicellular organism process	GO Process	0.0201	38
GO:004 8513	organ development	GO Process	0.0219	19
GO:000 6875	cellular metal ion homeostasis	GO Process	0.0221	4
GO:001 9752	carboxylic acid metabolic process	GO Process	0.0224	23
GO:000 9932	cell tip growth	GO Process	0.0227	6
GO:000 9888	tissue development	GO Process	0.0228	13
GO:001 0155	regulation of proton transport	GO Process	0.0229	2
GO:000 9408	response to heat	GO Process	0.023	8
GO:000 9653	anatomical structure morphogenesis	GO Process	0.0231	17
GO:190 1576	organic substance biosynthetic process	GO Process	0.0236	68
GO:003 4284	response to monosaccharide	GO Process	0.0236	4
GO:001 0541	acropetal auxin transport	GO Process	0.0253	3
GO:003 0433	ER-associated ubiquitin-dependent protein catabolic process	GO Process	0.0253	3
GO:003 6503	ERAD pathway	GO Process	0.0253	3
GO:001 5770	sucrose transport	GO Process	0.0253	3
GO:003 0244	cellulose biosynthetic process	GO Process	0.0255	4

GO:003 4622	cellular macromolecular complex assembly	GO Process	0.026	8
GO:003 0243	cellulose metabolic process	GO Process	0.0264	5
GO:005 5114	oxidation-reduction process	GO Process	0.0276	29
GO:003 3500	carbohydrate homeostasis	GO Process	0.0289	3
GO:000 0902	cell morphogenesis	GO Process	0.0291	9
GO:009 0558	plant epidermis development	GO Process	0.0294	8
GO:004 5089	positive regulation of innate immune response	GO Process	0.0297	4
GO:004 8731	system development	GO Process	0.0301	28
GO:003 1347	regulation of defense response	GO Process	0.0307	7
GO:000 9611	response to wounding	GO Process	0.0318	7
GO:006 0919	auxin influx	GO Process	0.0318	2
GO:001 5976	carbon utilization	GO Process	0.0318	2
GO:001 5850	organic hydroxy compound transport	GO Process	0.0345	4
GO:003 4976	response to endoplasmic reticulum stress	GO Process	0.0345	4
GO:003 0154	cell differentiation	GO Process	0.0357	15
GO:190 1701	cellular response to oxygen-containing compound	GO Process	0.0359	14
GO:000 9058	biosynthetic process	GO Process	0.0373	70
GO:007 1365	cellular response to auxin stimulus	GO Process	0.0388	8
GO:000 6694	steroid biosynthetic process	GO Process	0.0401	4
GO:190 1699	cellular response to nitrogen compound	GO Process	0.0407	5
GO:000 6334	nucleosome assembly	GO Process	0.0413	3
GO:001 0252	auxin homeostasis	GO Process	0.0413	3
GO:001 9748	secondary metabolic process	GO Process	0.0413	10
GO:004 3244	regulation of protein complex disassembly	GO Process	0.0413	3
GO:000 6066	alcohol metabolic process	GO Process	0.0419	7
GO:001 7157	regulation of exocytosis	GO Process	0.0422	2
GO:009 0332	stomatal closure	GO Process	0.0422	2

GO:0070574	cadmium ion transmembrane transport	GO Process	0.0422	2
GO:0043933	macromolecular complex subunit organization	GO Process	0.0423	15
GO:0007275	multicellular organismal development	GO Process	0.0427	36
GO:0022414	reproductive process	GO Process	0.0452	23
GO:0009958	positive gravitropism	GO Process	0.0453	3
GO:0015977	carbon fixation	GO Process	0.0453	3
GO:0000281	mitotic cytokinesis	GO Process	0.0453	4
GO:0044257	cellular protein catabolic process	GO Process	0.0472	9
GO:0042176	regulation of protein catabolic process	GO Process	0.048	4
GO:0010029	regulation of seed germination	GO Process	0.048	4